2009

Adaptation at a Shortened Length in Rabbit Femoral Artery

Melissa Bednarek
Virginia Commonwealth University

School of Medicine
Virginia Commonwealth University

This is to certify that the dissertation prepared by Melissa L. Bednarek entitled ADAPTATION AT A SHORTENED LENGTH IN RABBIT FEMORAL ARTERY has been approved by his or her committee as satisfactory completion of the dissertation requirement for the degree of Doctor of Philosophy

Paul H. Ratz, Ph.D., Dissertation Advisor, School of Medicine

George D. Ford, Ph.D., School of Medicine

Srinivasa M. Karnam, Ph.D., School of Medicine

Roland N. Pittman, Ph.D., School of Medicine

John E. Speich, Ph.D., School of Engineering

Diomedes E. Logothetis, Ph.D., Chair, Department of Physiology and Biophysics, School of Medicine

Jerome F. Strauss, III, M.D., Ph.D., Dean, School of Medicine

F. Douglas Boudinot, Ph.D., Dean, Graduate School

July 22, 2009

ADAPTATION AT A SHORTENED LENGTH IN RABBIT FEMORAL ARTERY

A Dissertation submitted in partial fulfillment of the requirements for the degree of Doctor of Philosophy at Virginia Commonwealth University.

by

MELISSA L. BEDNAREK
Bachelor of Science, St. Bonaventure University, 1998
Masters in Physical Therapy, MCP Hahnemann University, 2000

Director: PAUL H. RATZ, PH.D.
PROFESSOR, DEPARTMENTS OF BIOCHEMISTRY AND PEDIATRICS

Virginia Commonwealth University
Richmond, Virginia
August 2009

Acknowledgements

There are so many people without whom this project would not have been possible.

First, I would like to thank my advisor, Dr. Paul Ratz. For the many hours he spent with me during which I learned not only about smooth muscle and science but about life itself. His keen observations have helped me to develop both personally as well as professionally. Second, I would like to thank past Physiology Graduate Program Director, Dr. George Ford. Over the years, Dr. Ford connected me with career development opportunities that I would have not otherwise known about, not the least of which was introducing me to Dr. Ratz's research. Third, I would like to thank Dr. John Speich. The many conversations about adaptation, tissue differences and how to negotiate my first job have been invaluable. Finally, in addition to the above listed committee members, I would like to thank Dr. Roland Pittman and Dr. Murthy Karnam for their valuable insight into this project.

While in the lab, many people contributed to this project, both intellectually as well as through humor. Among them, Amy Miner, Dr. Silvina Alvarez, Atheer Almasri, Dr. Clint Collins, Dr. Corey Johnson, Brendan Browne, Kate Bowers, Jack Guan, Patrick Headley, and Hersch Bhatia.

While completing this degree, the love and support I have received from friends, both near and far, was immeasurable. The encouragement, suggestions, and comic relief through the many ups and downs of these past five years will never be forgotten.

Last, but certainly not least, I would like to thank my family. None of this would have ever been possible without their encouragement and unending love and support.

Table of Contents

Page

List of Figures

Page

List of Abbreviations

ASM ..... airway smooth muscle

$[Ca^{2+}]_i$ ..... intracellular calcium concentration

CaMKII ..... Ca^{2+}/calmodulin-dependent protein kinase

CS ..... contracting solution

FAK ..... focal adhesion kinase

F-actin ..... filamentous actin

G-actin ..... globular actin

L_0 ..... optimal length for muscle contraction

L_1 ..... loop 1

L_2 ..... loop 2

L-adaptation ..... length-adaptation

LD ..... loading

L_s ..... slack length

L-T ..... length-tension

MLCK ..... myosin light chain kinase

MLCp ..... phosphorylated 20 kDa myosin light chain

MLCP ..... myosin light chain phosphatase

N-WASp ..... neuronal Wiskott-Aldrich syndrome protein

PKC ..... protein kinase C

PSS ..... physiological salt solution

ROCK ..... rhoA kinase

RS ..... relaxing solution

SS ..... strain-softening

T_a ..... active tension

T_p ..... passive tension

TPR ..... total peripheral resistance

ULD ..... unloading

VOCs..... voltage-operated Ca^{2+} channels

VSM..... vascular smooth muscle

Abstract

ADAPTATION AT A SHORTENED LENGTH IN RABBIT FEMORAL ARTERY

By Melissa L. Bednarek, B.S., M.P.T.

A Dissertation submitted in partial fulfillment of the requirements for the degree of Doctor of Philosophy at Virginia Commonwealth University.

Virginia Commonwealth University, 2009

Major Director: Paul H. Ratz
Professor, Departments of Biochemistry and Pediatrics

It is well known that the overlap between the thick and thin filaments in striated muscle is responsible for the single active length-tension (L-T) curve. With the lack of visible striations, a sarcomeric unit has not been identified in smooth muscle. Though once thought to function like striated muscle via a sliding filament mechanism of contraction, recent studies on length-adaptation (L-adaptation) in airway smooth muscle (ASM), in which increased tension is generated with repeated contraction, have led to the hypothesis of a dynamic L-T curve in smooth muscle. Although more established in ASM, two studies have shown L-adaptation in vascular smooth muscle (VSM). In this project, the L-T curve over a 3-fold length range in rabbit femoral artery was investigated and the presence of more than one active and passive L-T curve was identified. The third of three

repeated KCL-induced contractions at a single, shortened length resulted in L-adaptation in which the phasic and tonic phases of contraction demonstrated a 10-15% increase in active tension (T_a) relative to the first contraction. Experiments investigating possible mechanism(s) responsible for this phenomenon demonstrated that neither an increase in $[Ca^{2+}]_i$ nor an increase in MLC_{20} phosphorylation was responsible for the increased tension. However, actin polymerization did appear to play a role in the L-adaptation of both phases of contraction. Thus directions for future research could include further study of actin polymerization in VSM that contributes to L-adaptation and may ultimately result in artery remodeling.

CHAPTER 1

Introduction

1.1 Smooth Muscle Physiology

The common function of all muscles is to contract. Contraction of skeletal muscle results in movement of bones while contraction of cardiac and the great majority of smooth muscles results in hollow organ dimensional changes. In particular, the smooth muscle contained in the walls of the vascular tree is responsible for regulating the diameter of the vessel. Changes in diameter and tension are possible through contraction of vascular smooth muscle (VSM).

As in striated muscle, calcium (Ca^{2+}) plays a key role in the mechanism of smooth muscle contraction. Voltage-operated Ca^{2+} channels (VOCs) open with depolarization of the smooth muscle membrane, thus allowing for the influx of Ca^{2+} down its concentration gradient (Figure 1.1). Calcium will then bind cooperatively with calmodulin, and the Ca^{2+}-calmodulin complex activates myosin light chain kinase (MLCK). Through its kinase activity, MLCK phosphorylates the 20 kDa regulatory light chain of myosin (MLC_{20}) thus facilitating interaction with actin and formation of tension-generating crossbridges. In the presence of ATP, contractions occur until MLC_{20} is dephosphorylated by myosin light chain phosphatase (MLCP). Through actin connections to dense bodies and ultimately to

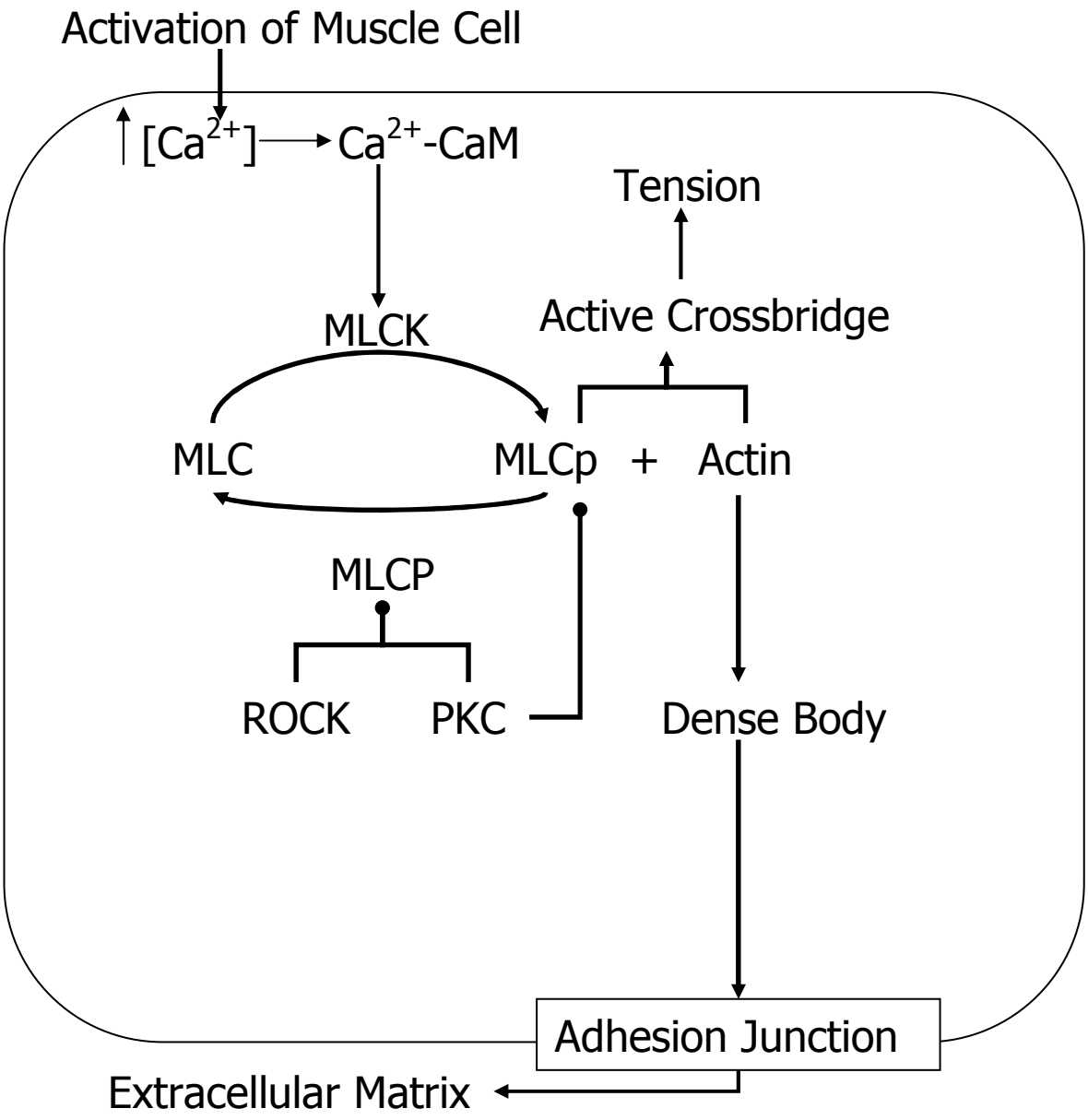

FIGURE 1.1: Diagram of Mechanism of Smooth Muscle Contraction
Diagram illustrating the mechanism of smooth muscle contraction, from activation through transmission of generated tension to the extracellular matrix. Also shown is the regulation of MLCP by ROCK and PKC as well as the regulation of MLCp by PKC.

the adhesion junction at the cell membrane, the tension generated by the crossbridges is transmitted to the extracellular matrix [15].

In addition to VOCs that open with membrane depolarization, there are additional routes through which Ca^{2+} may enter a smooth muscle cell. Chief among these routes are receptor-operated Ca^{2+} channels (ROCs) and store-operated Ca^{2+} channels (SOCs). When a neurotransmitter or hormone, such as norepinephrine, activates a G-protein coupled receptor (GPCR) additional cation channels, including ROCs and SOCs are opened. In the history of smooth muscle research, both depolarization and activation of GPCRs have been utilized as a means to activate tissue [99]. The stimulus utilized to depolarize is typically a high concentration potassium (K^+)-solution. The presence of additional extracellular K^+ will prevent movement of intracellular K^+ down its concentration gradient and thus result in membrane depolarization and opening of VOCs to initiate smooth muscle contraction. An advantage of tissue activation through depolarization is that GPCR and downstream signaling pathways are not activated, which has led to new information on Ca^{2+}-sensitivity of contraction [79].

1.2 Phases of a VSM Contraction

Upon activation, VSM demonstrates a characteristic biphasic contraction. The initial rapid rise in tension, phasic phase, is complete within approximately 10 sec after stimulation while the slow rise in tension, tonic phase, requires an additional 2-3 min to develop [103] (Figure 1.2). Conditions such as stimulus concentration and temperature have been shown to differentially affect these two phases[20, 103, 123].

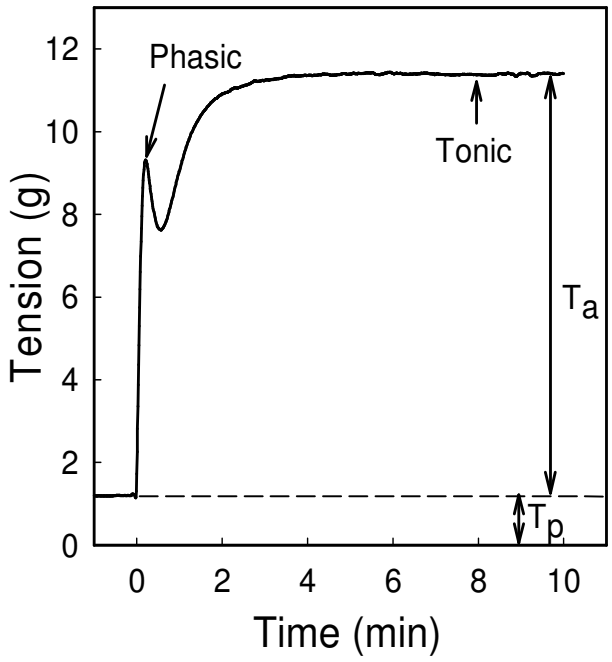

FIGURE 1.2: Representative Tension Tracing of Rabbit Femoral Artery Contraction
Representative time versus tension tracing for a K^+-induced rabbit femoral artery contraction. The development of the phasic phase active tension (T_a) is very rapid and brief while the development of the tonic phase T_a is slower and sustained. Also, note that total muscle tension is the summation of T_a and passive tension (T_p). Passive tension will be further discussion in Section 1.4.

Although the mechanism responsible for each phase of a VSM contraction is not fully known, some models have been proposed. K^+-induced VSM contractions are dependent on the influx of extracellular Ca^{2+} [42, 120] and there is evidence that each of the phases may be due to a different type of Ca^{2+} channel [43]. Extracellular Ca^{2+} may act in conjunction with depolarization-activated intracellular Ca^{2+} pools to generate tension [6, 55] and different sources of Ca^{2+} may be responsible for the different phases of contraction [81, 123].

Regardless of the source, it is generally accepted that a rise in myoplasmic Ca^{2+} levels is responsible for the phasic phase of smooth muscle contraction. What is less understood is the mechanism for sustained tension in the tonic phase with falling levels of myoplasmic Ca^{2+} and MLC_{20} phosphorylation [19, 45]. A model proposed by Murphy and colleagues to explain these findings is the latchbridge hypothesis [17, 35]. In this model, following muscle activation, crossbridges are dephosphorylated yet remain attached to create latchbridges that are capable of maintaining tension. Another model proposed to explain the maintenance of tonic force with decreased MLC_{20} phosphorylation invokes structural stability [78]. This model describes membrane activation of a Ca^{2+}-sensitive protein kinase C (PKC) that is able to phosphorylate intermediate filament proteins, such as desmin, and actin-binding proteins, such as filamin. When phosphorylated, filamin is able to interact with actin to provide a stable internal structure, and thus tonic force is maintained. Additional support for the involvement of PKC and actin in tonic force maintenance comes from the work of Wright and Hurn[123]. Low concentrations of the PKC inhibitor staurosporine or use of cytochalasin D, known to cap the (+) end of

filamentous actin (F-actin), selectively inhibits the tonic phase of a K^+-induced contraction of rat aorta.

1.3 Role of VSM in Regulation of Blood Pressure

A certain level of arterial blood pressure is required for adequate tissue perfusion. Because there is insufficient cardiac output to fully perfuse all vascular beds, blood flow must be regulated. Changes in cardiac output and total peripheral resistance (TPR) will result in changes in blood pressure. There are two main systems responsible for sensing and responding to changes in arterial blood pressure [15]. The first system is a quick-response system and involves baroreceptors located in the walls of the carotid sinus and aortic arch. With changes in blood pressure, there are changes in autonomic output to the heart and blood vessels. The effect of a decrease in blood pressure on VSM involves an increase in sympathetic activity, release of periarterial norepinephrine, activation of GPCRs causing vasoconstriction and an increase in TPR that will facilitate a compensatory rise in arterial blood pressure. The second system, the renin-angiotension II-aldosterone (RAA), is slower-acting and will facilitate a compensation for a decrease in blood pressure through its actions on the adrenal cortex, kidneys and vasculature. Although this system primarily involves changes in blood volume through the action of angiotension II-stimulated release of aldosterone, a secondary effect of angiotension II is vasoconstriction of arterioles. Thus, along with the heart and kidneys, the vascular system plays a role in the regulation of arterial blood pressure.

The regulation of blood pressure through changes in TPR occurs primarily at the level of the arteriole. Along with cardiac output, TPR determines the steady component of blood pressure [65]. A second component of blood pressure, the pulsatile component, is determined by ventricular ejection, large artery compliance and timing of reflected waves [65]. Thus, there are roles for both the microcirculation and macrocirculation in the regulation of blood pressure.

Based on their location in the vascular tree, a function of large arteries is to translate the intermittent pressure increase and resultant ejection of blood from the heart into a constant pressure and perfusion for distal tissues [87, 88]. This occurs through the "Windkessel" effect in which part of the stroke volume ejected during systole is immediately conducted distally while the other part is stored within the elastic vessel wall to be conducted during diastole. Based on their different functions, the smaller peripheral arteries are stiffer and thus conduct pulse waves faster than the larger central arteries. Thus, a forward-traveling pressure wave will ultimately meet stiffer arteries and generate a backward-traveling reflection pressure wave. The forward- and backward-traveling waves will summate to provide pulse pressure amplification down the vascular tree and, centrally, increase coronary artery perfusion during diastole. Any change in this balance of arterial stiffness, such as may occur with normal aging or pathology such as hypertension, will result in impaired blood flow. Over time, these changes can result in pathologic remodeling that includes an increase in vessel wall diameter with a decrease in lumen diameter[26, 89]. Thus, VSM in both small and large arteries play a critical role in the

regulation of arterial blood pressure. Rabbit femoral artery, a medium-sized muscular artery, was used for this project.

1.4 Passive Length-Tension (L-T) Relationship in Skeletal and Smooth Muscle

As a component of measured total tension, the passive tension (T_p) exerted by muscle plays an important role in muscle biomechanics. Therefore, the effect of length on T_p should be considered. Using isolated frog skeletal muscle fibers, Lakie and Robson [51] demonstrated that the length-history in the relaxed state was important in the passive tension that the fiber was able to develop. When the magnitude of the length response to a tension was compared with the response to the same tension applied following a period of length-oscillations, the latter length response was found to be approximately eight times larger. For a maximal increase in the post-oscillation response, a series of six to nine length oscillations were necessary. The magnitude of a third response decreased as the time interval between the second and third tension increased. This effect was attributed to crossbridge interactions. Using a permeabilized rabbit psoas muscle preparation, Campbell and Moss [10] later investigated length-history dependency of skeletal muscle in the presence of controlled levels of Ca^{2+}. Based on the investigators' definition of thixotrophy as "a time-dependent reduction in a muscle's resistance to stretch following movement," they found that muscle stiffness increased with increase levels of free Ca^{2+}. Thus, the link to $[Ca^{2+}]_i$ provided additional evidence for a role of cycling crossbridges in generation of T_p. This work was later expanded to suggest a role for crossbridges in T_p generation in cardiac muscle [11].

Despite the inherent complexity in VSM, such as the presence of basal tone and the large amount of connective tissue in the vessel wall, some have investigated T_p generation in VSM following length changes. One such study was that completed by Herlihy and Murphy [37] in which they set out to more fully characterize the passive and active tension of hog carotid artery over a series of lengths. They noted that different L-T_p curves could be obtained dependent on the protocol used to obtain T_p. The authors suggested that a series of stretches to a maximal length followed by release to shorter length provide the best estimate of T_p. Thus, the length-history of VSM affects T_p generated at a particular length. Wingard et al. [121] expanded on this work using a similar protocol to obtain T_p and also found the presence of two T_p curves. The T_p generated with gradual tissue lengthening exceeded that generated with gradual shortening and the authors attributed the difference in curves to an irreversible increase in the compliance of the tissue in contact with the steel mounting posts (Figure 1.3). Thus, following maximal stretch, the length of viable tissue capable of contributing to the T_p, as well as active tension (T_a), is reduced. Others have suggested a possible role for Ca^{2+}-independent crossbridges or passive structures as responsible for resistance to stretch [82].

More recent work by Speich and colleagues [100, 101] demonstrated that strips of rabbit detrusor smooth muscle displayed both a viscoelastic component and a strain-softening (SS) component following length-oscillations under passive conditions. They determined that the viscoelastic component was reversible with time while the SS component, initially thought to be irreversible, returned following muscle activation. Furthermore, the amount of stiffness that returned upon activation was found to be

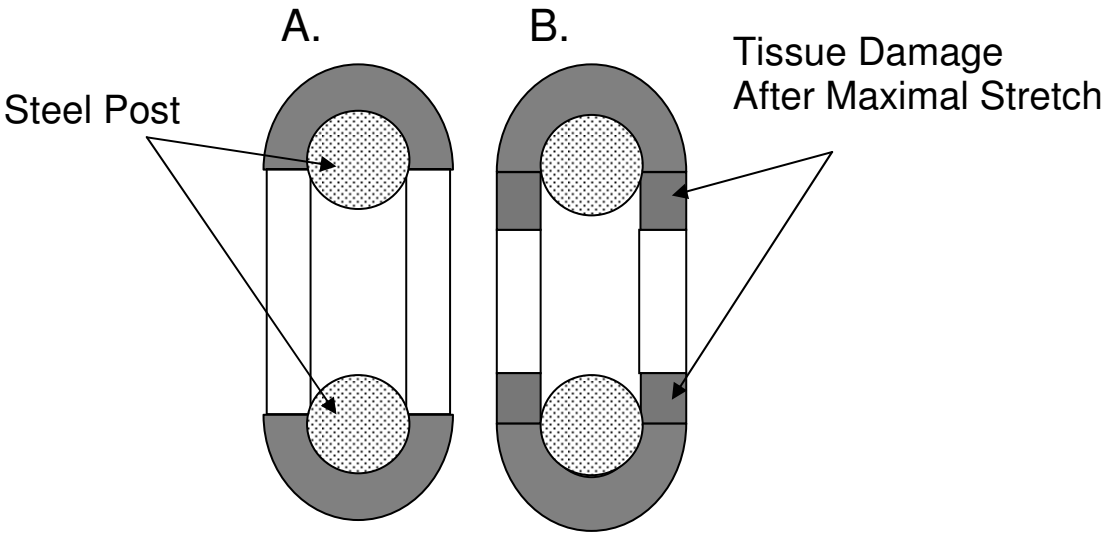

FIGURE 1.3: Diagram of Increased Tissue Compliance Evident with Stretch
Panel A illustrates that, when an artery ring is viewed end-on, there is a certain amount of tissue in contact with the steel mounting post. Following maximal stretch, this tissue is thought to be irreversibly damaged and thus, due to its position in series with the viable contractile tissue, increase the tissue compliance as shown in Panel B. Thus, in effect, the length of viable tissue is reduced following stretch to maximal length.

dependent on the muscle length at the time of activation. Thus, their work provided additional evidence for a role for crossbridges in the generation of T_p. A novel finding of this study was the involvement of Rho kinase (ROCK), as the return of SS-induced T_p was prevented in the presence of a ROCK inhibitor.

The studies just described involved a series of length changes prior to measurement of T_p. Experiments on airway smooth muscle (ASM) in rabbit investigated the effect of static changes in length on T_p [117]. When relaxed tissues were set for 24 h at lengths longer or shorter than a reference length, the shape of the subsequent passive L-T_p curve was similar to the reference but was shifted on the length-axis, to the right for tissues set at longer lengths and to the left for tissues set at shorter lengths. Thus it appears that ASM is capable of adapting to length changes with extended time at a particular length. This characteristic has been termed length-adaptation (L-adaptation).

1.5 Active L-T Relationship in Skeletal and Smooth Muscle

Through visualization of sarcomeric units, early work on skeletal muscle fibers demonstrated that the isometric tension generated by muscle activation was directly correlated to the amount of contractile filament overlap [29, 44]. Using a systematic approach in their now classic work, Gordon et al. [29] demonstrated the full L-T curve in frog skeletal muscle fibers. They reported that tension generation was nearly constant at sarcomere lengths from approximately 2.0 μ to 2.25 μ. Tension fell sharply at lengths both shorter and longer than those identified as the plateau, such that tension generation was only possible between lengths of 1.27 μ and 3.65 μ. This characteristic L-T relationship

was explained using the sliding filament mechanism of contraction. They suggested that each interaction between a thick and thin filament is able to generate a fixed amount of tension and the tension generated by the fiber as a whole is dependent on the amount of overlap between thick and thin filaments and thus the number of interactions. Based on the similar shape of the L-T_a curve, later experiments on smooth muscle strips provided evidence for a sliding filament mechanism of contraction similar to that just described for striated muscle [30, 37].

It has long been known that smooth muscle can contract over a large length range [122], although not all exhibit the dramatic 7-fold length change possible in urinary bladder smooth muscle [113]. Consistent with this idea, Herlihy and Murphy [37] noted that arterial strips generated tension at proportionately shorter muscle lengths than in skeletal muscle. Mulvany and Warshaw [63] later estimated that the working range of VSM was 0.38-fold L_0 to 1.82-fold L_0, where L_0 is the length at which the tissue is able to generate maximal tension. When relaxed, isolated smooth muscle cells stretched to lengths greater than resting produced similar forces to that achieved at resting length, Harris and Warshaw [36] interpreted these findings as evidence for a broad plateau in the L-T_a relationship. In VSM, the plateau has been shown to range from 0.9-fold L_0 to 1.19-fold L_0 [121].

The large length range over which smooth muscle has been shown to generate tension has called into question a static sarcomeric structure that is known to exist in skeletal muscle. As a sarcomeric-like unit has yet to be visualized in smooth muscle, alternative explanations for the observed L-T_a relationship have been put forth. An

element common to these explanations is the dynamic nature of the smooth muscle cell, contractile filament structure and/or actin cytoskeleton.

1.6 Terminology Related to the L-T Relationship in ASM

With advantages such as minimal connective tissue and the parallel arrangement of cells, ASM has been found to be ideal for the study of smooth muscle biomechanics [97]. Before further discussion of the dynamic nature of tension generation in smooth muscle, a brief discussion of agreed upon terminology in the field of ASM biomechanics and the application to this project is warranted.

With the expansion of the field over the past two decades, a group of over 40 researchers published an editorial in 2004 in which areas of current confusion in terminology were discussed as well as recommendations for standard terminology suggested [3]. The concept of a maximal/optimal force, L_0, achieved at a single length seems inappropriate, at least for ASM. These researchers determined that ASM can adapt to lengths shorter and longer than a reference length by developing additional tension, and therefore suggested using terminology such as "in situ length" or "arbitrarily chosen reference length." These researchers also suggested that the term L-adaptation be used to refer to "time-dependent force recovery and the subsequent shift in the length-force relationship." While it is now clear that ASM can L-adapt, the possibility that VSM can likewise readjust the degree of T_a when moved away from L_0 remains controversial.

For this project, L_0 was defined as the muscle length at which the T_p was 13% ±3% of the T_a (unpublished observation of PH Ratz) at that particular length. The protocol used to

obtain this length was very reproducible and was modified from two studies on VSM by Murphy and colleagues [37, 121]. The protocol is more fully described in the Materials and Methods section. For the purpose of this project, L-adaptation was defined as increased tension generated upon repeated activation at a single length.

1.7 L-adaptation of T_a in Smooth Muscle Involves Changes in Myofilament Structure

One idea that first emerged in the mid-1990's to explain the long range of smooth muscle function was structural changes that occur in the contractile filaments with length changes [24, 74]. With the inability to visualize the contractile structures, these investigators used indirect measures of function to gain insight into ASM. With muscle lengthening at constant activation, they found a decrease in velocity of shortening proportional to an increase in tension [24, 93]. The model proposed by these investigators to explain these findings was based on the knowledge that tensions generated by crossbridges positioned in parallel add while crossbridges positioned in series increase speed of shortening. More specially, they hypothesized that as muscle length increases so too does the number of contractile units in series [24].

Additional support for a model in which thick filaments, specifically, transition from a parallel to series arrangement with increasing muscle length can be found in pioneering work performed 40 years ago that demonstrated that thick filaments were capable of assembling upon muscle activation and partially dissolving upon muscle relaxation [85]. Evidence of an increase in myosin filament density with activation came from studies with rat anococcygeus muscle [27, 28, 124] that were later corroborated by porcine ASM

studies that showed that the time necessary for thick filament polymerization could account for the mechanical properties of adaptation [98]. The degree to which thick filaments polymerize upon activation appears to be tissue dependent, as the thick filament density in the rat anococcygeus increased 23% [124] upon activation compared to the 144% increase in porcine ASM [39]. Kuo et al. [50] demonstrated that an oscillation-induced decrease in thick filament density could be reversed with repeated contraction. This group later suggested that it is the length of the ASM that regulates the amount of thick filaments present in the cell [49].

To further the role that the thick filaments may play in this dynamic process of L-adaptation, Seow suggested that their formation may be guided by the thin filament network [92]. Indeed, *in vitro* studies in *Dictyostelium* have shown that the interaction between myosin monomers and fully-formed thin filament networks accelerates the rate of polymerization of myosin [54]. A later study suggested that phosphorylation of the MLC may regulate the thin filament-mediated myosin polymerization [1]. Thus, attention was turned to the actin thin filament network and its regulation.

There is a large amount of actin present in smooth muscle. Cohen and Murphy [12] found significantly higher actin content in pig arterial tissues (carotid, thoracic aorta and left anterior descending coronary arteries) as compared to nonarterial smooth muscle tissues (esophagus, trachea, intestine and uterus). With further investigation of arteries of different sizes, no differences in actin, myosin or tropomyosin content was found [13]. Four types of actin are known to exist in smooth muscle: α-smooth muscle, γ-smooth muscle, β-non-muscle and γ-non-muscle [23, 115]. Some have suggested that the relative

amount of each type of actin in smooth muscle tissue relates to the amount of contractile activity of the tissue [23]. Some actin filaments are engaged with myosin for the formation of tension-generating crossbridges while other actin filaments provide structural stability to the cell through connections to dense bodies and adhesion junctions. Attempts to assign different functions to the different actin isoforms have met with varying results as Drew et al. [18] found polymerization of the isoforms to be random in swine stomach while North et al. [66] and Kim et al. [47] found the isoforms to localize to specific areas of smooth muscle cells.

Regardless of actin isoform specificity, it was necessary to determine if, like the myosin thick filaments, actin thin filaments polymerize upon activation. Using different techniques, Mehta and Gunst [57] and Herrera et al. [40] confirmed that indeed actin polymerization does occur with activation of ASM with the latter group showing that both myosin and actin polymerization are length-sensitive. One of the techniques used by Mehta and Gunst [57] involved use of latrunculin A and cytochalasin D. Latrunculin A is a naturally occurring agent that has been shown to bind with globular actin, G-actin, monomers in a 1:1 ratio and thus impair the ability of a smooth muscle cell to recruit G-actin for polymerization [16]. As reviewed by Cooper [14], cytochalasin D is a naturally occurring agent that binds to the barbed end of filamentous (F)-actin at low concentrations (0.2 μM) while it binds to G-actin monomers at higher concentrations (2-20 μM). In their experiments on canine ASM strips, Mehta and Gunst found that tension declined in a dose-dependent manner in the presence of either agent while the presence of latrunculin A had no effect on MLC phosphorylation but the presence of cytochalasin D resulted in a dose-

independent decline in MLC phosphorylation as compared to untreated control strips. The findings regarding the effect of muscle length on MLC phosphorylation had previously been shown by Youn et al. [126]. With the ability to clamp calcium levels through the α-toxin permeabilization technique, Mehta and Gunst confirmed that the effect of cytochalasin D on MLC phosphorylation was not mediated through changes in calcium signaling. Another important result of their work pertained to the length-dependent sensitivity of actin polymerization inhibitors. When muscle strips were contracted with and without latrunculin A at L_0, 0.8 L_0 and 0.6 L_0, there was significantly more tension inhibition at the longer lengths. Thus the effect of muscle length on tension generation is lost in the presence of latrunculin A yet retained in the presence of cytochalasin D.

Despite the useful information gained from mechanical studies of isometric contraction using muscle strips or rings, it is important to consider the *in vivo* environment of the tissues in the whole animal. To that end, some have conducted studies on arteries that are cannulated and pressurized to create isobaric conditions. Versus the measurement of T_a generated with an isometric contraction using a wire myograph setup, the lumen diameter is measured upon stimulation in a pressure myograph setup. An important study illustrating possible differences in the behavior of small arteries under isometric and isobaric conditions was completed by Buus et al. [8]. They showed that although there was no difference in the T_p relationship using a wire versus pressure myograph, there were differences in the active responses. When activated through α-1 adrenergic receptor agonist noradrenaline or phenylephrine, pressurized vessels showed an increased sensitivity to stimulation that was dose dependent. However, when the GPCR system was

bypassed with use of K^+-stimulation, there were no differences between experimental methods. Similar responses to norepinephrine were found in rat [22]and rabbit [21] mesenteric arteries. These effects, however, may be related to the small size of the arteries studied as Tanko et al. [111] showed that medium size porcine coronary arteries are more sensitive to agonist and K^+-stimulation under isometric versus isobaric conditions. Taken together, these results illustrate that care should be exercised when interpreting results of isometric arterial studies as representative of the *in vivo* condition.

With this in mind, inhibitors of actin polymerization have been used in the *in vivo*-like pressurized model. Using small rat mesenteric arteries and isobaric conditions, Shaw et al. [94] demonstrated that, as in isometric conditions, there is a concentration-dependent decrease in vasoconstriction with agonist stimulation in the presence of cytochalasin D. In their studies with latrunculin B, these authors found a concentration-dependent decrease in the sustained agonist-induced vasoconstriction but not the peak phase. While it appears that the peak and sustained phases of contraction were inhibited equally at all tested concentrations of cytochalasin D (0.1 μM to 5.0 μM), the differential effect of latrunculin B on the phases increased with the higher concentrations tested. Furthermore, these authors showed that these reductions in vasoconstriction were not due to alteration of $[Ca^{2+}]_i$, as measured with the calcium indicating dye indo-1. A reduction in sustained vasoconstriction with no effect on $[Ca^{2+}]_i$ was found upon K^+-stimulation in the presence of cytochalasin D and latrunculin B. The authors did not comment on the effect of phasic K^+-induced tension in the presence of the inhibitors. Thus studies with acetylcholine [57], α-adrenergic [94], and K^+-stimulation [94, 112] show no change in $[Ca^{2+}]_i$ in the presence

of cytochalasin, however, a simultaneous decrease in tension and $[Ca^{2+}]_i$ has been shown with muscarinic stimulation [112].

1.8 L-adaptation of T_a in Smooth Muscle Involves Regulation of the Contractile Apparatus

In addition to changes in the structure of the myosin and actin filaments per se, another possible source for the length-dependent changes unique to smooth muscle might be found in the regulation of activation of the actomyosin crossbridges. In the early 1980's, Price and colleagues [76] demonstrated a length-dependency in dog anterior tibial artery through activation with agonist stimulation or depolarization. The optimal length of the artery, L_{max}, was determined as the length at which maximal T_a was generated with electrical field stimulation. When compared to two shorter lengths and a longer length, they found that arteries were most sensitive to stimulation at L_{max}. With further attention to lengths greater than L_{max}, this group found that indeed sensitivity to norepinephrine stimulation continues to increase as length increases [77]. They suggested that an increase in $[Ca^{2+}]_i$ may be responsible for the length-dependent sensitivity evident in VSM. Calcium was also implicated in the reduced force development when activated ASM was moved to a shortened length [31]. Furthermore, Rembold and Murphy [83] found that $[Ca^{2+}]_{i,}$ as measured with aequorin, decreased at lengths below L_0. Thus the decreased myoplasmic level of Ca^{2+} at lengths below L_0 was thought to play a role in the decrease in tension at shorter lengths. Although the results of Van Heijst et al. showed a sensitivity to α-adrenergic stimulation that was dependent on length in intact tissues, especially in rabbit

femoral artery, their experiments on skinned muscle did not show a change in Ca^{2+}-sensitivity to length [114].

Upon stimulation, $[Ca^{2+}]_i$ in smooth muscle binds with calmodulin, thus forming a complex capable of activating MLCK that will phosphorylate MLC_{20} and begin crossbridge cycling. Thus, with the knowledge that $[Ca^{2+}]_i$ is dependent on smooth muscle length up to L_0 [83] it was reasonable to next investigate what, if any, effect length has on the level of MLC_{20} phosphorylation. Using swine carotid arteries and K^+-stimulation, Hai [34] measured both peak and steady-state MLC_{20} phosphorylation at slack length, L_0 and 1.5 L_0. Relative to L_0, at the longest length there was a significant decrease in peak phosphorylation while at slack length there was significant decrease in peak and steady-state phosphorylation. When two contractions at L_0, separated by 1 hr of relaxation, were completed there were no changes in peak or steady-state phosphorylation levels. This was in contrast to the significant decrease in peak phosphorylation that was found in the second contraction when the same protocol was completed on tissues at slack length. Thus, it appears that the level of MLC_{20} phosphorylation that corresponds to the peak of contraction is sensitive to lengths both above and below L_0 while steady-state phosphorylation is only sensitive at shortened lengths. In permeabilized swine VSM, myosin phosphorylation levels were found to be insensitive to lengths shorter and longer than L_0 [61]. The decrease in MLC_{20} phosphorylation in tissues shorter than L_0 is evident in ASM stimulated with acetylcholine or K^+ [59] as well as carbachol [125, 126]. In contrast, Wingard et al. [121] showed similar levels of steady-state MLC phosphorylation in K^+-depolarized swine carotid arteries at lengths ranging from 0.6 L_0 to 1.8 L_0.

1.9 L-adaptation of T_a in Smooth Muscle Involves Changes in the Regulation of the Actin Cytoskeleton

When investigation of ASM stiffness, thought to be indicative of the number of crossbridges participating in tension generation, demonstrated insensitivity to length, Gunst et al. suggested a structure in series with the tension generating crossbridges may be responsible for length dependent changes in smooth muscle [33]. One possibility for this structure was the actin cytoskeleton. As the function of a smooth muscle cell is to generate tension, which must then be transmitted to extracellular structures, Gunst and colleagues have done much to elucidate important signaling involved in regulation of the actin cytoskeleton in ASM over the past 15 years. Studies of cell signaling downstream of the cell membrane thought to regulate the actin cytoskeleton will be briefly reviewed. Integrins, located at the adhesion junction on the smooth muscle cell membrane, appear to be a physical link between the extracellular matrix and cytosolic structures. These proteins span the cell membrane and are capable of transducing chemical and mechanical signals both from the extracellular matrix to the cytosol and vice versa [25]. From the results of cell culture studies [7], the cytosolic kinase focal adhesion kinase (FAK) has been implicated in signal transduction pathways through integrins. Also among the proteins present at the adhesion junction is paxillin, which has been shown to be phosphorylated upon activation of ASM and necessary for tension development [70, 73, 118]. At least *in vitro*, FAK is capable of phosphorylating paxillin [5]. What is interesting to note is that loss of FAK in ASM has been shown to decrease $[Ca^{2+}]_i$ and MLC phosphorylation with subsequent decrease in tension generation [106] while loss of paxillin affects tension

generation but apparently through a mechanism not involving $[Ca^{2+}]_i$ and MLC phosphorylation [108, 109]. Thus the possibility exists that mechanisms for crossbridge cycling and actin polymerization diverge at the level of FAK. Phosphorylation of both FAK and paxillin was length-sensitive upon activation of ASM, with trends mirroring the L-T relationship in smooth muscle for lengths less than L_0 [105]. An additional protein at the adhesion junction, talin, is capable of binding directly to the cytoplasmic domain of integrins as well as actin filaments [9, 90] while α-actinin is recruited to integrins with ASM activation [127]. Thus, these early studies provided evidence for a role of membrane proteins as signaling changes in muscle length.

Unlike the cell culture model in which early studies of adhesion signaling were based, the small GTPase Rho does not appear to be an upstream regulator of FAK nor paxillin phosphorylation [58]. However, another member of the family of small GTPases, Cdc42, does appear to play a more upstream role in the regulation of actin polymerization in ASM. Agonist stimulation in ASM has been shown to activate Cdc42, which may result in regulation of actin polymerization through activation of neuronal Wiskott-Aldrich syndrome protein (N-WASp) and actin-related protein complex (Arp 2/3) [107]. The adaptor protein Crk II, known to interact with paxillin upon stimulation [108], has been shown to regulate the activation of Cdc42 and thus, ultimately, N-WASp [110]. Moving downstream to the level of actin filament nucleation by Arp 2/3 [41], N-WASp activation of Arp 2/3 is necessary for actin polymerization in response to contractile stimulation [128].

Despite the lack of an upstream role for Rho in the transduction of extracellular signals, Rho has been shown to be involved in regulation of actin polymerization. One of the known effectors of Rho is Rho kinase (ROCK), a serine/threonine kinase. As one of its many functions inside a cell, ROCK has been shown to phosphorylate Thr 508 of LIM kinase 1 (LIMK1) which, when activated, is capable of phosphorylating and inactivating cofilin [2, 53, 69]. Thus, activation of Rho and subsequently ROCK, LIMK1 and cofilin will prevent the actin depolymerizing function of cofilin. A second known effector of Rho is p140mDia, a member of the formin-related family of proteins that participate in cell structure regulation, and is thought to interact with profilin [119]. In contrast to cofilin, profilin has been shown to play a role in actin polymerization in the presence of thymosin β4 [71]. Thus, it appears that Rho may participate in the stabilization of the actin cytoskeleton via stabilization of cofilin and activation of profilin.

1.10 Studies of L-adaptation in VSM

As was presented, there is a significant amount of literature on L-adaptation in ASM including possible mechanisms. There are, however, only two studies investigating the L-adaptive response of VSM to changes in length. In the first, using rabbit carotid artery and electrical field stimulation, Seow [91] showed a decrease in isometric T_a upon activation 2 min following change to a length shorter or longer than the reference length (L_{ref}). T_a significantly increased when activated at the same length 27 min later. When T_p was investigated, measurements 27 min after length change showed a decrease in stiffness as compared to shortly after length change. Seow concluded that adaptation in T_a and T_p in

VSM, although incomplete, was time dependent. Adaptation of T_a was evident through a series of isometric contractions every 5 min throughout the recovery period. What does not appear to be accounted for in this important study is the possible role that the repeated contraction may have had on L-adaptation in VSM. A more recent study by the same group investigated L-adaptation in sheep pulmonary artery [104]. As in the previous study, a decrease in T_a was evident upon release of the muscle from L_{ref} to either 0.8 or 0.6 L_{ref} that improved over a 30 min period during which the muscle was activated every 5 min. Although there was improvement in T_a for muscle released to either shortened length, only the muscle released to 0.6 L_{ref} demonstrated a significant increase from stimulation immediately upon release to the stimulation when fully adapted. Despite smaller absolute values, the same pattern of recovery was evident for T_p as for T_a.

1.11 Project Objectives/Outline

Although the concept of smooth muscle L-adaptation is widely accepted in ASM, a complete mechanism is still not known nor is the extent to which these findings can be applied in other tissues. With the limited studies on L-adaptation in VSM in particular, the early studies just presented have only begun to characterize L-adaptation. Length-dependent changes in VSM tension generation are clinically important in the regulation of arterial blood pressure, especially in light of conditions such as hypertension.

With the differing views of a static versus dynamic L-T curve in smooth muscle, it was necessary to first characterize the full L-T curve in this preparation with a focus on possible differential effects of length on the phasic and tonic phase of contraction. With

appreciation for the role that T_p plays in generation of total force, the effect of length-history on T_p was investigated. The L-adaptation of T_a present in VSM was then more fully characterized, again with a focus on any differences in adaptation between the two phases. The next goal was to investigate the role of crossbridge regulation on L-adaptation through measurement of $[Ca^{2+}]_i$, and MLC_{20} phosphorylation. The role of $[Ca^{2+}]_i$ was further investigated through β-escin permeabilized tissue experiments in which $[Ca^{2+}]_i$ was tightly controlled. Using pharmacologic agents known to affect actin polymerization, a possible role for this process in L-adaptation was also studied.

CHAPTER 2

Materials and Methods

2.1 Tissue Preparation

All experiments involving rabbits were conducted within the appropriate animal welfare regulations and guidelines and were approved by the Virginia Commonwealth University Institutional Animal Care and Use Committee. In brief, adult New Zealand White rabbits were pre-anesthetized prior to death through sternotomy, as the heart was used for other investigations. Femoral arteries were carefully dissected out and cleaned of adhering tissue and either used immediately or stored in physiological salt solution (PSS) at 0-4˚C for later experimentation. The PSS composition was 140 mM NaCl, 4.7 mM KCl, 1.2 mM $MgSO_4$, 1.6 mM $CaCl_2$, 1.2 mM Na_2HPO_4, 2.0 mM morpholino-propanesulfonic acid (adjusted to pH 7.4), 0.02 mM EDTA (to chelate heavy metals) and 5.6 mM D-glucose. Immediately prior to an experiment, the vessel endothelium was disrupted with a roughened metal rod and the artery was cut into rings ranging from 2-4 mm in length. The tissue was then secured between two pins in an aerated myograph tissue chamber (Danish Myo Technology) or an aerated muscle chamber (Radnoti Glass Technology, Monrovia, CA) containing PSS maintained at 37˚C. One pin was connected to a micrometer for length changes while the other was connected to an isometric force transducer. With the

exception of permeabilized tissue experiments, all tissues were activated through K^+-depolarization.

2.2 L_0 Determination

With the exception of the full L-T curve protocol, the optimum muscle length for each tissue was determined using an abbreviated L-T curve protocol adapted from the work of Murphy and colleagues [37, 121] (Figure 2.1). With a 0.5 g load, tissues were first warmed to 37˚C for 30-60 min followed by a 5 min K^+-induced contraction to determine tissue viability (wake-up). Tissues were then washed in PSS and allowed to relax for 15 min. Based on the maximal T_a achieved for each tissue during wake-up, the T_p that would be 13 ± 3% of the T_a was calculated (release value). Tissues were then stretched in 0.5 g increments and allowed to stress relax for 5 min before the next stretch. Tissues were stretched to a load 1 g above the release value and then quick-released to break any crossbridges. Following 15-30 seconds at the released value, tissues were again activated for 5 min followed by a wash in PSS for 15 min. The T_p obtained following release and just prior to contraction and the maximal T_a obtained during contraction were used to calculate the release value for the second L_0 determination. A minimum of two L_0 determinations were completed prior to each experimental protocol.

With the exception of the full L-T curve protocol and the T_p protocols, all studies were conducted in the presence of 1 μM phentolamine to block potential α-adrenergic receptor activation caused by release of norepinephrine from periarterial nerves. All

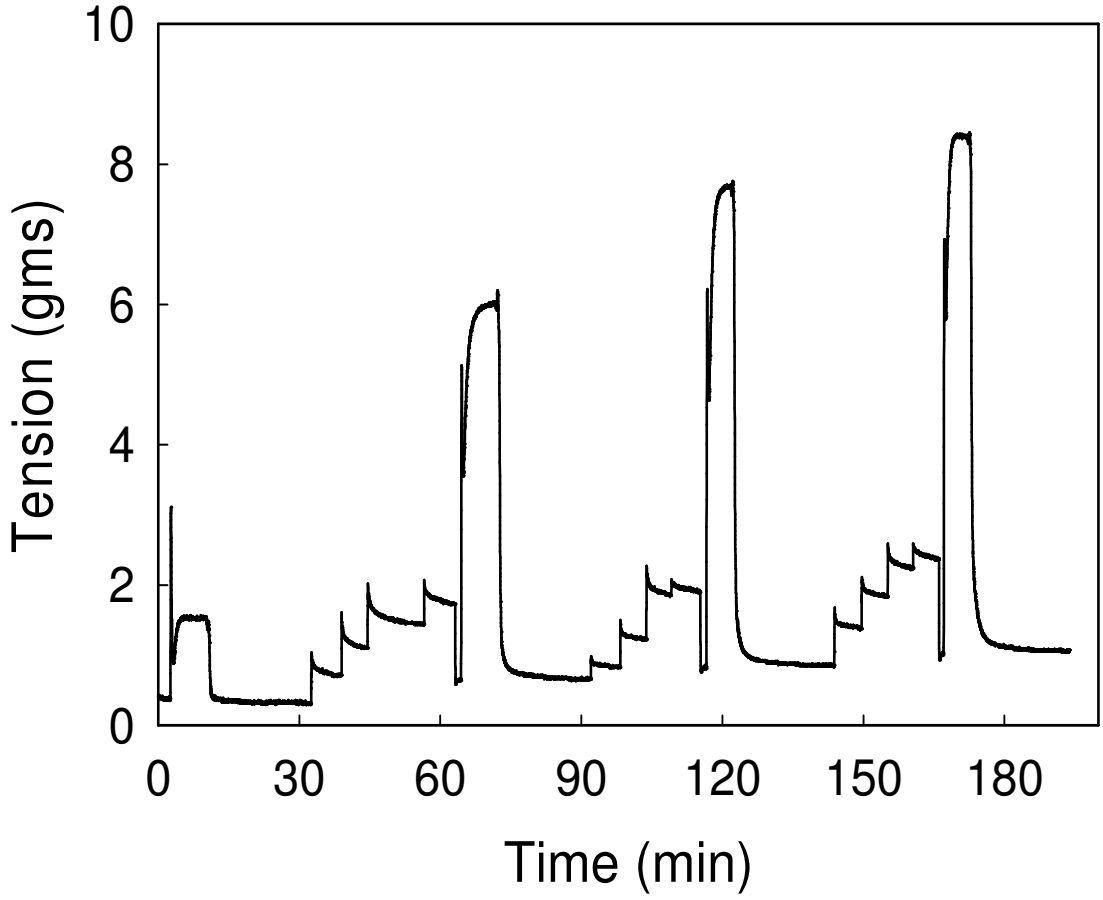

FIGURE 2.1: Representative Tension Tracing for L_0 Determination
Representative time versus tension tracing for a wake-up contraction followed by 3 L_0 determinations. Note that an L_0 determination consists of a series of 0.5 g stretches, release to a shorter length (to determine T_p) followed by muscle activation (to determine T_a) and then relaxation. The ratio of T_p to Ta is calculated with a goal of 13 ± 3%. A minimum of 2 L_0 determinations were completed before each experimental protocol where indicated.

tension experiment data was then normalized to the steady-state tension achieved at 1.0 L_0 in the presence of 1 μM phentolamine. Data was acquired through an analog-digital converter board (National Instruments) and analyzed using DasyLab 8.0 (DasyTech, Amherst, NH).

2.3 $[Ca^{2+}]_i$

Simultaneous tension and $[Ca^{2+}]_i$ were measured in femoral artery rings. Following L_0 determination, tissues were loaded for 2 h with 7.5 μM fura-2-PE3 (acetoxymethyl ester) and 0.01% (w/v) Pluronic F-127 to enhance solubility. Fluorescence emission intensities at 510 nm collected by a photomultiplier tube were expressed as excitation ratios (340/380 nm, DeltaRam V; Photon Technology International, Lawrenceville, NJ) using Felix software (Photon Technology International). Background fluorescence, determined by incubating tissues in 4 mM $MnCl_2$ plus 20 μM ionomycin, was subtracted before calculating the fluorescence ratios. Tension data obtained was normalized to the steady-state tension achieved at 1.0 L_0 in the presence of 1 μM phentolamine while calcium data normalized to the corresponding steady-state calcium signals.

2.4 Tissue Permeabilization

Following L_0 determination, femoral artery rings were washed in a calcium-free "relaxing solution" (RS) comprised of 74.1 mM potassium methanesulfonate, 4.0 mM magnesium methanesulfonate, 4.0 mM Na_2ATP, 4.0 mM EGTA, 5.0 mM creatine phosphate, 30.0 mM PIPES adjusted to pH 7.1 with 1N KOH and ionic strength 0.18 with

additional 0.5 M potassium methanesulfonate. Tissues were chemically permeabilized with 100 μM β-escin for 45 min at 4˚C then 15 min at 30˚C. Treatment with β-escin at low temperature has been shown to slow penetration and/or binding of β-escin to the surface of smooth muscle membrane [56]. Following permeabilization, artery rings were washed with RS and incubated for 20 min at 30˚C in RS containing 10 μM A23187, a Ca^{2+} ionophore that will deplete the sarcoplasmic reticulum Ca^{2+}. Tissues were then activated with a "contracting solution" (CS) that contained 1M $CaCl_2$ stock added to RS in amounts as determined by WEBMAXC [72] for a final pCa 6.0 and pH of 7.1. Tissues at L_0 were contracted in the presence of 1 μM phentolamine for 10 min prior to the start of the protocol. All experimental data was then normalized to the steady-state tension achieved with this contraction. After each contraction during an experimental protocol, tissues were washed with mixture of RS and 10 μM A23187.

2.5 Western Blot

Phosphorylation of MLC_{20} was measured by Western blot analysis of artery ring homogenates. In brief, artery rings at $0.75L_0$ or $1.25L_0$ and at basal or steady-state contraction were quick-frozen in an acetone-dry ice slurry, thawed to room temperature in an acetone mixture with 6% trichloroacetic acid, 10 mM dithiothreitol (DTT) and 30 mM NaF, homogenized in a buffer containing 1% SDS, 10% glycerol, 20 mM DTT, 25 mM Tris·HCl (pH 6.8), 5 mM EGTA, 1 mM EDTA, 50 mM NaF, 1 mM sodium orthovanadate, 20 μg/ml leupeptin, 20 μg/ml aprotinin, and 20 μg/ml (4-amidino-phenyl)-methane-sulfonyl fluoride, heated, clarified by centrifugation, and stored at -20º C or immediately

assayed for protein concentration. Proteins were separated by electrophoresis followed by Western blotting. MLC_{20} was identified using p-Ser19-anti-MLC_{20} rabbit polyclonal antibody and anti-MLC_{20} mouse monoclonal antibody (Sigma; St. Louis, MO) was assessed to quantify loading accuracy.

2.6 Protocol for Full L-T Curve

Following equilibration, rather than an abbreviated length-tension curve to determine L_0, tissues were subjected to a full L-T curve protocol. Tissues were preconditioned with a series of 10 1-g stretches maintained for 3 min each before release to slack length, L_s. Tissues then underwent a series of three contractions at L_s with 5 min of relaxation in PSS between each. Next, tissues were taken through a series of length changes, with the number, relative step size and duration as indicated in Figure 2.2. After a 3 min period to allow for equilibration following length change, tissues were contracted for 7 min and relaxed for 5 min before the next length change. Note the smaller length steps at the top of the L-T curve in an effort to identify L_0 as accurately as possible. After T_a was obtained at each length for loading (LD) and unloading (ULD), tissues were washed and incubated in a calcium-free solution for 10 min. Tissues were then taken through the same length steps LD and ULD as before and the T_p determined at each length. To allow for stress relaxation with increasing lengths and to ensure that a true T_p was measured, tissues were stretched to 0.05 mm above the desired length and allowed to stress-relax for 1 min prior to release to the desired length where tissue was maintained for 2 min before next length change. As stress relaxation is not a concern with decreases in length, tissues were released directly to

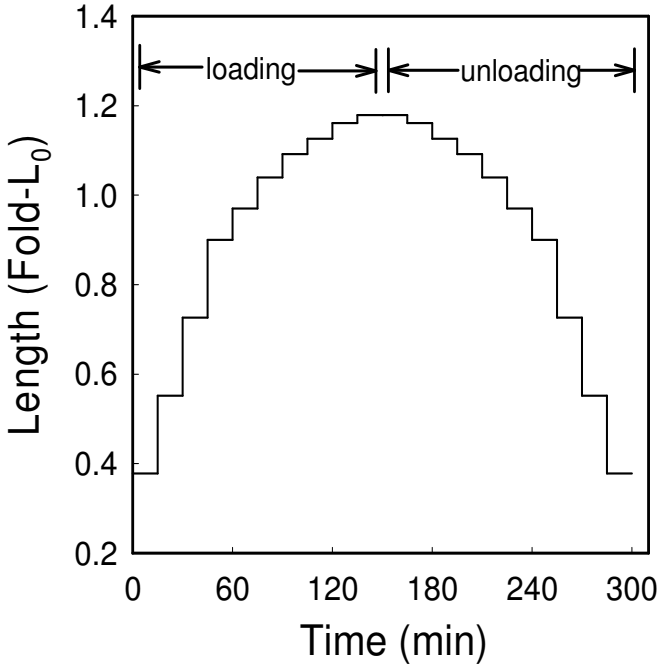

FIGURE 2.2: Diagram of Full L-T Curve Protocol
Illustration of the full L-T curve protocol length-steps. The protocol included 3 min to equilibrate to a new length, 7 min for muscle activation and 5 min for relaxation prior to change to a different length. The number, duration and relative length of each step is shown. Note that loading (LD) refers to increasing length steps while unloading (ULD) refers to decreasing length steps.

the desired length when descending the L-T curve. The steady-state T_p measurements at each length obtained during LD, or ULD, were subtracted from the total tension measurements obtained at the same length during LD, or ULD, to determine T_a. The phasic and tonic T_a values and steady-state T_p values were obtained for each step and normalized to maximal phasic T_a achieved upon LD.

A similar protocol was used to study the length-history dependence of T_p with the following modifications. Following determination of L_0 through an abbreviated L-T curve, two contractions at L_0 were completed followed by 2 contractions at slack length (L_s). Next, in a set of two tissues, one tissue was pre-conditioned to maximal length of 1.42-fold L_0 while the other was not. Tissues were then taken through two series of LD and ULD at lengths 0.8-fold L_0, L_0, 1.2-fold L_0 and 1.4-fold L_0 (Figure 2.3). To account for stress relaxation during LD, tissues were stretched 2% above the desired length for 2 min prior to release to desired length. T_p at L_0 and one shorter and one longer length were then compared. Only one measurement was obtained at 1.4-fold L_0, thus there was no comparison for LD and ULD available. Tissues were then contracted at L_s and L_0 to ensure viability following the series of stretches. All tissues were found to be viable at the end of the protocol (data not shown).

2.7 Protocol for L-Adaptation at a Shortened Length

Following determination of L_0 through an abbreviated L-T curve and a normalization contraction at L_0 in the presence of 1 μM phentolamine (T_0), tissues were maintained either at control length L_0 or released to a shortened length 0.8-fold L_0 for 5 min. Tissues then

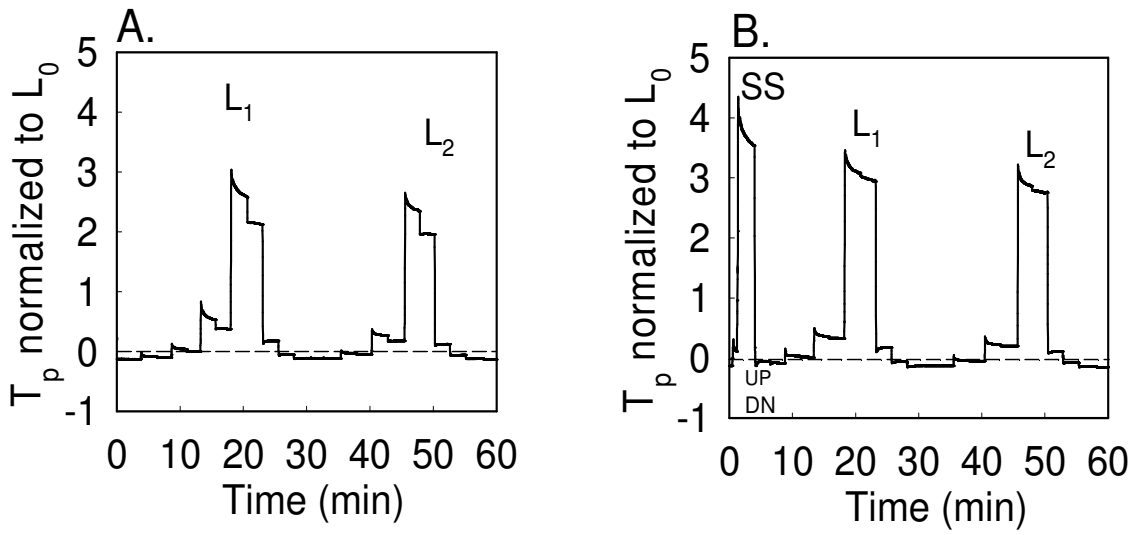

FIGURE 2.3: Representative Tension Tracing for Length-History Dependent T_p Protocol

Representative time versus tension tracing, normalized to L_0, for investigation of length-history dependency of T_p. In Panel A, tissues were taken through two series (L1 and L2) of length steps of 0.8-fold L_0, L_0, 1.2-fold L_0, and 1.4-fold L_0 during LD followed by ULD (T_p at longest length only obtained once). In Panel B, tissues were first strain-softened (SS) to length 1.42-fold L_0 prior to the series of length steps.

underwent a series of three K^+-induced contractions at constant length, each of which was 10 min in duration followed by at least 15 min of relaxation in PSS (Figure 2.4). Phasic measurements were obtained ~20 sec after activation while tonic measurements were obtained 10 min after activation. This protocol was modified to include a stretch to 1.2 L_0 or a contraction at the stretched length of 1.2 L_0 between contractions 1 (T_1) and contraction 2 (T_2) when investigating the role of intracellular structures on adaptation (Figure 2.5). For studies involving the β-escin permeabilized tissue, this protocol was again used with the T_a values obtained at steady-state.

2.8 Protocol for Drug Studies

Following determination of L_0 through the abbreviated L-T curve protocol and a normalization contraction at L_0 in the presence of 1 μM phentolamine, all tissues underwent a second 10 min contraction followed by 15 min relaxation prior to the introduction of drug. Tissues were then incubated with vehicle, 2 μM latrunculin B (binds G-actin monomers), 0.2 μM cytochalasin D (caps the (+) end of F-actin), 0.3 μM H-1152 (ROCK inhibitor) or 10 nM nifedipine (blocks L-type Ca^{2+} channels) for 15-30 min. The vehicle/drug was then present in all subsequent buffer changes for the remainder of the experiment. Following two contractions at L_0, two tissues were incubated in vehicle while two other tissues were incubated in drug. Following another two contractions, one tissue in vehicle and one tissue in drug were released to a shortened length 0.8-fold L_0 while the other two remained at L_0. All tissues then underwent a series of three contractions to

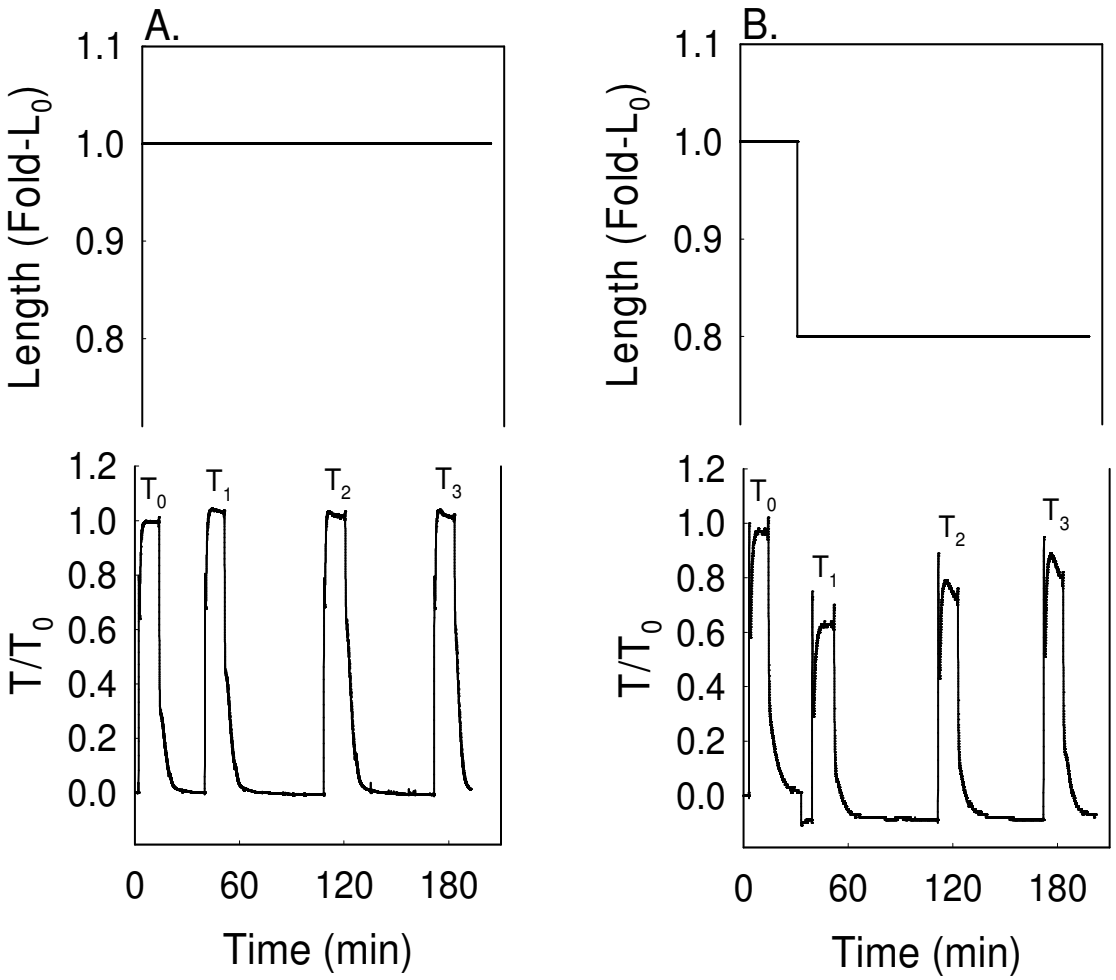

FIGURE 2.4: Representative Tension Tracing for L-adaptation at a Shortened Length

Length changes and representative time versus tension tracings for investigation of adaptation at a shortened length. Panel A indicates that the length was held constant at L_0 over the course of 4 contractions, with T_0 as a reference contraction to which data was later normalized. Panel B indicates that following T_0, length was decreased to 0.8-fold L_0 for 3 contractions.

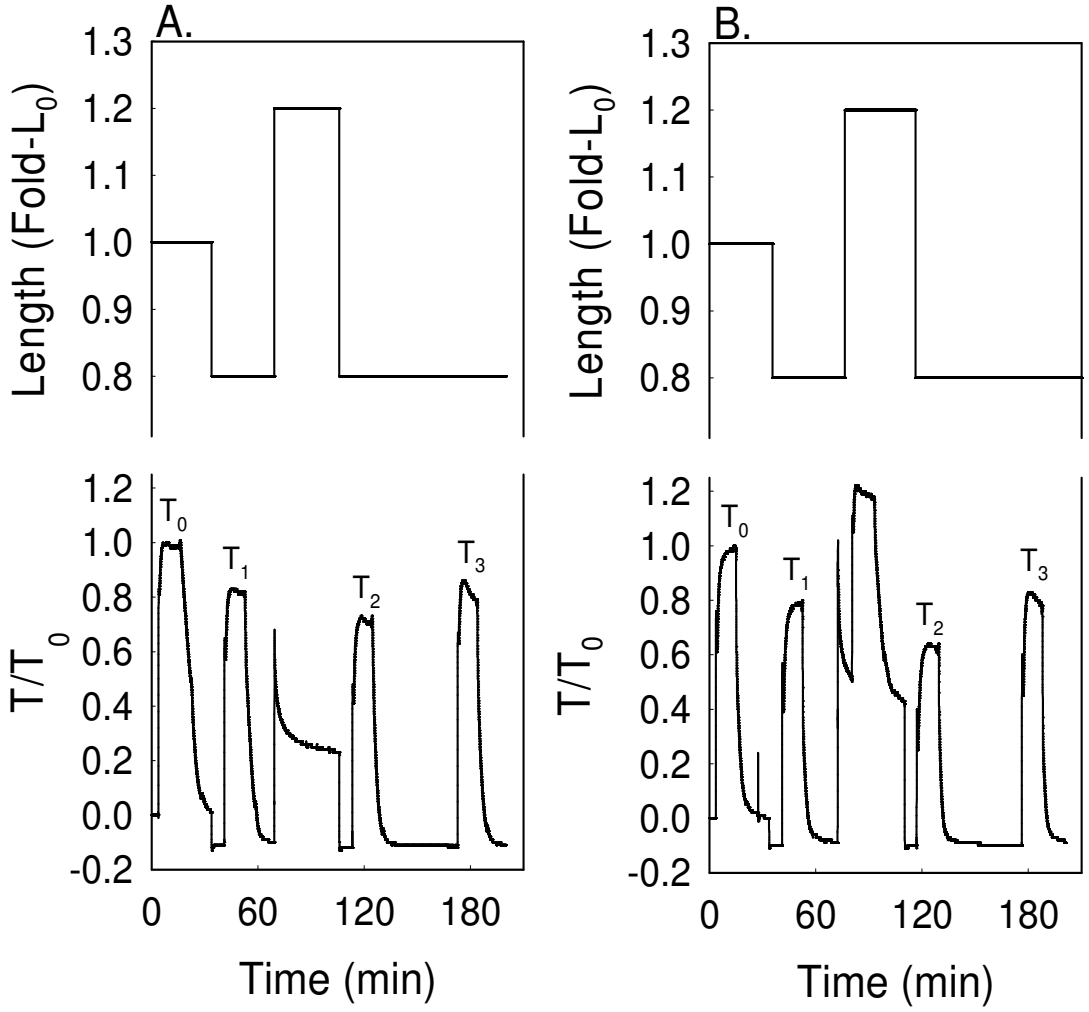

FIGURE 2.5: Representative Tension Tracing for Interruption of L-adaptation at a Shortened Length

Length changes and representative time versus tension tracings for investigation of interruption of adaptation at a shortened length. Panel A indicates that all contractions were completed at a shortened length 0.8-fold L_0 with a stretch to 1.2-fold L_0 between T_1 and T_2. Panel B indicates that for some studies, the tissue was additionally contracted at the stretched length of 1.2 –fold L_0. T_0 is a reference contraction to which data was later normalized.

investigate the effect of the vehicle versus drug with repeated contraction at a shortened length (Figure 2.6).

2.9 Drugs

Phentolamine, β-escin and nifedipine were from Sigma, St. Louis, MO. A23187 was from Fisher Scientific, Fair Lawn, NJ. Ionomycin was from LC Laboratories, Woburn, MA. Fura-2-PE3 (acetoxymethyl ester) and Pluronic F-127 were from TEF Labs, Austin, TX. Latrunculin B, cytochalasin D, H-1152, KN-92 and KN-93 were from Calbiochem, La Jolla, CA. β-escin was dissolved in RS. Nifedipine and ionomycin was dissolved in ethanol. A23187, latrunculin B, cytochalasin D and KN-92 were dissolved in dimethyl sulfoxide (DMSO) and all other compounds were dissolved in deionized water. Ethanol and DMSO were added at a final concentration no greater than 0.1%.

2.10 Statistical Analysis

Statistics were completed using either Microsoft Excel 2003 or Prism 3.0 (GraphPad Software, San Diego, CA). The null hypothesis was examined using Student's *t* test (when two groups were compared) or using a one-way ANOVA (when more than two groups were compared). To determine differences between groups after ANOVA, the Student-Newman-Keuls post hoc test was used. An exception was the Dunnett's multiple comparison test used to determine differences between T_a pre-drug to T_a post drug in the presence of inhibitors of actin polymerization. In all cases, the null hypothesis was rejected at $p < .05$. For each study described, the *n* value was equal to the number of rabbits used in the study.

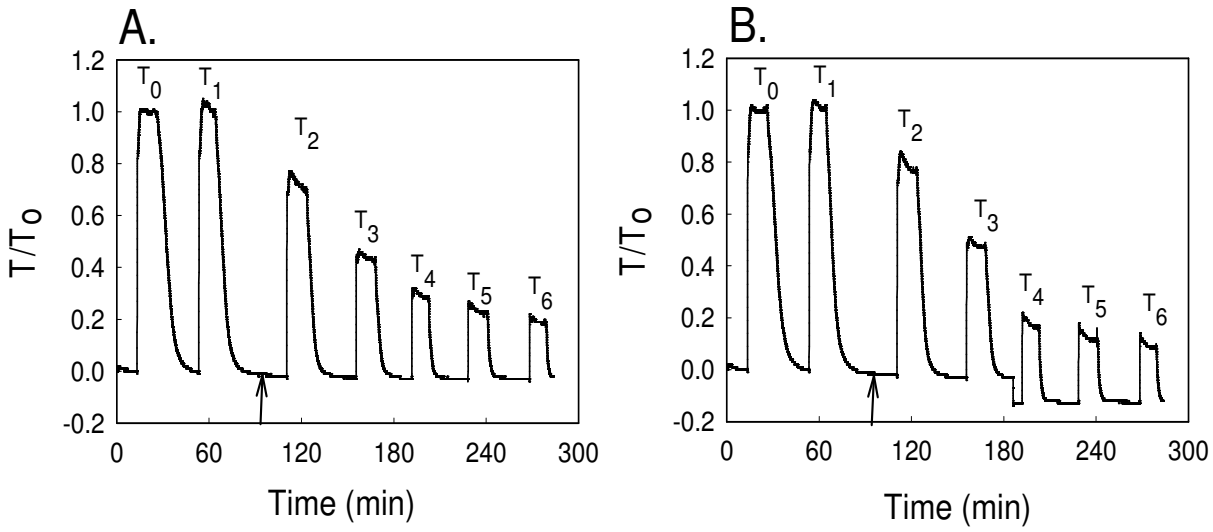

FIGURE 2.6: Representative Tension Tracing for the Effect of Drugs on L-adaptation at a Shortened length

Representative time versus tension tracings for investigation of drugs on adaptation at a shortened length. Panel A indicates that the length was held constant at L_0 over 2 contractions prior to introduction of vehicle/drug, indicated with the arrow. Remaining contractions at L_0 were conducted in the presence of vehicle/drug. Panel B indicates that following T_3, tissue was shortened to 0.8-fold L_0 for a series of 3 contractions (T_4-T_6). Thus, the effect of length on VSM contraction in the presence of vehicle/drug was investigated.

CHAPTER 3

Results

3.1 Full L-T Curve

With differing thoughts on the static versus dynamic nature of the L-T curve in VSM, it was necessary to determine the T_a and T_p over a 3-fold length change in rabbit femoral artery preparation used for these studies. With an interest in the ascending limb and plateau of the L-T curve, and referencing previous work that estimated these lengths, the muscle lengths studied ranged from 0.38-fold L_0 to 1.18 fold L_0. T_p increased with length, with steeper increases evident beyond length L_0 (Figure 3.1A). Beginning at shorter lengths, tissues generated increasing amounts of phasic and tonic T_a up to length L_0. Beyond L_0, tension began to decrease. Although present in both phasic and tonic T_a curves, a broad plateau was most evident in phasic T_a from 0.97-fold L_0 to 1.09-fold L_0.

When taken at the same length, two different T_p, phasic T_a and tonic T_a curves were evident dependent on whether the tissue was being LD or ULD (Figure 3.1A and B). Loading occurred when tissues were stretched to a longer length followed by equilibration, activation, relaxation and stretch to a new longer length. Unloading occurred when tissues were released to a shorter length, allowed to equilibrate, activated, and relaxed followed by

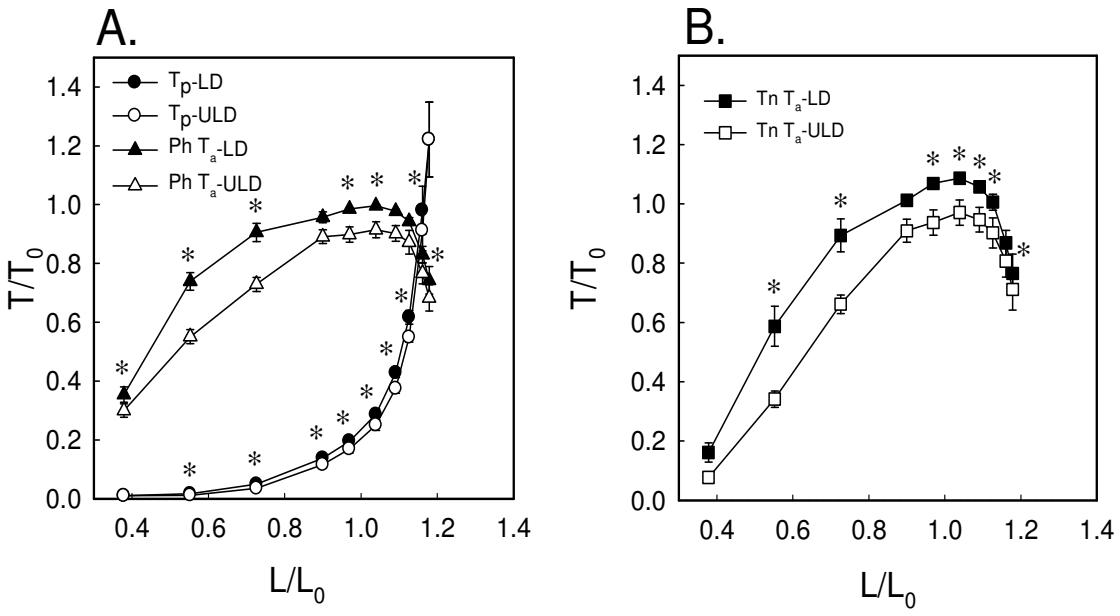

FIGURE 3.1: Phasic and Tonic L-T Curves
Length versus tension over 3-fold length change in rabbit femoral artery. Panel A illustrates the two curves obtained for phasic T_a and for T_p while Panel B illustrates the two curves obtained for tonic T_a. Curves obtained either during either loading (LD) or unloading ULD). ∗ indicates $p < .05$ LD versus ULD. n=4.

release to a new shorter length. Differences between LD and ULD curves for all tensions measured were significant at most lengths. Thus it appears that length- history, stretch versus release, affects both T_p and T_a in rabbit femoral artery.

Phasic versus tonic T_a were further investigated at each length. At short lengths, phasic T_a is greater than tonic T_a, while at lengths approaching L_0, tonic T_a is greater than phasic T_a. Thus, there is a crossover in the strength of phasic T_a and tonic T_a on the ascending limb of the L-T_a curve (Figure 3.2A). When tissue is LD, this crossover occurs at 0.73-fold L_0 while it occurs at 0.90 -fold L_0 when ULD (data not shown). This relationship is further illustrated in Figure 3.2B as a rapid decrease in phasic T_a relative to tonic T_a as lengths approach L_0.

In conclusion, these data suggested that the phases of a rabbit femoral artery contraction are differentially affected by muscle length. Additionally, length-history may play a role as the crossover in the strength of the phases occurred at different lengths dependent on LD versus ULD.

3.2 Length-History Dependency of T_p

The length-history dependency of T_p was further investigated in a separate set of experiments. Tissues were either strain-softened (SS; Figure 3.3B) to the maximal length for the protocol (1.42-fold L_0) or were not SS (Figure 3.3A). Tissues were then LD and ULD through two series of length-steps, Loop 1 (L_1) and Loop 2 (L_2). Lengths investigated were 0.8-fold L_0, 1.0-fold L_0 and 1.2-fold L_0. Tissues were allowed to

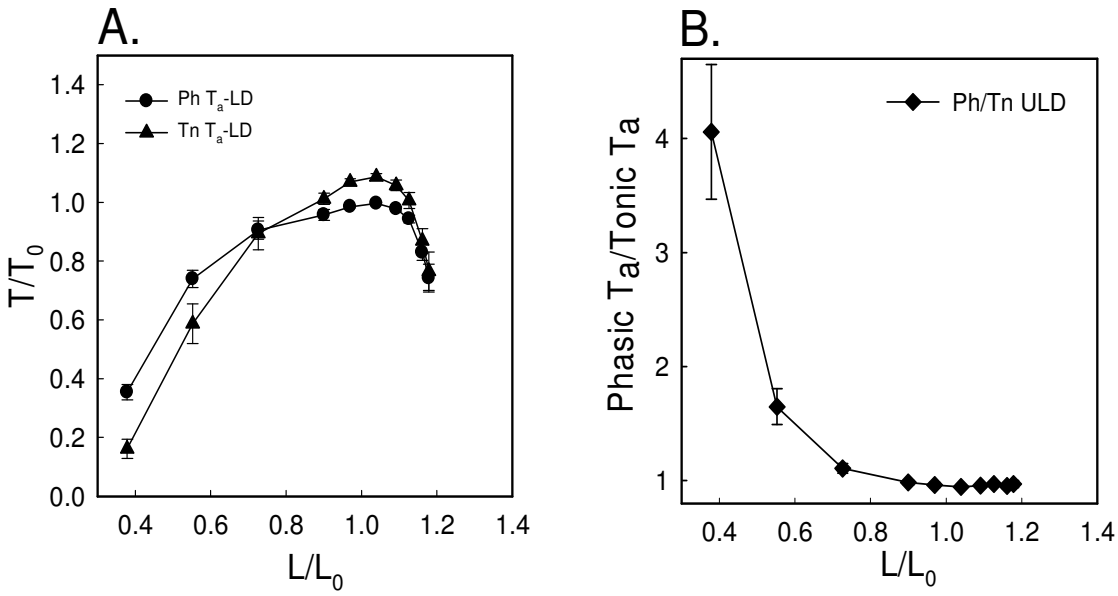

FIGURE 3.2: Effect of Length on Phasic T_a and Tonic T_a
Length versus tension over 3-fold length change in rabbit femoral artery. Panel A illustrates the crossover in T_a such that tonic T_a exceeds phasic T_a at lengths greater than 0.73-fold L_0 during LD. Panel B further illustrates the sensitivity to length evident with a rapid decrease in phasic T_a relative to tonic T_a at lengths approaching L_0. n=4.

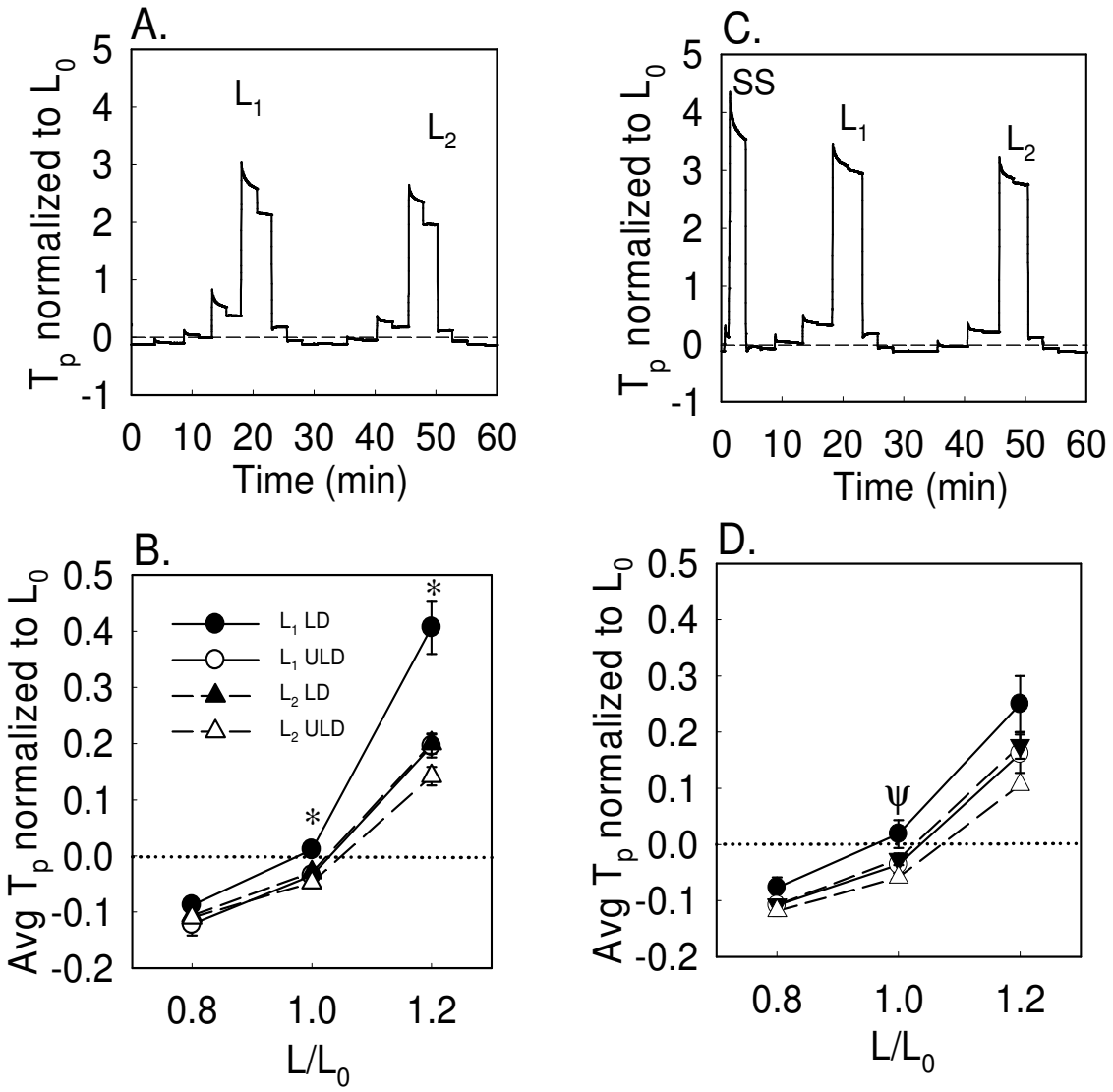

FIGURE 3.3: Effect of Length-History on T_p
Panels A and C illustrate representative time versus tension tracings for T_p measured at three different length steps with (Panel C) and without (Panel A) strain-softening (SS). All data normalized to L_0. T_p at L_0 and 1.2-fold L_0 was significantly higher during L_1 LD in tissues that were not SS (Panel B). T_p was significantly higher at L_0 during L_1 LD versus L_2 ULD in tissues that were SS. * and ψ indicate $p< .05$ for above comparisons. n=5.

equilibrate at each length before measurement of T_p. In tissues that were not SS, the T_p obtained during L_1 LD was significantly higher at L_0 and 1.2-fold L_0 when compared to the same lengths of L_1 ULD, L_2 LD and L_2 ULD. In tissues that were SS prior to L_1, the only significant difference was found between L_1 LD and L_2 ULD at length 1.0-fold L_0. Additionally, the T_p obtained at 1.2-fold L_0 in the tissue with no SS was significantly higher compared to the T_p obtained during L_1 LD in SS-tissues.

Thus, T_p of rabbit femoral artery is dependent on length-history at lengths L_0 and longer. For lengths below L_0, prior length-history does not appear to affect T_p. Also, for tissues measured at long lengths, the presence of SS will result in a significant decrease in T_p upon first LD as compared to tissues that were not SS.

3.3 Effect of Repeated Contraction on T_a

Inherent in the full L-T protocol is a series of repeated contractions, each at a different length. With a focus on the ascending limb of the L-T curve, the effect of repeated contraction at a single, shortened length 0.8-fold L_0 on phasic and tonic T_a was assessed. Additionally, the 3 min time point was assessed in an attempt to elucidate the transition from phasic T_a at approximately 10-20 seconds to tonic T_a at approximately 5 min. An example time versus tension tracing for 5 repeated contractions is shown in Figure 3.4A with the average phasic, 3 min and tonic T_a achieved in Figure 3.4B. Phasic and tonic T_a did increase with repeated contraction, with the greatest increase between T_1 and T_2 followed by T_2 to T_3. Relative to T_1, there was no significant increase in phasic or tonic T_a at T_5 versus T_3 (Figure 3.4C). The T_a at 3 min was also increased with repeated

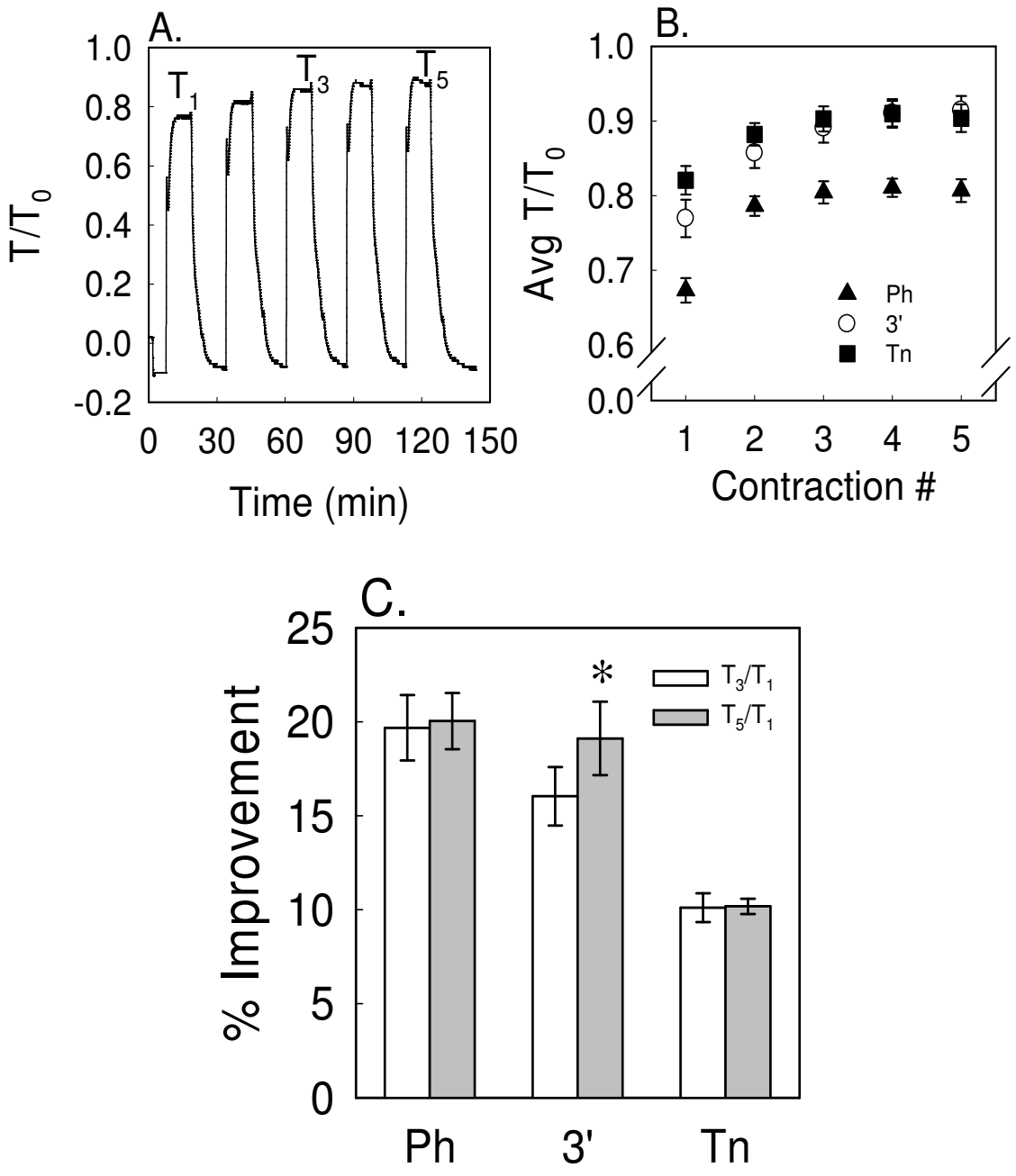

FIGURE 3.4: Effect of Repeated Contraction at a Shortened Length
Panel A shows a representative time versus tension tracing for a series of five repeated contractions at a shortened length 0.8-fold L_0. Panel B illustrates the average increase in phasic, 3 min, and tonic T_a over the series of five contractions. Panel C shows that there is only significant improvement in the 3 min time point beyond T_3. * indicates $p < .05$ for T_3/T_1 versus $T_5/_1$. n=7.

contraction, however, a significant increase relative to T_1 was found between T_3 and T_5 ($p<.05$).

Thus, three contractions appeared appropriate to study L-adaptation of phasic and tonic T_a. Additionally, these data suggested that either the activation process or the additional time necessary for additional contractions will result in higher T_a at the 3 min time point.

3.4 Effect of Time and Duration of Contraction on T_a

Due to the lengthy nature of the full L-T protocol, the effect of time on T_a development was considered. The phasic, 3 min, and tonic T_a developed in a tissue at a shortened length 0.8-fold L_0 at time zero was compared to the same time points in a second tissue that was activated 100 min later (T_1-delay; Figure 3.5A). Only the 3 min time point was found to be significantly ($p<.05$) improved in the delayed contraction (Figure 3.5B). Therefore, it appeared that time alone will improve the T_a achieved at the transitional 3 min time point in a rabbit femoral artery contraction.

In the full L-T curve protocol, the duration of the contraction at each length step was 7 min. The effect of a longer duration of a K^+-induced contraction was thus investigated. Tissues that remained activated for greater than 10 min demonstrated an additional rise in T_a beyond that achieved during the tonic phase. This second rise achieved a maximum (MAX) in an average of 34 min. When compared to the phasic, 3 min and tonic T_a achieved during the third of three repeated contractions, where L-adaptation

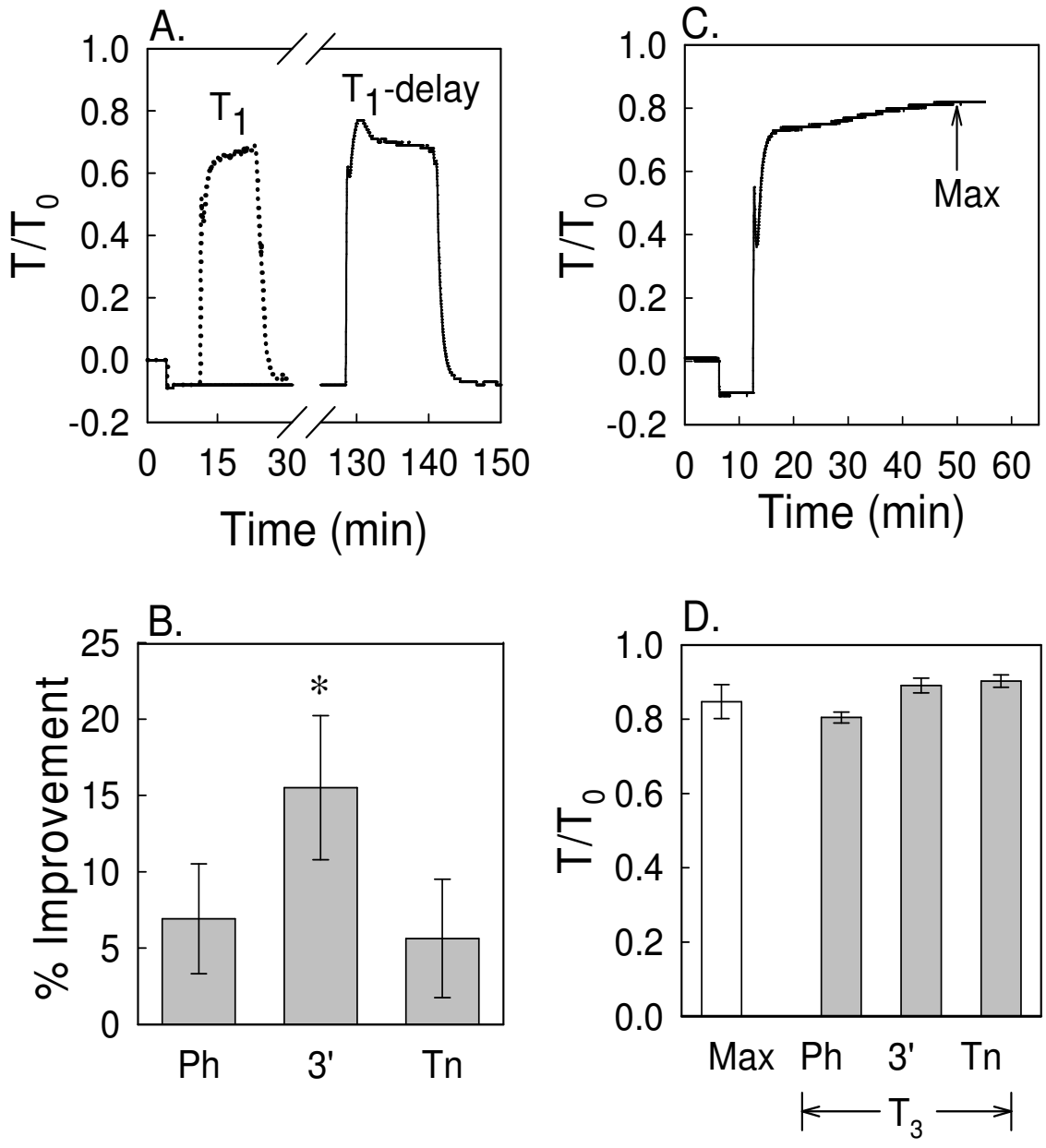
A.
1.0
0.8
0.6
0.4
0.2
0.0
-0.2
T/T0
T1
T1-delay
0
15
30
130
140
150
Time (min)
C.
1.0
0.8
0.6
0.4
0.2
0.0
-0.2
T/T0
Max
0
10
20
30
40
50
60
Time (min)
B.
25
20
15
10
5
0
% Improvement
*
Ph
3'
Tn
D.
1.0
0.8
0.6
0.4
0.2
0.0
T/T0
Max
Ph
3'
Tn
T3

FIGURE 3.5 (on previous page): Effect of Delayed and Sustained Contraction at Shortened Length

Panel A shows a representative time versus tension tracing for a contraction 100 min after (T_1-delay) a reference contraction (T_1). Panel B shows that only the 3 min time point was significantly improved ($p < .05$) in the T_1-delay contraction relative to T_1. Panel C shows a representative time versus tension tracing for a sustained contraction, noting an additional increase in tension beyond tonic, indicated by Max. Max T_a occurs at an average of 34 min after activation. Panel D indicates that the T_a achieved at Max of a sustained contraction is not different from the T_a achieved during any phase of the third of 3 repeated contractions (T_3). n=7.

appears complete, there were no differences (Figure 3.5D). Thus the same amount of T_a in rabbit femoral artery can be achieved through either a sustained contraction of at least 34 min or a minimum of three repeated contractions.

Based on the above results, the 3 min time point was concluded to be an additional phase of contraction that significantly increased with time alone. This time point did not, however, provide additional information related to the phasic and tonic components of contraction and was thus not used in further analyses.

3.5 L-adaptation of T_a at a Shortened Length

With three consecutive contractions of less than 34 min duration established as appropriate to study the phasic and tonic phases of a rabbit femoral artery contraction, L-adaptation at a shortened length was further investigated.

First, the phasic and tonic T_a achieved with repeated contraction at length L_0 were investigated. No significant increase in either phase of T_2 or T_3, relative to T_1 was found (Figure 3.6A, Figure 3.6C and Figure 3.6D). Next, the phasic and tonic T_a achieved with repeated contraction at a shortened length 0.8-fold L_0 were studied. Relative to T_1, both phases were significantly greater during T_2 and T_3 (Figure 3.6B, Figure 3.6C and Figure 3.6D).

With L-adaptation defined as the increase in tension with repeated contraction, it was important to quantify the amount of increased T_a by the third repeated contraction at a shortened length. Relative to L_0, the phasic T_a at 0.8-fold L_0 increased an average of

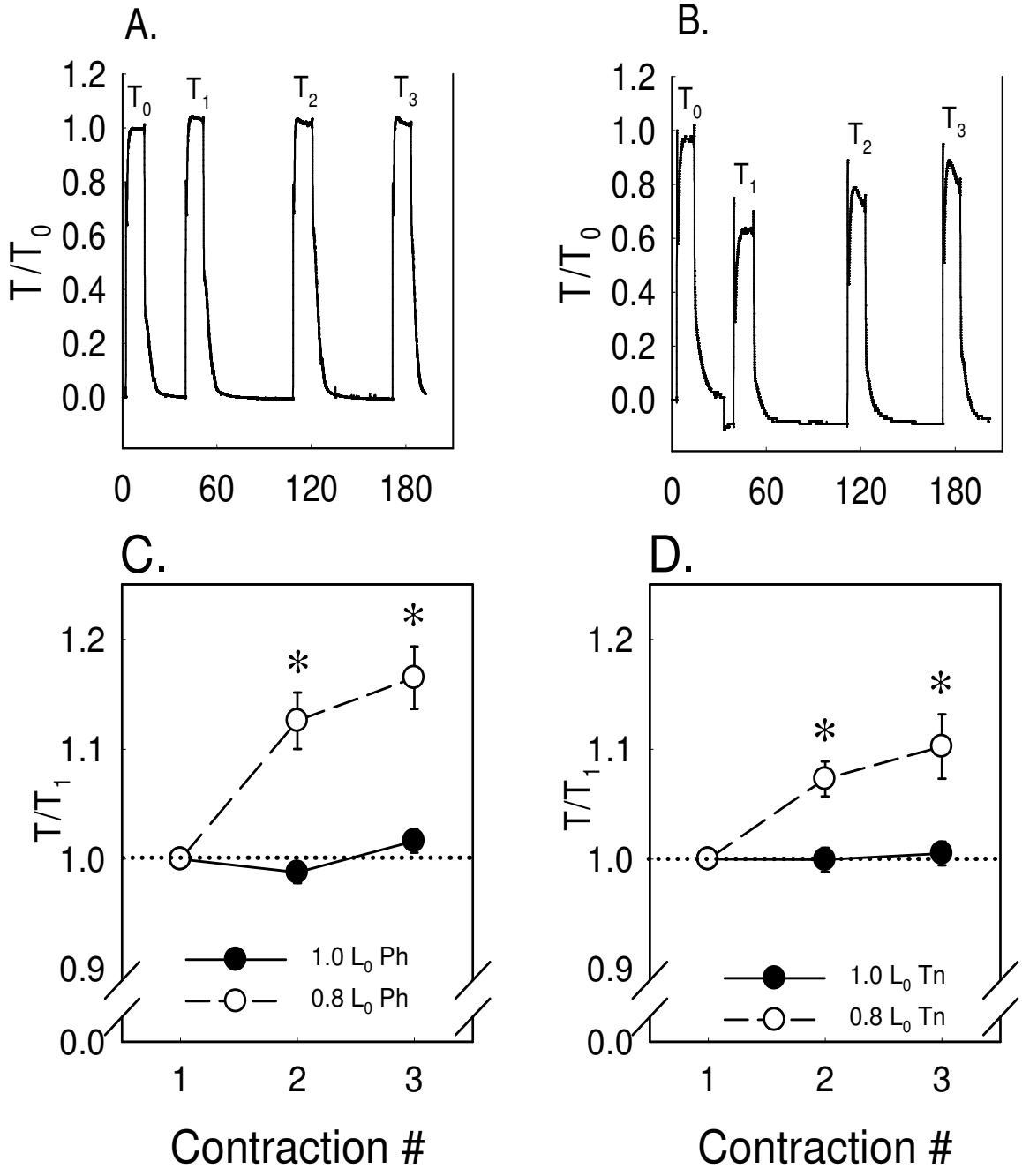
A.
B.
C.
D.
T/T0
T/T1
T0
T1
T2
T3
1.2
1.0
0.8
0.6
0.4
0.2
0.0
0
60
120
180
1.1
0.9
1
2
3
*
1.0 L0 Ph
0.8 L0 Ph
1.0 L0 Tn
0.8 L0 Tn
Contraction #

FIGURE 3.6 (on previous page): Effect of L-adaptation at a Shortened Length on Phasic T_a and Tonic T_a

Panels A and B are representative time versus tension tracings for repeated contraction at L_0 and 0.8-fold L_0, respectively. In Panel C, the average phasic T_a, relative to T_1, achieved over two subsequent contractions is shown for length 1.0-fold L_0 and 0.8-fold L_0. In Panel D, the average tonic T_a, relative to T_1, achieved over two subsequent contractions is shown for each length. * indicates $p < .05$ between lengths at either T_2 or T_3. n= 9-10.

14.72% (SEM = 3.19, n=9) while the tonic T_a increased 9.87% (SEM = 3.24, n=9). These increases in T_a were significant as shown in Figure 3.7.

In conclusion, L-adaptation does not occur at length L_0, but does occur at a shortened length of 0.8-fold L_0. Additionally, although there was a larger percent increase in L-adaptation in the phasic phase versus tonic phase, this difference was not statistically significant.

3.6 Role of $[Ca^{2+}]_i$ in L-adaptation of T_a at a Shortened Length

The results presented thus far indicate that while L-adaptation does not occur at length L_0, it does occur at shortened length 0.8-fold L_0. Thus having characterized L-adaptation in rabbit femoral artery, insight into a cellular mechanism was of interest. Based on the known mechanism of smooth muscle contraction (refer to Figure 1.1) and the role that Ca^{2+} plays in cell signaling, a role for $[Ca^{2+}]_i$ to mediate the increase in T_a with L-adaptation was investigated.

The $[Ca^{2+}]_i$ signal, as measured with the calcium indicator fura, was measured simultaneously with T_a during the L-adaptation protocol just described. Relative to T_1, a significant increase in phasic and tonic T_a was again seen at T_2 and T_3 (Figure 3.8C and Figure 3.8E). However, there were no significant differences in the simultaneous Ca^{2+} signal obtained during either phase of T_2 nor T_3 (Figure 3.8D and Figure 3.8F). It should be noted that in these set of experiments, relative to T_1, there was a decrease in phasic T_a at length L_0 at T_3 and an increase in phasic T_a at length 0.8-fold L_0. However, when taken

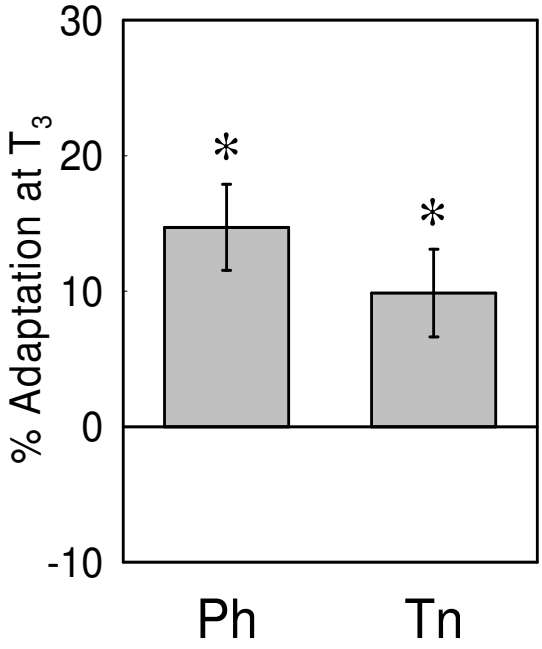

FIGURE 3.7: L-adaptation at a Shortened Length of the Phasic and Tonic Phase
Bar graph illustrating the increase in phasic and tonic T_a on the third repeated contraction at shortened length 0.8-fold L_0, thus L-adaptation. * indicates $p < .05$ versus 0. n= 9.

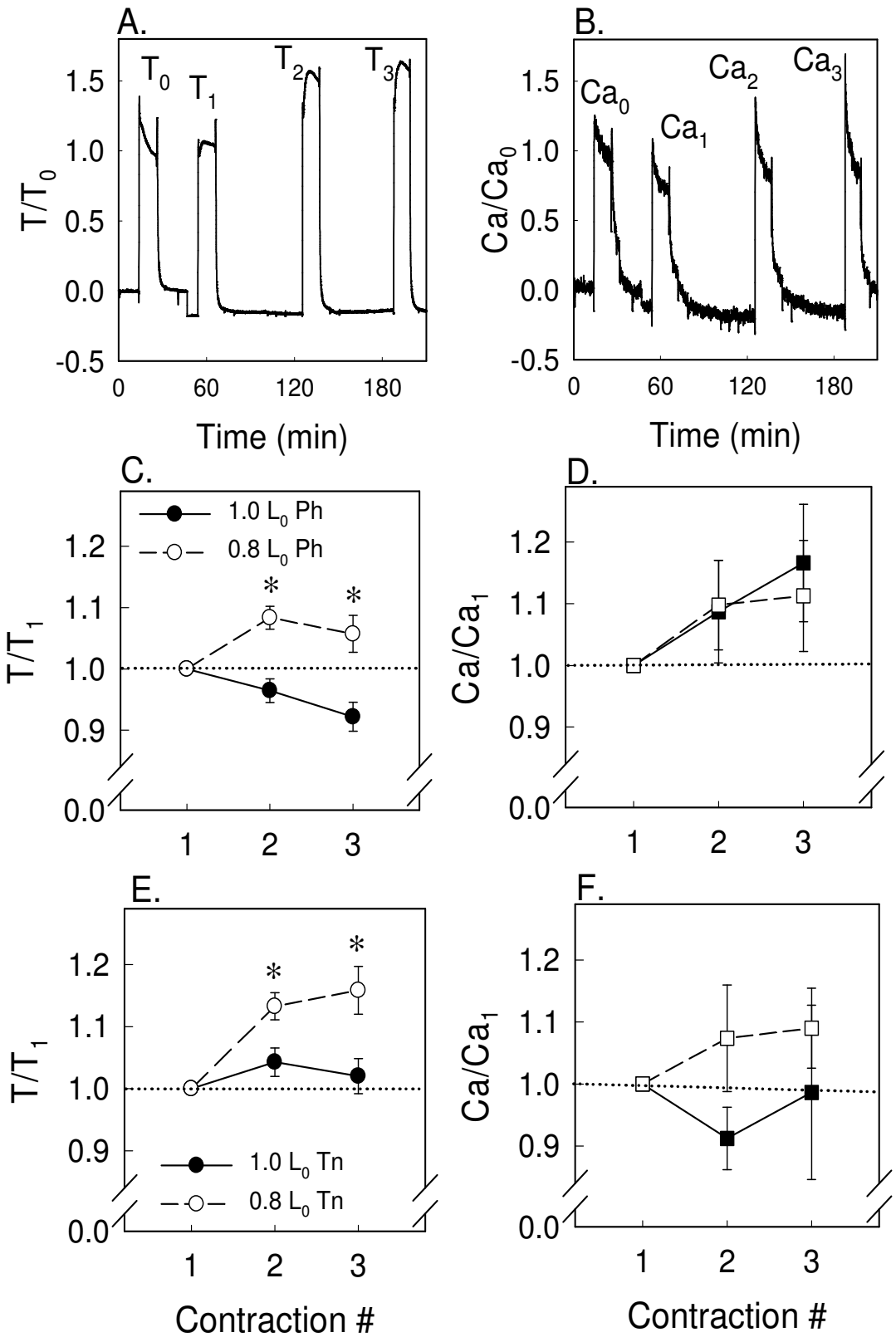
A.
T0
T1
T2
T3
T/T0
Time (min)
B.
Ca0
Ca1
Ca2
Ca3
Ca/Ca0
Time (min)
C.
1.0 L0 Ph
0.8 L0 Ph
T/T1
D.
Ca/Ca1
E.
1.0 L0 Tn
0.8 L0 Tn
T/T1
Contraction #
F.
Ca/Ca1
Contraction #

FIGURE 3.8 (on previous page): Effect of $[Ca^{2+}]_i$ on L-adaptation at a Shortened Length

Panel A is a representative time versus tension tracing that was obtained simultaneously with the $[Ca^{2+}]_i$ signal represented in Panel B. Panels C and E demonstrate phasic and tonic T_a L-adaptation as previously discussed. Panels D and F indicate no significant changes in the $[Ca^{2+}]_i$ signal for the phasic nor tonic components of contraction relative to T_1. * indicates $p < .05$ between lengths at either T_2 or T_3. n= 4.

together there was significant phasic L-adaptation at T_3. Despite a trend toward an increase, at no time point, during either phase, was the Ca^{2+} signal significantly different relative to T_1. Thus, the increase in T_a evident with repeated contraction does not appear to be mediated through an increase in $[Ca^{2+}]_i$, as measured at approximately 20 sec (phasic) and 10 min (tonic) into contraction.

3.7 Role of MLC_{20} Phosphorylation in L-adaptation of T_a at a Shortened Length

Phosphorylation of MLC_{20} is another important point of regulation in smooth muscle contraction and was thus investigated as a possible participant in L-adaptation. For the myosin phosphorylation studies, one modification was made to the L-adaptation protocol previously described. To capture any length-dependent differences in phosphorylation that may exist, the difference in the lengths compared were exaggerated. In the L-adaptation experiments previously described, length L_0 was used as a control. In the myosin phosphorylation experiments, all tissues were adapted to a longer length, 1.25-fold L_0, to serve as control. In the L-adaptation experiments previously described, 0.8-fold L_0 was used as a shortened length at which L-adaptation occurs. In the myosin phosphorylation experiments, tissues were released to shortened length 0.75-fold L_0. For both control and shortened lengths, tissues were then quick-frozen at one of the following four time points: (1) basal level prior to T_4, (2) steady state K^+-induced T_4 contraction, (3) basal level prior to T_6 or (4) steady state K^+-induced T_6 contraction (Figure 3.9A and B). Relative to T_4, there were no differences in basal levels of tension of T_6 at 0.75-fold L_0 as compared to 1.25-fold L_0. However, there was significantly more tension generated at the

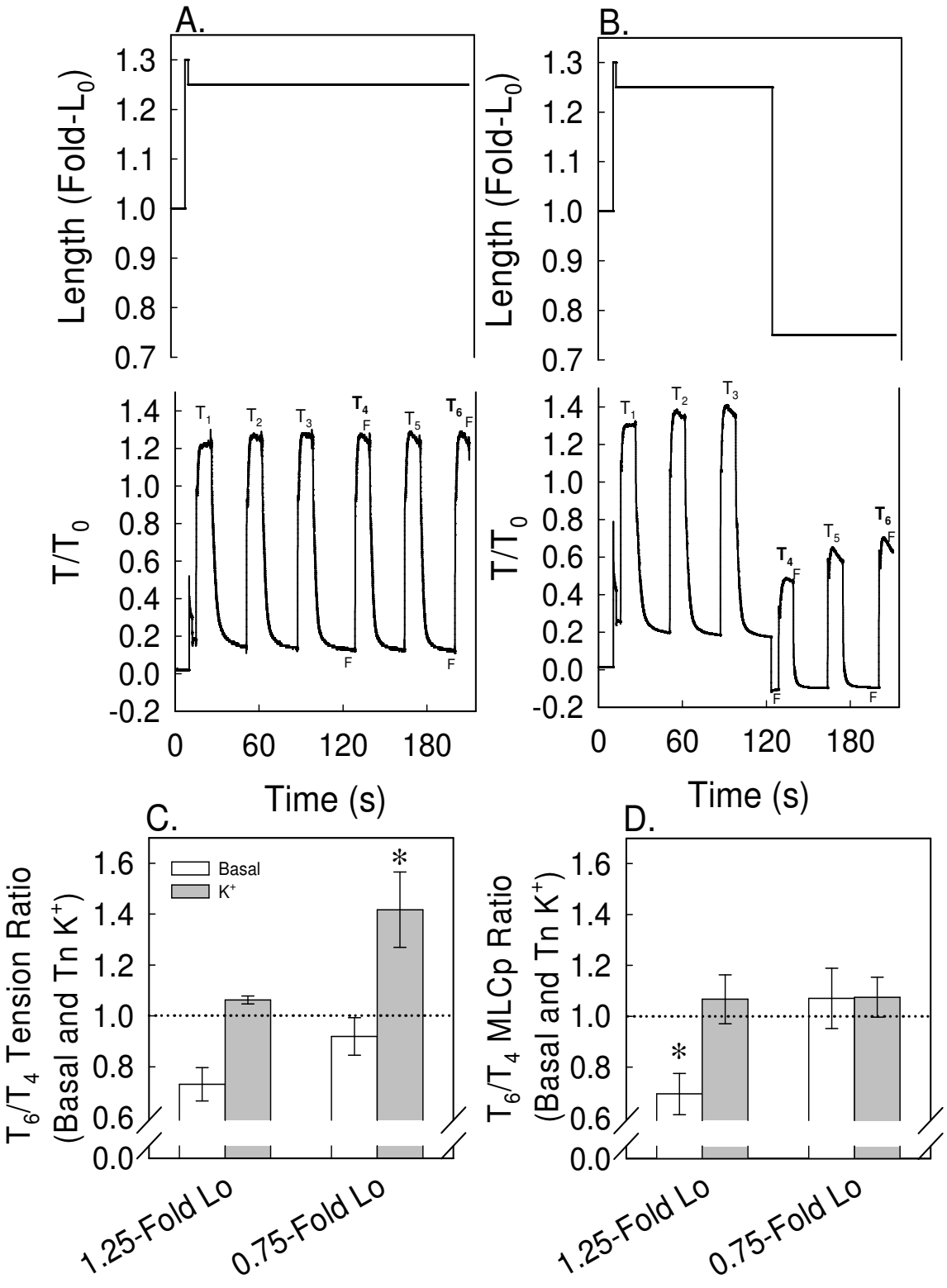
A.
B.
Length (Fold-L0)
T/T0
Time (s)
T1
T2
T3
T4
T5
T6
F
C.
D.
Basal
K+
T6/T4 Tension Ratio
(Basal and Tn K+)
T6/T4 MLCp Ratio
(Basal and Tn K+)
*
1.25-Fold Lo
0.75-Fold Lo

FIGURE 3.9 (on previous page): Effect of MLC_{20} Phosphorylation on L-adaptation at Shortened Length

The top portions of Panel A and Panel B illustrate protocol length changes while the bottom portions are representative time versus tension tracing for tissues adapted at 1.25-fold L_0 (A) and 0.75-fold L_0 (B). All tissues were first stretched to 1.30-fold L_0 to allow for stress relaxation before release and adaptation at 1.25-fold L_0. Panel C demonstrates the increase in T_a at shortened length 0.75-fold L_0 while Panel D illustrates no changes in MLC_{20} phosphorylation with K^+-activation. F indicates a time point at which a tissue was quick frozen. $*$ indicates $p < .05$ between lengths at either basal or during activation. n= 4.

shortened length, as compared to the control length, with K^+-activation (Figure 3.9C). Western blot analysis demonstrated a significantly lower amount of basal MLC_{20} phosphorylation at control length relative to shortened length, but no length-dependent differences upon K^+-activation (Figure 3.9D). Thus, an increase in MLC_{20} phosphorylation does not appear responsible for the increase in T_a generated with repeated contraction at a shortened length.

3.8 Effect of Inhibitors of Actin Polymerization on Contraction at L_0

As L-adaptation was not explained by an increase in $[Ca^{2+}]_i$ nor an increase in phosphorylated MLC_{20}, a role for regulation of actin thin filaments was investigated. Before the effect of inhibitors of actin polymerization could be assessed in a series of three repeated contractions at shortened length, their effect on a K^+-induced contraction at L_0 was assessed. Depending on the mechanism by which each drug prevents actin polymerization, differential effects on the phasic and tonic phase were evident.

Cytochalasin D inhibits actin polymerization by capping the (+) end of F-actin and thus prevents the addition of G-actin. When 0.2 μM cytochalasin D was added between two consecutive contractions at L_0, there was a significant decrease in both phasic and tonic T_a (Figure 3.10B). Following an additional 4 contractions, cytochalasin D further reduced the phasic and tonic T_a such that phasic and tonic phases produced nearly equivalent amounts of tension. When the data was analyzed as a percent inhibition of the pre-drug contraction, there was significantly more inhibition at T_6 versus T_2, and in the tonic component versus the phasic component (Figure 3.10C). Thus, through this indirect

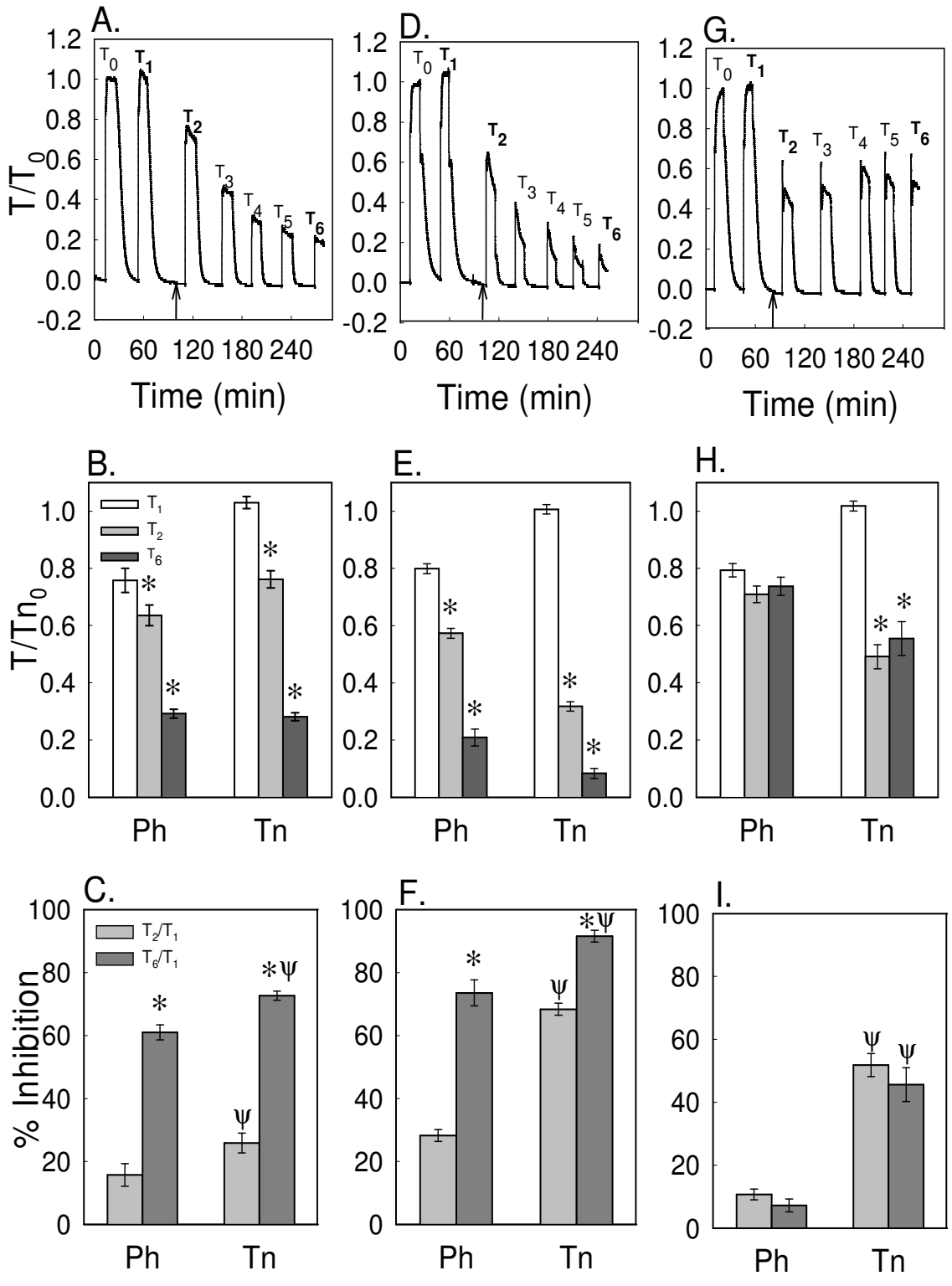
A.
D.
G.
T/T0
Time (min)
B.
E.
H.
T/Tn0
Ph
Tn
C.
F.
I.
% Inhibition
T2/T1
T6/T1

FIGURE 3.10 (on previous page): Effect of Inhibitors of Actin Polymerization on Contraction at L_0

Panels A, D and G illustrate representative time versus tension tracings for repeated contractions at L_0 in the presence of 0.2 μM cytochalasin D, 2 μM latrunculin B and 0.3 μM H-1152, respectively. The introduction of drug is indicated by the arrow. Panels B, E and H show the normalized tension prior to introduction of cytochalasin D, latrunculin B and H-1152, respectively, and then post-drug at T_2 and T_6 with * indicating $p < .05$ differences relative to T_1. Panels C, F and I illustrate the percent inhibition of phasic and tonic T_a relative to T_1 for cytochalasin D, latrunculin B and H-1152, respectively with * indicating $p < .05$ between T_2 and T_6 and ψ indicating $p < .05$ between phases. n= 5-6.

measure, an increase in F-actin appears to play a role in both the phasic and tonic components of contraction with a larger effect on the tonic phase.

Latrunculin B inhibits actin polymerization by binding 1:1 with free G-actin monomers. Similar to cytochalasin D, when 2 μM latrunculin B was added between two consecutive contractions at L_0, there was a significant decrease in both phasic and tonic T_a (Figure 3.10E). An additional 4 contractions in the presence of latrunculin B further reduced the phasic and tonic T_a, with a greater effect on the tonic phase. Compared to the pre-drug contraction, there was almost complete inhibition of the tonic phase after four contractions (Figure 3.10F). Thus, although cytochalasin D and latrunculin B significantly inhibit the tonic phase more than phasic phase, quantitatively, the effect appeared greater in the presence of latrunculin B. Thus, it appears that free G-actin monomers are necessary for both phases of VSM contraction, with the lack thereof more pronounced in the tonic phase.

Through ROCK, Rho is thought to stabilize cofilin and activate profilin, thus providing a stable actin cytoskeleton. H-1152 is an inhibitor of ROCK and thus has effects on the stability of the actin cytoskeleton. When 0.3 μM H-1152 was added between two consecutive contractions at L_0, there was a significant decrease in the tonic phase only (Figure 3.10H and I). Additionally, although the decrease in tonic T_a remained significant following four contractions as compared to pre-drug, there was no progressive inhibition of the tonic phase with repeated contraction (Figure 3.10I). Thus, it appears that Rho is important in only the tonic phase of contraction presumably through its effect on cofilin and profilin.

In conclusion, these studies demonstrate that actin polymerization is a necessary component of rabbit femoral artery contraction, with the effects more prominent in the tonic phase of contraction.

3.9 Role of $[Ca^{2+}]_i$ as Mediator of Inhibition of Actin Polymerization

In the presence of cytochalasin D and latrunculin B, a decrease in the phasic and tonic T_a generated by rabbit femoral artery was evident. The possibility that these agents inhibited contraction by blocking Ca^{2+} channels was considered. Thus a series of experiments were completed that investigated $[Ca^{2+}]_i$ in the presence of inhibitors of actin polymerization.

Using the same protocol illustrated in Panels A, D and G in Figure 3.10, simultaneous tension and $[Ca^{2+}]_i$ measurements were obtained. As previously shown, relative to pre-drug, there was a significant decrease in both phasic and tonic tension in the presence of 0.2 μM cytochalasin D (Figure 3.11A). This decrease did not appear to be due to a decrease in Ca^{2+} as phasic $[Ca^{2+}]_i$ remained the same as pre-drug and tonic $[Ca^{2+}]_i$ significantly increased (Figure 3.11B). The same trends were true in the presence of 2 μM latrunculin B. In the presence of decreased tension generation, phasic $[Ca^{2+}]_i$ was not changed and tonic $[Ca^{2+}]_i$ significantly increased (Figure 3.11C and D). Thus, a concurrent decrease in $[Ca^{2+}]_i$ did not appear responsible for the decrease in T_a evident when actin polymerization is inhibited. It is interesting to note that $[Ca^{2+}]_i$ during the tonic phase of the contraction significantly increased while the T_a has significantly decreased.

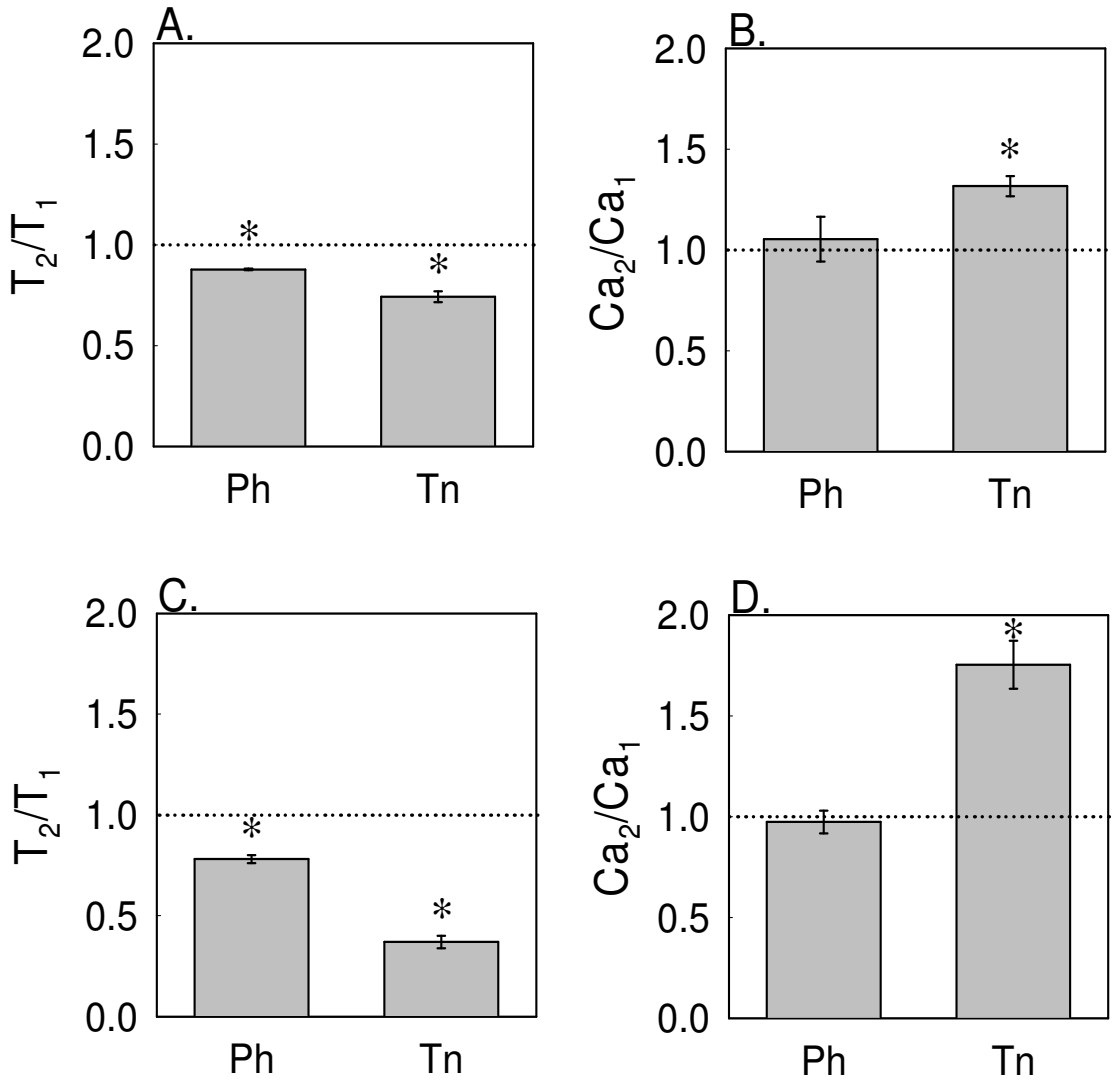

FIGURE 3.11: Effect of Inhibitors of Actin Polymerization on $[Ca^{2+}]_i$ on Contraction at L_0

Bar graphs illustrating significant decreases in phasic and tonic T_a in the presence of 0.2 uM cytochalasin D (Panel A) and 2 uM latrunculin B (Panel C). During simultaneous $[Ca^{2+}]_i$ measurements in the presence of each drug, phasic Ca^{2+} remained the same as pre-drug while tonic Ca^{2+} significantly increased. * = $p < .05$ relative to pre-drug. n=3.

3.10 Effect of Inhibitors of Actin Polymerization on L-adaptation of T_a at a Shortened Length

Having established the effect of actin polymerization on the development of phasic and tonic T_a in rabbit femoral artery maintained at L_0, it was of interest to investigate the role of actin polymerization on the L-adaptation of phasic and tonic T_a at a shortened length. The protocol utilized to investigate cytochalasin D, latrunculin B and vehicle control DMSO was previously presented in the Figure 2.6 of the Materials and Methods. The complex nature of the protocol and data analysis warrants further description before the results are presented.

Following introduction of the drug and two contractions at L_0, one tissue was maintained at length L_0 while a second tissue was released to shortened length 0.8-fold L_0 for three remaining contractions in the protocol (T_4, T_5, and T_6). Representative time versus tension tracings at lengths L_0 and 0.8-fold L_0, respectively, are shown for DMSO (Figure 3.12 Panel A and B), cytochalasin D (Figure 3.12 Panel C and D) and latrunculin B (Panel E and F). First, all phasic and tonic T_a achieved at T_6 were normalized to its own T_a achieved during T_4 to account for individual differences in tissues. Next, data at 0.8-fold L_0 was normalized to data at L_0 to account for the effect of the drug on contractions at L_0. The increase in force above 1, indicating no difference in generation of T_a between T_4 and T_6, was converted to a percentage and interpreted as the amount of L-adaptation the tissue displayed.

For ease of comparison, the L-adaptation that tissue displays in the absence of drug illustrated in Figure 3.7 is shown again in Panel A of Figure 3.13. Both phases of a

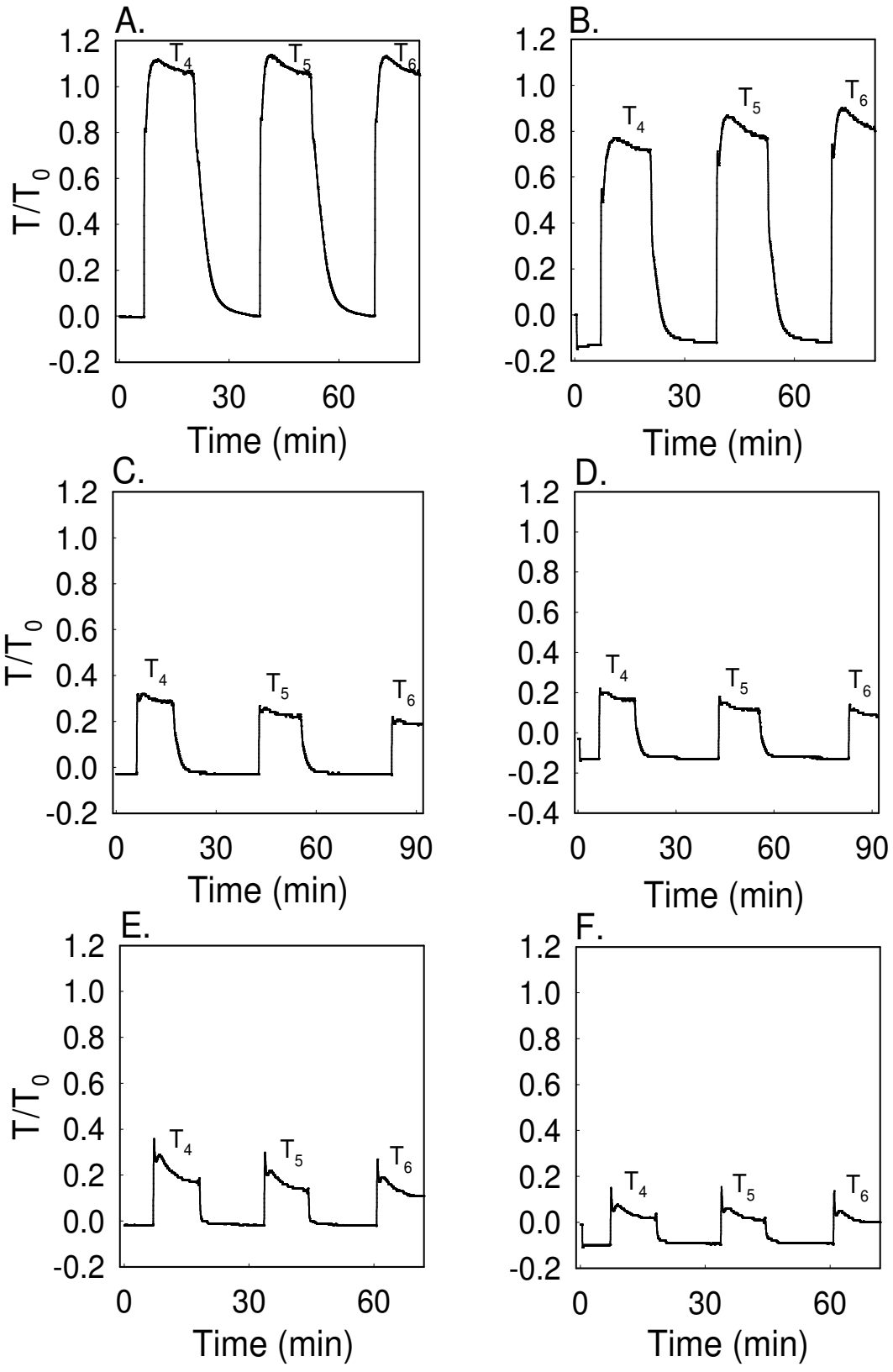
A.
B.
C.
D.
E.
F.
T/T0
Time (min)
T4
T5
T6

FIGURE 3.12 (on previous page): Representative Tension Tracing in the Presence of Inhibitors of Actin Polymerization at L_0 and at a Shortened Length
Representative time versus tension tracings for the investigation of L-adaptation of T_a over three contractions at length L_0 and 0.8-fold L_0. Panel A and B illustrate vehicle control DMSO, Panels C and D 0.2 μM cytochalasin D and Panels E and F 2 μM latrunculin B.

femoral artery contraction demonstrate a significant increase in T_a, on average 15% for the phasic component and 10% for the tonic component. The vehicle control (DMSO) for cytochalasin D and latrunculin B does not affect adaptation as there is an average of 15% increase in the phasic phase and 9% increase in the tonic phase (Figure 3.13B). In contrast, there is loss of significant adaptation in the presence of cytochalasin D, with less than 1% adaptation in both phases (Figure 3.13C). In the presence of latrunculin B, significant adaptation of the phasic phase remains (24%) while the 7% L-adaptation of the tonic phase is not significant (Figure 3.13D). Thus, although actin polymerization is necessary for L-adaptation of phasic and tonic T_a in femoral artery, with significant phasic adaptation in the presence of latrunculin B, it appears that the source of G-actin is one other than free monomers in the cytosol.

The effect of ROCK inhibition was also investigated. In the presence of H-1152, significant adaptation of 19% remained while the 6% adaptation in the tonic phase was not significant (Figure 3.13E). Thus, ROCK appears to play a significant role in the tonic phase of L-adaptation.

To further investigate a possible role for Ca^{2+} participation in L-adaptation of T_a, the effect of the L-type Ca^{2+} channel blocker nifedipine on L-adaptation was investigated. When used at 10 nM, significant adaptation in phasic (9.7%) and tonic (13%) T_a remained (Figure 3.13F).

In summary, these results demonstrate that phasic L-adaptation is dependent, at least in part, on the growth of actin through the addition of G-actin monomers to F-actin. Tonic

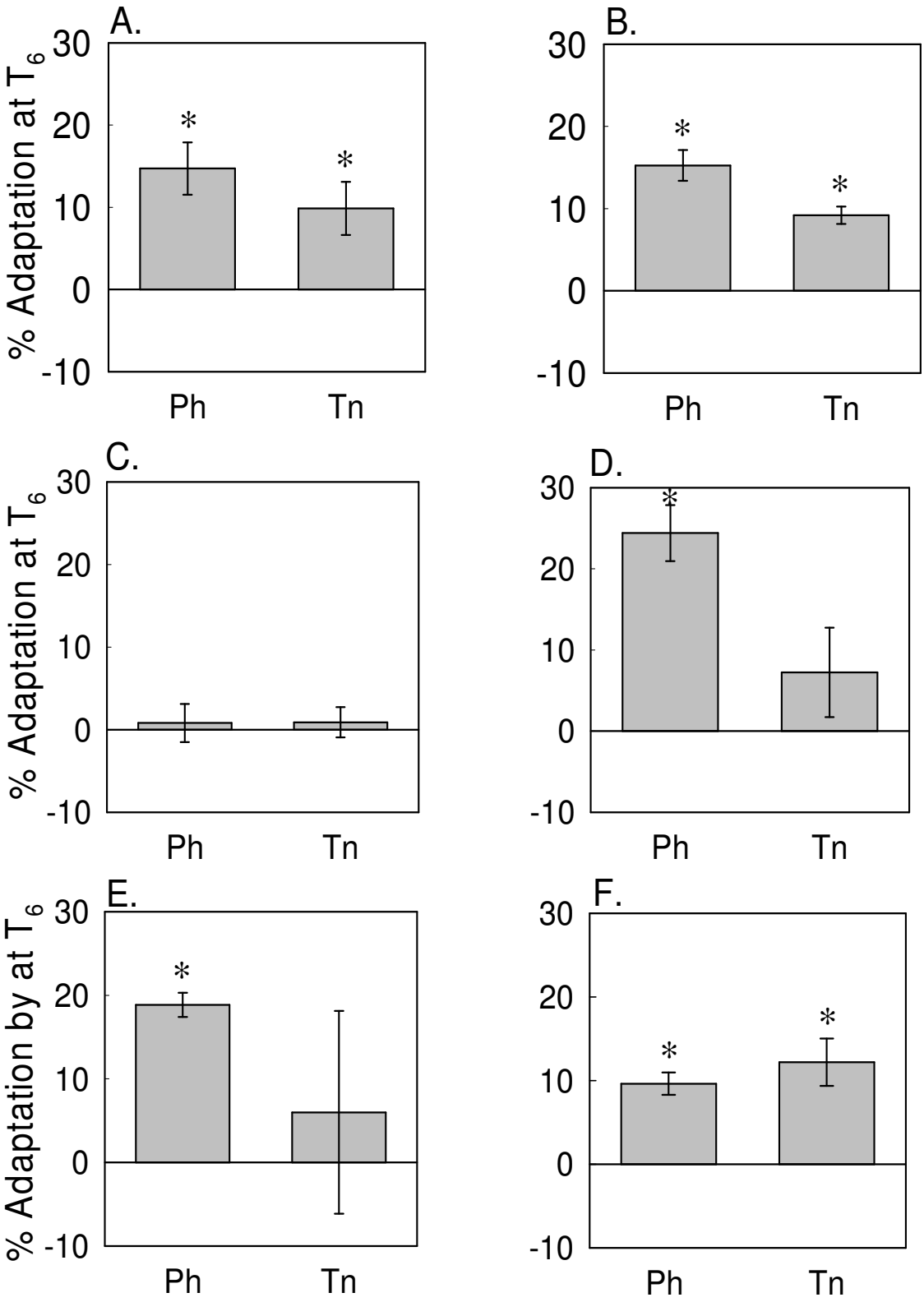
A.
B.
C.
D.
E.
F.
% Adaptation at T6
% Adaptation by at T6
30
20
10
0
-10
Ph
Tn
*

FIGURE 3.13 (on previous page): Effect of Inhibitors of Actin Polymerization on L-adaptation of T_a at a Shortened Length

Bar graphs illustrating the amount of phasic and tonic adaptation at shortened length 0.8-fold L_0 in the presence of no drug (Panel A), vehicle control DMSO (Panel B), 0.2 μM cytochalasin D (Panel C), 2 μM latrunculin B (Panel D), 0.3 μM H-1152 (Panel E) and 10 nM nifedipine (Panel F). * = $p < .05$ compared to 0. n= 5-12.

L-adaptation appears to be more complex and appears to be affected not only by availability of the (+) end of F-actin to which G-actin monomers can add but also the activity of regulators of actin polymerization (i.e. cofilin and profilin).

3.11 L-adaptation of T_a at a Shortened Length in β-escin Permeabilized Tissue

A possible role for Ca^{2+} was further investigated in β-escin permeabilized tissue of rabbit femoral artery. With the selective damage to cellular processes inherent in a permeabilized tissue preparation there is a gradual decrease in the tension generation with time and repeated contraction (Figure 3.14A). Despite this difficulty, L-adaptation of T_a was studied at optimal length and a shortened length through activation with pCa 6.0. Due to the nature of the muscle activation in this preparation, only the steady-state phase of contraction was investigated in this preparation. Panel B in Figure 3.14 illustrates the gradual decrease with time and four repeated contractions in tissues at length L_0 and at 0.8-fold L_0. Thus, to study L-adaptation in this preparation, differences in the rate of degradation between the two lengths were interpreted as "apparent adaptation." In Figure 3.14C, apparent adaptation was significant in the third and fourth repeated contraction at 0.8-fold L_0 relative to L_0. Significant steady-state apparent L-adaptation remained in the presence of cytochalasin D, latrunculin B and H-1152 (Figure 3.14D).

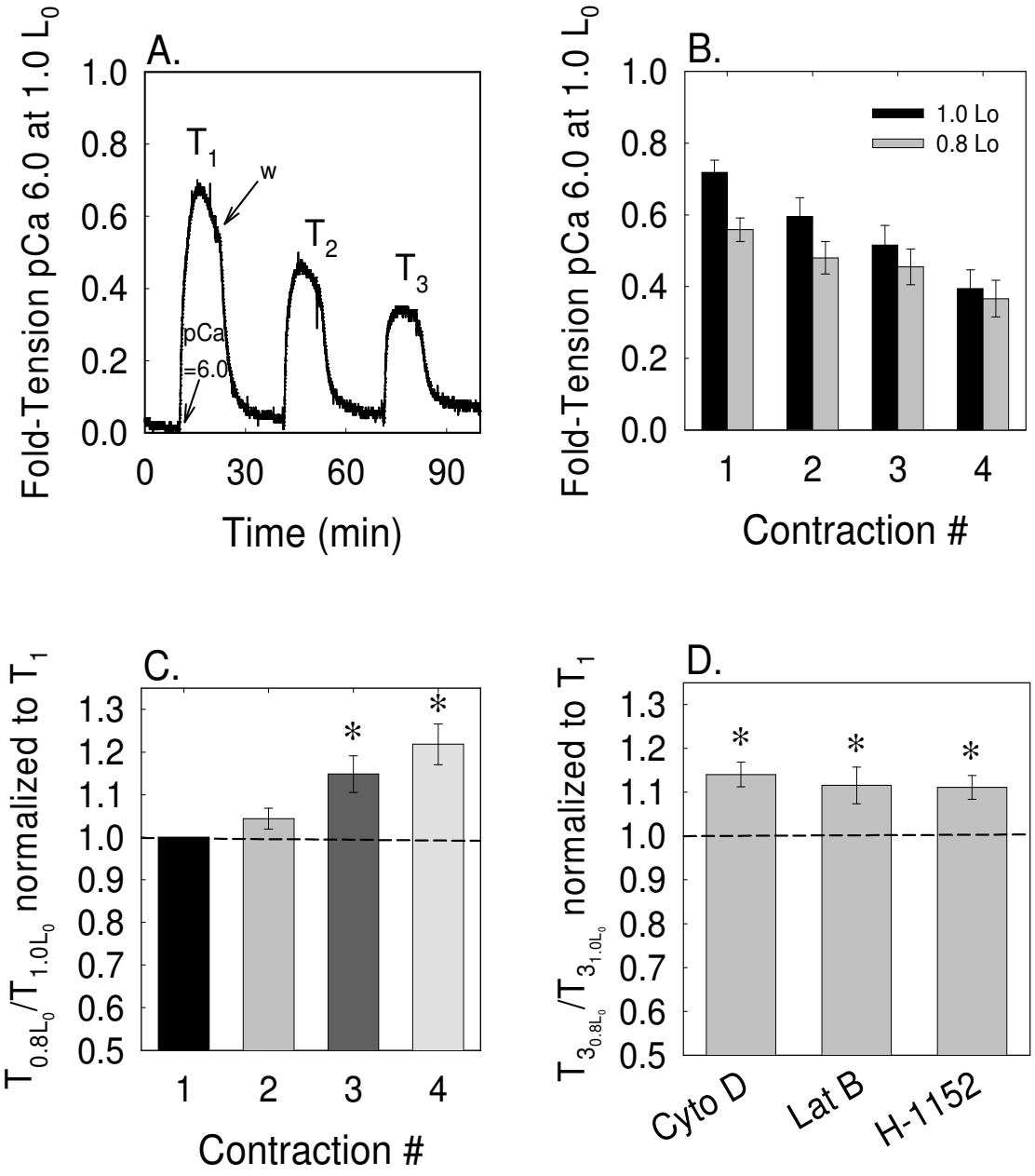
A.
Fold-Tension pCa 6.0 at 1.0 L0
1.0
0.8
0.6
0.4
0.2
0.0
T1
w
T2
T3
pCa
=6.0
0
30
60
90
Time (min)
B.
Fold-Tension pCa 6.0 at 1.0 L0
1.0 Lo
0.8 Lo
1
2
3
4
Contraction #
C.
T0.8L0/T1.0L0 normalized to T1
1.3
1.2
1.1
1.0
0.9
0.8
0.7
0.6
0.5
*
*
1
2
3
4
Contraction #
D.
T3 0.8L0/T3 1.0L0 normalized to T1
1.3
1.2
1.1
1.0
0.9
0.8
0.7
0.6
0.5
*
*
*
Cyto D
Lat B
H-1152

FIGURE 3.14 (on previous page): Effect of β-escin Permeabilization of L-adaptation of T_a at a Shortened Length

Panel A illustrates representative time versus tension tracing in a β-escin permeabilized tissue preparation with muscle activation with pCa 6.0. Panel B demonstrates the average tensions generated over 4 contractions at length L_0 and 0.8-fold L_0. Panel C demonstrates the "apparent adaptation" (refer to text for full description) present with repeated contraction at 0.8-fold L_0 while Panel D illustrates adaptation in the presence of 0.2 μM cytochalasin D, 0.2 μM latrunculin B and 0.3 μM H-1152. ∗ indicates $p < .05$ compared to 1. n= 4-10.

3.12 Effect of Inhibitors of MLCK on L-adaptation of T_a at a Shortened Length

As studies with fura Ca^{2+} indicating dye, nifedipine and permeabilized tissue preparation did not demonstrate a role for Ca^{2+} in the L-adaptation of T_a, the next downstream molecule, calcium-calmodulin (Ca^{2+}-CaM), was briefly investigated. In addition to calmodulin, another intracellular Ca^{2+} binding partner is Ca^{2+}-calmodulin-dependent protein kinase II (CaMKII),which has been shown to be activated with K^+-stimulation and suggested to play a role in maintenance of tonic T_a in VSM (Rokolya and Singer 2000). To study L-adaptation, a series of three contractions (T_1, T_2, T_3) were completed either at L_0 or 0.8-fold L_0 in the presence of KN-93, a CaMKII inhibitor, or KN-92, a negative control for KN-93. As KN-92 is dissolved in DMSO and KN-93 is dissolved in deionized water, additional controls included measurement of L-adaptation in the presence of DMSO or deionized water and phentolamine. Figure 3.15 illustrates example tension versus time tracings for tissues at 0.8-fold L_0 in the presence of deionized water (Panel A), DMSO (Panel B), KN-92 (Panel C) and KN-93 (Panel D). Regardless of length, tissues in the presence of KN-93 demonstrated decreases in both phases of contraction, with effects more pronounced in the tonic phase. The effect of KN-93 and KN-92 were investigated in tissues from the same animal, however, length differences were investigated between animals and thus statistics not completed. Therefore, when data from different animals were randomly paired, a decrease in both phases of T_a generation was evident when CaMKII was inhibited (Figure 3.16 E and F).

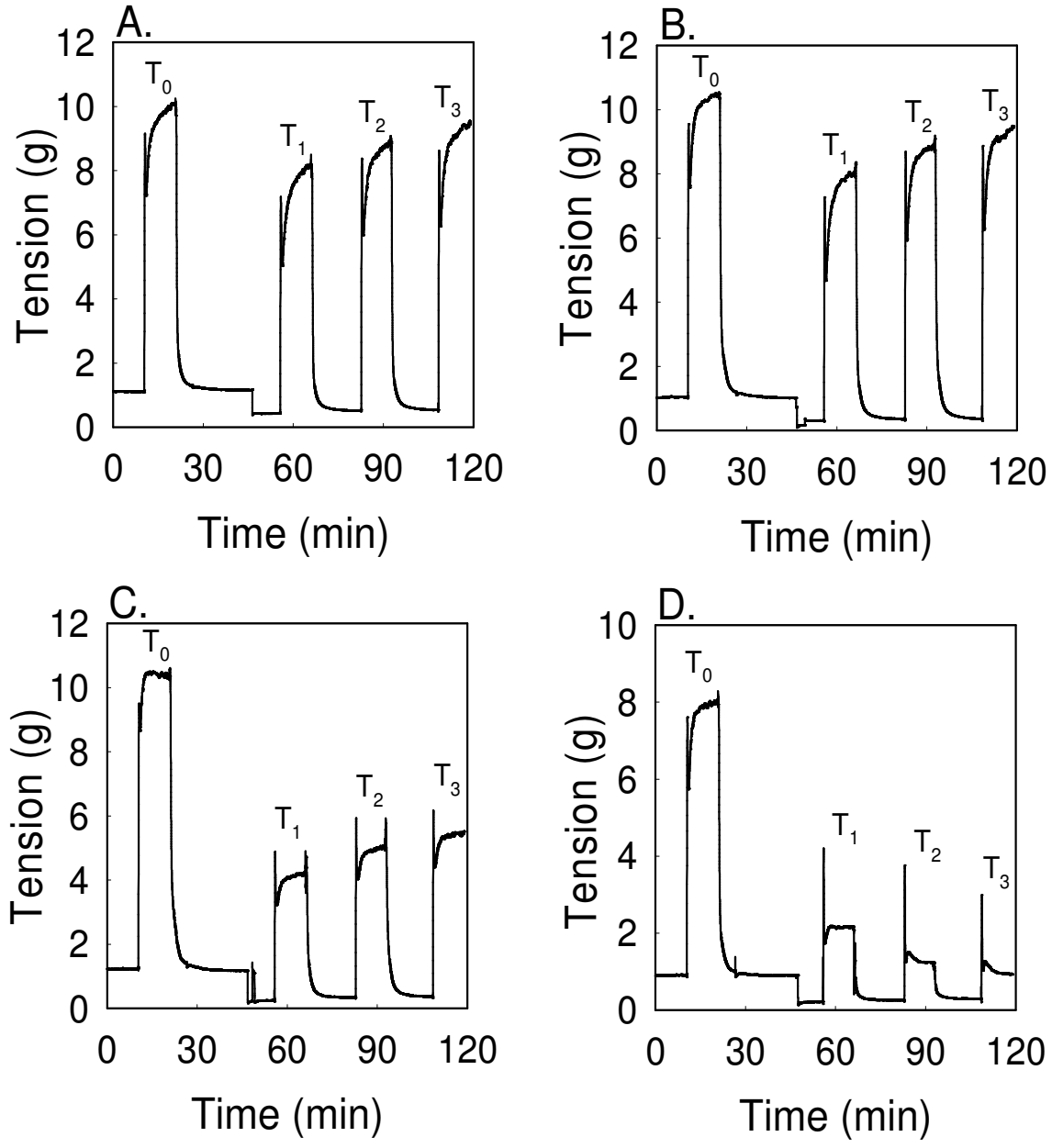

FIGURE 3.15: Representative Tension Tracing in the Presence of CaMKII Inhibitor
Representative time versus tension tracings in the presence of 1 μM phentolamine (Panel A), DMSO (Panel B), 1 μM KN-92 (Panel C) and 1 μM KN-93 (Panel D).

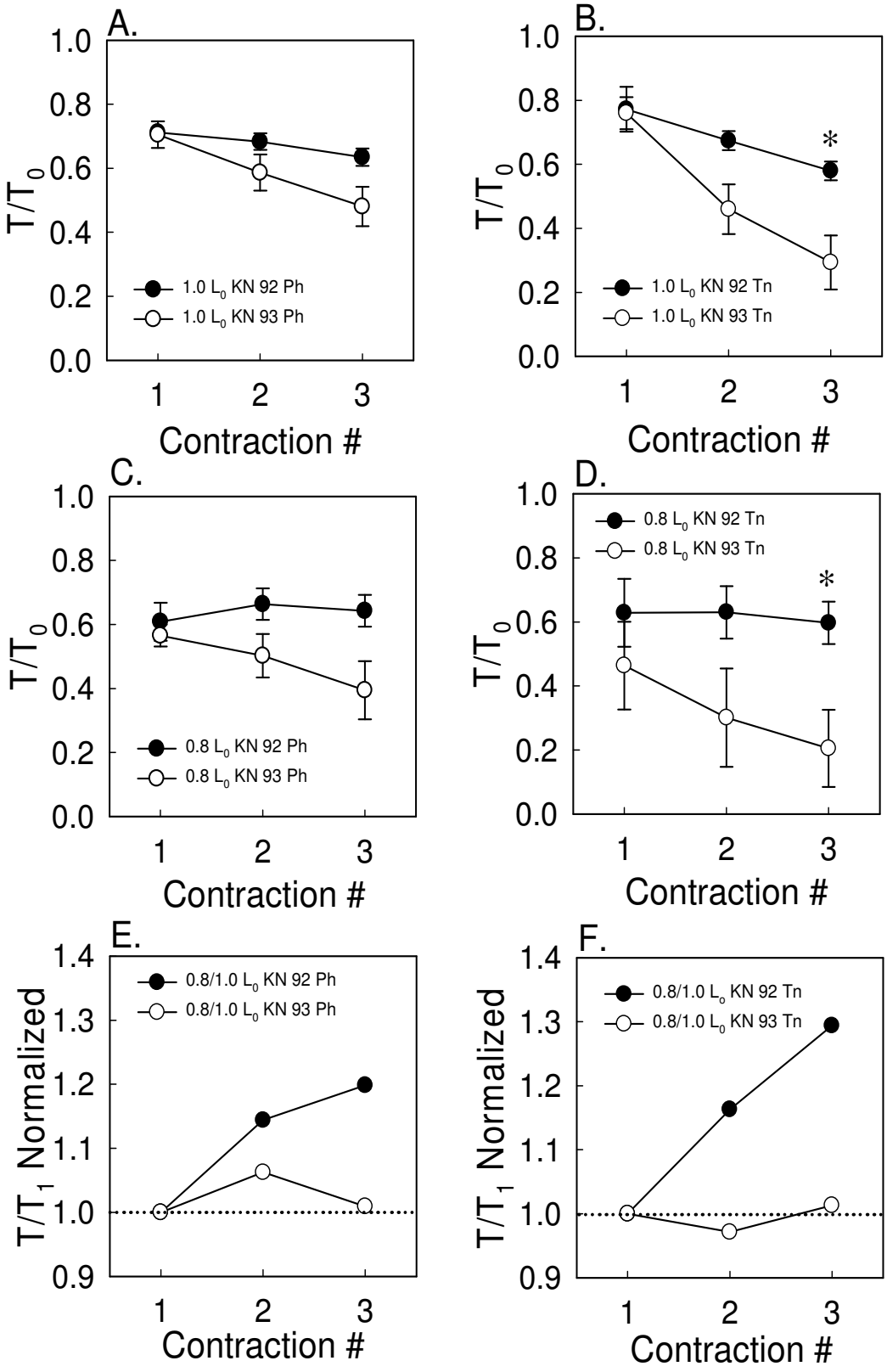
A.
B.
C.
D.
E.
F.
T/T0
T/T1 Normalized
Contraction #
1.0 L0 KN 92 Ph
1.0 L0 KN 93 Ph
1.0 L0 KN 92 Tn
1.0 L0 KN 93 Tn
0.8 L0 KN 92 Ph
0.8 L0 KN 93 Ph
0.8 L0 KN 92 Tn
0.8 L0 KN 93 Tn
0.8/1.0 L0 KN 92 Ph
0.8/1.0 L0 KN 93 Ph
0.8/1.0 Lo KN 92 Tn
0.8/1.0 L0 KN 93 Tn
*

FIGURE 3.16 (on previous page): Effect of CaMKII Inhibitor on L-adaptation of T_a at a Shortened Length

Average T_a over three repeated contractions at length L_0 (Panel A and B) and 0.8-fold L_0 (Panel C and D) in the presence of KN-92 and KN-93. Panel E and Panel F demonstrate an increase in phasic and tonic T_a KN-92 tissues relative to KN-93 tissues. * indicates $p < .05$ between drugs. n= 3 at each length.

3.13 Effect of Stretch versus Stretch and Contraction on L-adaptation of T_a at a Shortened Length

Having started this project with an investigation of the effect of stretch on T_p, in a last series of experiments, the effect of stretch on L-adaptation of T_a at a shortened length was studied. All tension measurements were taken at 0.8-fold L_0, however, a stretch to 1.2-fold L_0 was completed between T_1 and T_2 (Figure 3.17A). While stretch was thought to break intracellular and/or extracellular connections, the effect of a contraction at a stretched length was also investigated (Figure 3.17B).

Relative to pre-stretch (T_1), both the phasic and tonic T_a in a contraction post-stretch (T_2) was significantly decreased (Figure 3.17C and D). This was also seen in tissues subjected to contraction at long length. Phasic and tonic T_a returned to levels at or above pre-stretch upon a subsequent third contraction (T_3). It is interesting to note that the addition of a contraction at long length significantly decreased tonic T_a as compared to stretch alone (Figure 3.17 D). The decrease in phasic and tonic T_a generation was more pronounced with a greater stretch to 1.4 L_0 (data not shown). Decreased $[Ca^{2+}]_i$ levels do not appear to play a role in the decreased phasic and tonic T_a generation following stretch or stretch and contraction (Figure 3.18).

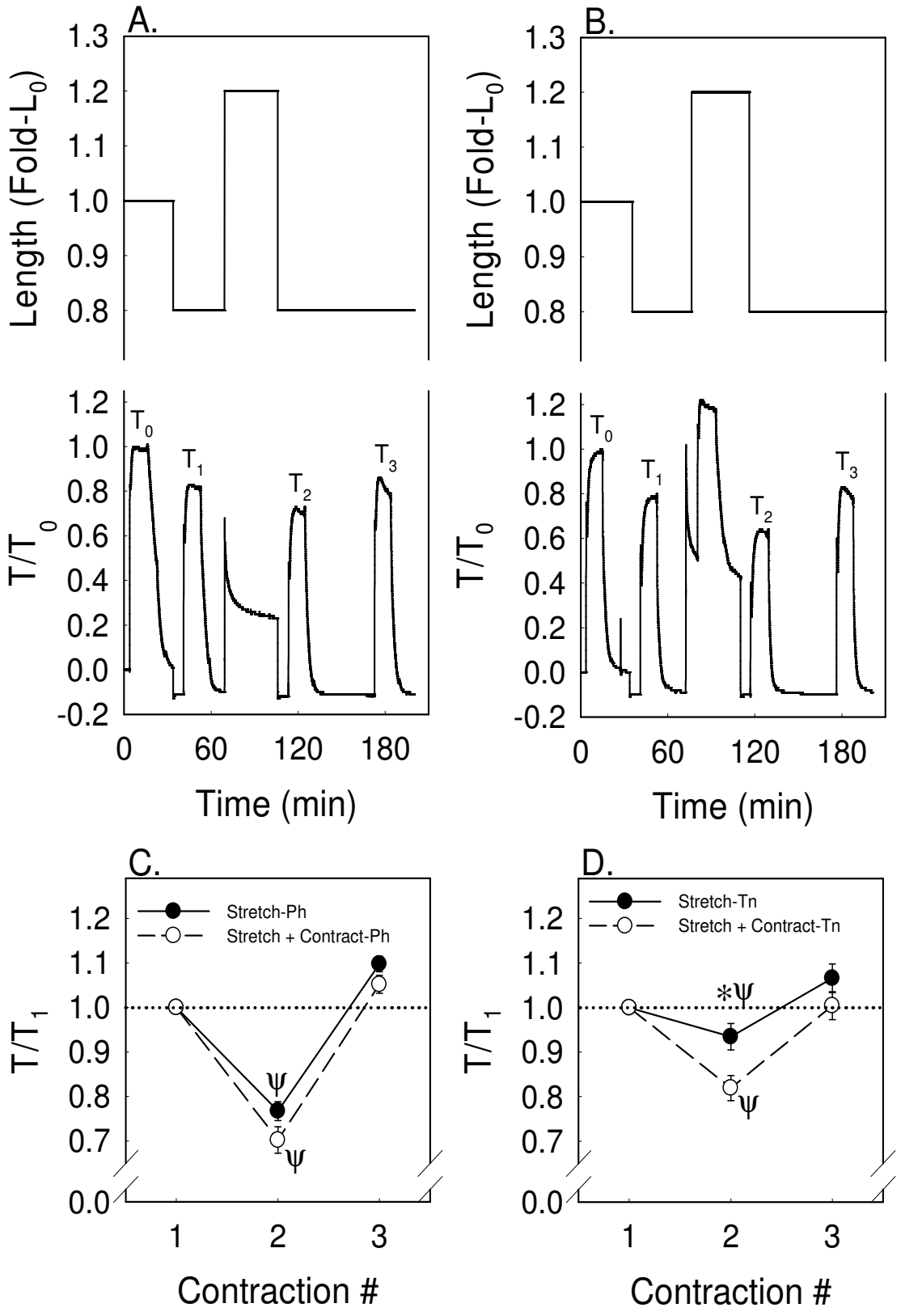
A.
B.
Length (Fold-L0)
T/T0
T0
T1
T2
T3
Time (min)
C.
D.
T/T1
Stretch-Ph
Stretch + Contract-Ph
Stretch-Tn
Stretch + Contract-Tn
ψ
*ψ
Contraction #

FIGURE 3.17 (on previous page): Effect of Stretch versus Stretch and Contraction on L-adaptation of T_a at a Shortened Length

Representative time versus tension tracing of 3 consecutive contractions, T_1, T_2, and T_3, at a shortened length 0.8 L_0 with a stretch to 1.2 L_0 completed between T_1 and T_2 (Panel A) and contraction at the stretched length completed between T_1 and T_2 (Panel B). Average phasic (Panel C) and tonic (Panel D) tension values normalized to T_1 over 3 consecutive contractions are shown. Note additional decrease in tension in tissue when contraction completed at the stretched length. * indicates $p < .05$ stretch compared to stretch + contract for a single contraction. ψ = $P < .05$ compared to 1.0. n = 5-11.

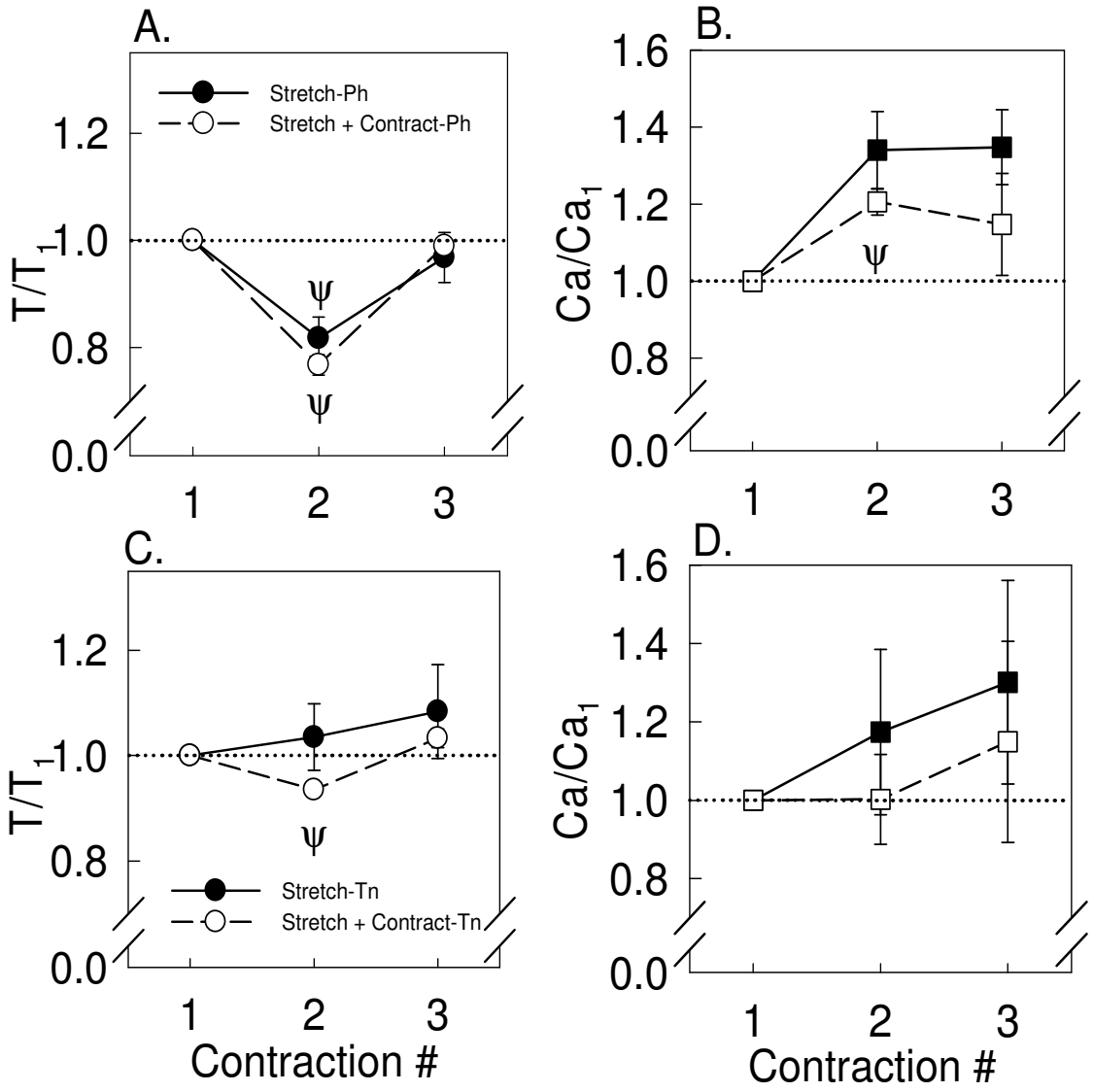

FIGURE 3.18: Effect of $[Ca^{2+}]_i$ on Stretch versus Stretch and Contraction
Panel A shows the average phasic and Panel C shows the average tonic tension values normalized to T_1 over three consecutive contractions at length 0.8 L_0 with stretch to 1.2 L_0 completed between T_1 and T_2 or stretch and contraction completed between T_1 and T_2. The corresponding $[Ca^{2+}]_i$ signals during phasic (Panel B) and tonic (Panel D) phases of contraction are also shown. * indicates $p < .05$ stretch compared to stretch + contract for a single contraction. ψ = $P < .05$ compared to 1.0. n = 3.

CHAPTER 4

Discussion

The main findings of this project include the presence of a dynamic T_p and T_a L-T curve in rabbit femoral artery and that tissues contracted three times at a shortened length displayed significant L-adaptation in both the phasic and tonic phases. Attempts to elucidate a mechanism for this phenomenon showed that neither an increase in $[Ca^{2+}]_i$ nor an increase in MLC_{20} phosphorylation were responsible for the increased tension, however, actin polymerization did appear to play a role in the L-adaptation of both phases of contraction (Figure 4.1).

With the awareness that the length-history of VSM affects the T_p at a particular length, and to facilitate comparison between studies, the method utilized to measure T_p in this project was a modification of that used previously [37, 121]. With a focus on the ascending limb of the L-T curve, similar to the results of Wingard et al. [121], two T_p curves were found with the tension greater with tissue LD versus tissue ULD. Wingard et al. attributes this difference to tissue damage that occurs with stretch to long lengths such that there is a subsequent decrease in viable VSM capable of generating tension. In separate experiments, tissues naïve to maximal stretch (1.4-fold L_0) demonstrated a significant increase in T_p upon first stretch to 1.2-fold L_0 as compared to a second stretch to 1.2-fold L_0 in the same tissue or another tissue previously stretched to 1.4-fold L_0.

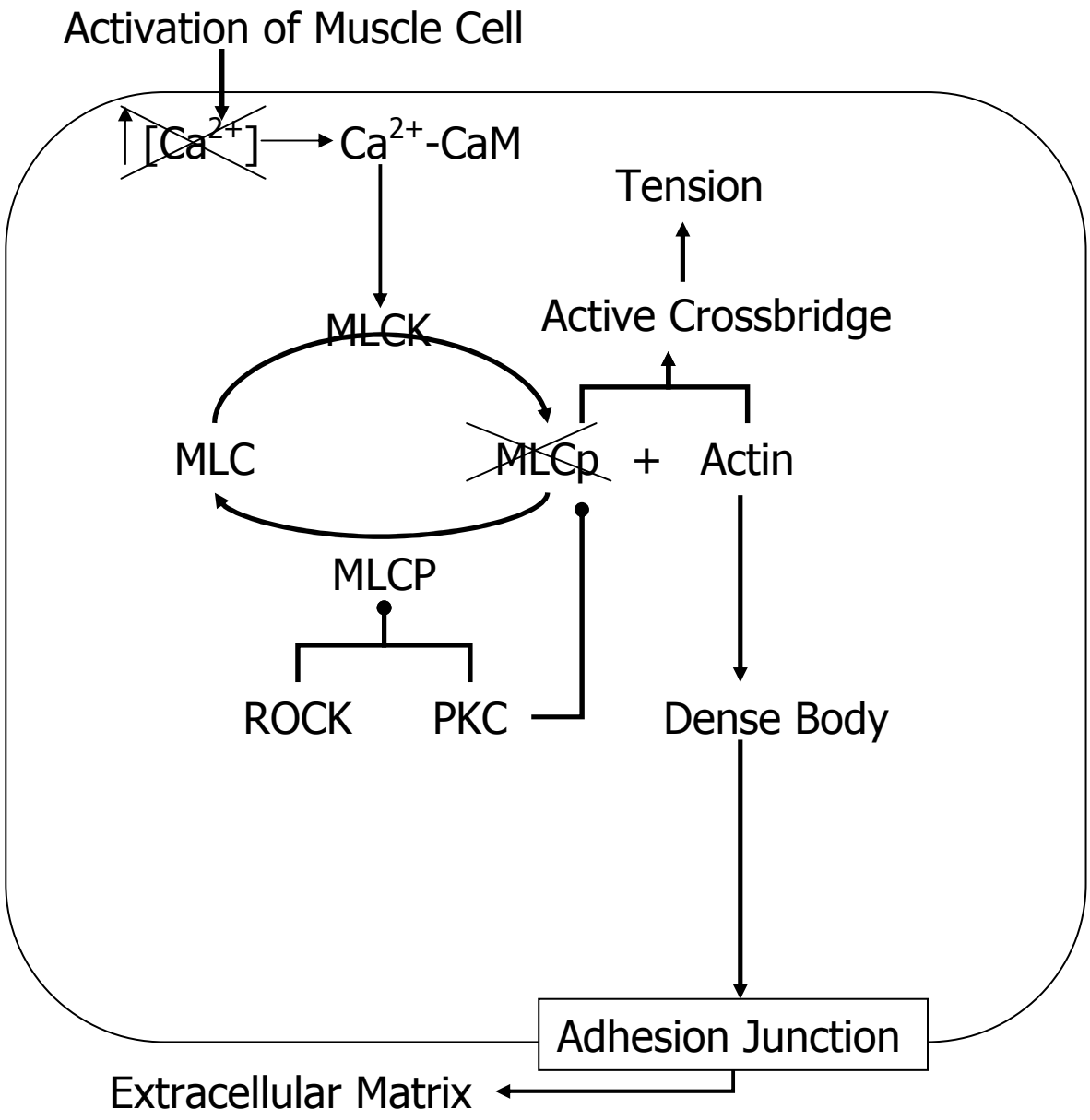

FIGURE 4.1: Diagram of Mechanism of Smooth Muscle Contraction Relative to L-adaptation at a Shortened Length

Diagram illustrating the mechanism of smooth muscle contraction, from activation through transmission of generated tension to the extracellular matrix. Note that results of this project provided evidence that neither $[Ca^{2+}]_i$ nor MLC_{20} phosphorylation were responsible for L-adaptation, however, actin polymerization does play a role.

Although it is possible that tissue damage was responsible for this difference, it was not thought to be likely based on further interpretation of the full L- T curve results. In this protocol, tissues were preconditioned, activated at a series of increasing lengths, activated at a series of decreasing lengths followed by measurement of T_p. Due to stress relaxation, to obtain a true T_p at the longest length, tissues were stretched to a length 0.05 mm longer than at any time previously in the protocol. Although it is possible that this stretch of less than 2% of the L_0 resulted in tissue damage, and thus the decreased T_p with ULD, it is not thought to be likely as it has been estimated that the series elastic component in VSM is not affected until lengths 7.2% of L_0 [38]. Additional studies are necessary to determine the mechanism responsible for the difference in T_p with LD and ULD. A possible role for crossbridges in generating T_p exists as Speich et al. found that activation can reverse the effect of strain-softening in rabbit detrusor smooth muscle [100, 101].

Furthermore, the presence of the two T_a curves agrees with the findings of Wingard et al. [121]. However, again, tissue damage was not thought to be responsible as the increased T_a with LD versus ULD was found when tissues were first gradually shortened and then gradually lengthened (data not shown). The presence of two L-T_a curves for each phase of contraction was a novel finding in this study and further investigation revealed that the tonic phase was more sensitive to length changes below L_0 as compared to the phasic phase.

The L-adaptation in VSM demonstrated in the present project confirmed the findings of the two previous studies by Seow [91] and Syyong et al. [104]. Seow reported that L-adaptation was dependent on time, however, the protocol used to adapt the tissues

included periodic muscle activation. Thus, in this project, the effect of time versus repeated contraction at a single length was more fully investigated. It appeared that the effect of time on T_a is dependent on the state of the muscle, relaxed or contracted. When a relaxed tissue was contracted 100 min after a second reference tissue, the phasic and tonic T_a were not significantly different between tissues (Figure 3.5B). However, when a tissue was maintained in a contracted state for 120 min, the maximal T_a was not significantly different than phasic nor tonic T_a of a third repeated contraction (Figure 3.5D). Thus, the maximal T_a of VSM can be achieved through a sustained contraction of average 34 min duration or upon a third repeated contraction.

This project appears to be the first to determine a cellular mechanism(s) responsible for L-adaptation at a shortened length in VSM. Both phases of contraction demonstrated L-adaptation but were investigated separately throughout all experiments. As the mechanism(s) responsible for each phase are not fully understood, it was hoped that the phenomenon of L-adaptation might be used as tool to reveal information about the mechanisms regulating these phases.

The importance of Ca^{2+} as a signaling molecule in the regulation of crossbridges in smooth muscle is well known. Some have observed a decrease in myoplasmic $[Ca^{2+}]_i$ in VSM at short lengths [83] while others have not found the same in ASM [32]. Therefore, in a series of three separate experiments, the possibility that an increase in $[Ca^{2+}]_i$ was responsible for the increased tension evident with repeated contraction at a shortened length was investigated. The first set of experiments utilized a Ca^{2+}-indicating dye and did not show a length dependent difference in $[Ca^{2+}]_i$ with repeated contraction. Of note,

similar to the studies in ASM, $[Ca^{2+}]_i$ trended toward an increase during both phases of contraction at a shortened length and the phasic phase at length L_0. Ratz et al. [80] previously showed that $[Ca^{2+}]_i$ in VSM trends toward an increase upon a second contraction at length L_0. A second set of experiments investigating the role of $[Ca^{2+}]_i$ involved a β-escin permeabilized tissue preparation. With the disruption of the cell membrane, the amount $[Ca^{2+}]_i$ available for muscle contraction can be precisely controlled through the contracting solution. When tissue was activated with a constant pCa 6.0 solution, the apparent L-adaptation at a shortened length was evident in this preparation and was taken as evidence that an increase in $[Ca^{2+}]_i$ was not responsible for the increase in tension with repeated contraction. A third, and final, set of experiments provided evidence that $[Ca^{2+}]_i$ was not playing a role in L-adaptation. In the presence of a low concentration of the L-type Ca^{2+}-channel blocker nifedipine, the tissue continued to display a significant phasic and tonic L-adaptation at a shortened length.

Having explored an upstream regulator of VSM contraction, attention was turned further downstream to regulation of crossbridge activation through phosphorylation level of MLC_{20}. Using a modified protocol to capture small differences in phosphorylation that may exist between tissues at a control length and tissues at shortened length, no difference in phosphorylation levels were found to correspond with the increase in T_a with repeated contraction. Interestingly, a significant decrease in the basal myosin phosphorylation was found by the third repeated contraction in control length tissues despite lack of a decrease in T_a. Hai [34] reported that steady-state active stress and myosin phosphorylation were not different between two repeated contractions at length L_0. Although no statistical

differences were presented, from the data included, a trend toward a decrease in levels of myosin phosphorylation with a second repeated contraction is evident. As compared to a shortened length, the decreased basal levels of myosin phosphorylation at control length should be considered as a possible contributor to the lack of differences with K^+-induced activation. Further studies investigating basal levels of myosin phosphorylation at different tissues lengths with repeated contraction are warranted.

As changes in myosin based regulation of crossbridge activation did not appear responsible for L-adaptation, attention was turned to the actin thin filament. As compared to striated muscle, there is a greater actin to myosin ratio present in smooth muscle. Thus, the possibility exists that polymerization of actin upon muscle activation results in the formation of additional crossbridges with resultant increase in tension. Previously, others [4, 123] have shown the effect of the F-actin capping agent cytochalasin to be limited to the slow phase of contraction in rat aortic rings. While the present results demonstrated an effect greater in the tonic phase, significant inhibition was evident in both phases that increased with repeated contraction at L_0 (Figure 3.10 B and C). Likewise, some have found no effect of latrunculin B on a K^+-induced contraction [47] while the results presented here indicated increased inhibition with repeated contraction in both the phasic and tonic phases of an L_0 contraction (Figure 3.10 E and F). Reasons for these differences are not known but may be tissue or drug concentration dependent. When the effect of the ROCK inhibitor H-1152, known to affect actin polymerization through LIMK1 and cofilin, were investigated at length L_0, there was no effect on the phasic phase but a significant inhibition of the tonic phase, which is consistent with previous work [80] (Figure 3.10 H

and I). The effects of cytochalasin B do not appear to be mediated through changes in $[Ca^{2+}]_{i.}$ (Figure 3.11 B), in agreement with work by Obara and Yabu [67], nor do the effects of latrunculin B appear Ca^{2+}-mediated (Figure 3.11 D).

The possible effect of inhibition of actin polymerization on L-adaptation in VSM was investigated. For both phasic and tonic T_a, within tissue differences between contractions and the differential effect of length on the T_a generated in the presence of the inhibitor were accounted for. The results indicated that the addition of G-actin monomers to the (+) end of F-actin is necessary for L-adaptation of both the phasic and tonic phases of VSM contractions, evident with the results in the presence of cytochalasin D (Figure 3.13C). Additionally, it appears that different sources of G-actin are responsible for the actin polymerization necessary for each phase, with the source for the tonic phase including free G-actin monomers as evident with the lack of significant L-adaptation in the presence of latrunculin B (Figure 3.13D). Although speculative, an alternative source of G-actin for the phasic phase could theoretically include G-actin bound to thymosin β_4 that is freed upon muscle activation to participate in actin polymerization. The results of L-adaptation in the presence of H-1152 indicate that actin polymerization involving ROCK is limited to the tonic phase as phasic L-adaptation remained. The importance of actin polymerization in the tonic phase of VSM contraction has been previously shown in studies such as that by Rembold et al. [84], however, the role of actin polymerization in the phasic phase appears to be a novel finding in this project.

The role of crossbridge regulation through the myosin thick filament was investigated in this project and not found to affect L-adaptation in VSM. Structural

changes in the actin thin filament, through polymerization, were, however, found to participate in L-adaptation. A possibility for future studies would involve investigation of crossbridge regulation through the actin thin filament. Two possible actin-binding proteins that are thought to participate in regulation of actin include caldesmon and calponin (reviewed in [62]). Capable of binding with actin, tropomyosin, myosin and calmodulin, caldesmon is uniquely situated to affect crossbridge function. Through its ability to bind with actin, calponin has been suggested to participate in crossbridge regulation through inhibition of the myosin ATPase.

Another signaling molecule, CaMKII, was briefly investigated in this project. As reviewed by Kamm and Stull [46], at higher $[Ca^{2+}]_i$ than necessary to activate MLCK and thus increase MLC_{20} phosphorylation, CaMKII is activated and can phosphorylate MLCK at a site that will result in the dissociation of calmodulin and thus decrease its activity. It is thus possible that inhibition of CaMKII, through an agent such as KN-93, will limit the normal inhibition of MLCK present at higher $[Ca^{2+}]_i$ and result in increased tension generation. In contrast to what was expected, yet consistent with the findings of others [48, 86], the present results indicated that there was a decrease in both phasic and tonic tension at L_0 and 0.8-fold L_0 with KN-93. In the presence of the negative control, KN-92, there were minimal to no decreases in tension at the two lengths studied. Taken together, these results indicated that L-adaptation at a shortened length is abolished for both the phasic and tonic phases in the presence of KN-93 (Figure 3.16 E and F). The mechanism for decrease in tension in the presence of a CAMKII inhibitor is not yet clear but involvement of mitogen-activated protein kinase (MAPK) has been suggested [48]. A role for

CaMKIIβ in maintaining polymerized F-actin in developing neurons has recently been shown [52].

The effect of an interruption in L-adaptation was also briefly explored in this project. With an intervening stretch or a contraction at a stretched length, a decrease in both phasic and tonic T_a was evident (Figure 3.17) that did not appear to be the result of a change in $[Ca^{2+}]_i$ (Figure 3.18).

It is of particular clinical interest to consider the response of VSM stretch on tension generation. Through continuous, intra-arterial blood pressure monitoring in both normotensive and hypertensive patients it has been shown that blood pressure follows a circadian rhythm [60]. In both groups, blood pressure was found to be highest mid-morning and then progressively fell throughout the day and evening to reach a 24-hour low at 3 AM. O'Brien et al. [68] reported "non-dippers" as a subset of hypertensive patients who do not demonstrate the normal diurnal variation in blood pressure, as defined by a 10 mm Hg decrease in systolic blood pressure and a 5 mm Hg decrease in diastolic blood pressure from day to night. The lack of a nocturnal decrease in blood pressure in these hypertensive patients has been linked to stroke, left ventricular hypertrophy, heart failure, myocardial infarction, and sudden death [68, 102, 116]. The mechanism responsible for circadian rhythm of blood pressure is not yet fully understood, however, a role for the sympathetic nervous system (SNS) has been suggested [72, 96]. A study by Sherwood et al. [95] provided further evidence for the role of the SNS as it pertains to nocturnal decreases in blood pressure. They found that the drop in excretion of urinary catecholamines, from day to night, was significantly less in the "non-dipper" subjects.

Additionally, they found that the subjects exhibited no difference in the responsiveness of β-adrenergic receptors, however, "non-dippers" demonstrated an increase in α_1-receptor sensitivity compared to "dippers." Thus, the authors concluded that the higher level of nighttime blood pressure in "non-dippers" may be due to an increased vasoconstriction, with resultant increased TPR. Thus with evidence of more than one L-T_a curve in VSM, the possibility exists that the arteries of "non-dippers" are unable to adapt to another curve when blood pressure is typically lower during nighttime hours. For small resistance arteries, this may result in changes in TPR while for larger conduit arteries this may result in changes in stiffness.

The L-adaptation studied in this project was of a relatively short duration. A study by Naghshin et al. [64] demonstrated that following longer term (7 days) adaptation at a shortened length in ASM, re-adaptation to a longer length became more difficult to complete. The authors note that perhaps chronic effects may be reversed if the muscle was adapted to the longer length over a longer period of time. Thus the possibility of remodeling of arteries chronically adapted to a short length exists. As reviewed by Prewitt, Rice and Dobrian [75], vessels are capable of different types of remodeling, dependent on their size. The arterioles undergo an inward, eutrophic remodeling in which lumen diameter is reduced while wall thickness is maintained. This is in contrast to the outward hypertrophy remodeling that large arteries undergo in which luman diameter is maintained while wall thickness increases. As previously presented, a role has been suggested for integrins and focal adhesion proteins as tranducers of mechanical stimuli to intracellular signaling. Thus, these important sites on the smooth muscle cell membrane

may provide a possible link between actin polymerization that appears to play a role in L-adaptation at a shortened length and consequent long term remodeling of the arterial tree.

References

References

1. Applegate, D. and J.D. Pardee, *Actin-facilitated assembly of smooth muscle myosin induces formation of actomyosin fibrils.* J Cell Biol, 1992. **117**(6): p. 1223-30.
2. Arber, S., et al., *Regulation of actin dynamics through phosphorylation of cofilin by LIM-kinase.* Nature, 1998. **393**(6687): p. 805-9.
3. Bai, T.R., et al., *On the terminology for describing the length-force relationship and its changes in airway smooth muscle.* J Appl Physiol, 2004. **97**(6): p. 2029-34.
4. Battistella-Patterson, A.S., S. Wang, and G.L. Wright, *Effect of disruption of the cytoskeleton on smooth muscle contraction.* Can J Physiol Pharmacol, 1997. **75**(12): p. 1287-99.
5. Bellis, S.L., J.T. Miller, and C.E. Turner, *Characterization of tyrosine phosphorylation of paxillin in vitro by focal adhesion kinase.* J Biol Chem, 1995. **270**(29): p. 17437-41.
6. Bozler, E., *Role of calcium in initiation of activity of smooth muscle.* Am J Physiol, 1969. **216**(3): p. 671-4.

7. Burridge, K. and M. Chrzanowska-Wodnicka, *Focal adhesions, contractility, and signaling.* Annu Rev Cell Dev Biol, 1996. **12**: p. 463-518.

8. Buus, N.H., E. VanBavel, and M.J. Mulvany, *Differences in sensitivity of rat mesenteric small arteries to agonists when studied as ring preparations or as cannulated preparations.* Br J Pharmacol, 1994. **112**(2): p. 579-87.

9. Calderwood, D.A., et al., *The Talin head domain binds to integrin beta subunit cytoplasmic tails and regulates integrin activation.* J Biol Chem, 1999. **274**(40): p. 28071-4.

10. Campbell, K.S. and R.L. Moss, *A thixotropic effect in contracting rabbit psoas muscle: prior movement reduces the initial tension response to stretch.* J Physiol, 2000. **525 Pt 2**: p. 531-48.

11. Campbell, K.S., J.R. Patel, and R.L. Moss, *Cycling cross-bridges increase myocardial stiffness at submaximal levels of Ca2+ activation.* Biophys J, 2003. **84**(6): p. 3807-15.

12. Cohen, D.M. and R.A. Murphy, *Differences in cellular contractile protein contents among porcine smooth muscles: evidence for variation in the contractile system.* J Gen Physiol, 1978. **72**(3): p. 369-80.

13. Cohen, D.M. and R.A. Murphy, *Cellular thin filament protein contents and force generation in porcine arteries and veins.* Circ Res, 1979. **45**(5): p. 661-5.

14. Cooper, J.A., *Effects of cytochalasin and phalloidin on actin.* J Cell Biol, 1987. **105**(4): p. 1473-8.

15. Costanzo, L.S., *Physiology*. 2nd ed. 2002, Philadelphia: Saunders.

16. Coue, M., et al., *Inhibition of actin polymerization by latrunculin A.* FEBS Lett, 1987. **213**(2): p. 316-8.

17. Dillon, P.F., et al., *Myosin phosphorylation and the cross-bridge cycle in arterial smooth muscle.* Science, 1981. **211**(4481): p. 495-7.

18. Drew, J.S., C. Moos, and R.A. Murphy, *Localization of isoactins in isolated smooth muscle thin filaments by double gold immunolabeling.* Am J Physiol, 1991. **260**(6 Pt 1): p. C1332-40.

19. Driska, S.P., M.O. Aksoy, and R.A. Murphy, *Myosin light chain phosphorylation associated with contraction in arterial smooth muscle.* Am J Physiol, 1981. **240**(5): p. C222-33.

20. Droogmans, G. and R. Casteels, *Temperature-dependence of 45Ca fluxes and contraction in vascular smooth muscle cells of rabbit ear artery.* Pflugers Arch, 1981. **391**(3): p. 183-9.

21. Dunn, W.R., G.C. Wellman, and J.A. Bevan, *Enhanced resistance artery sensitivity to agonists under isobaric compared with isometric conditions.* Am J Physiol, 1994. **266**(1 Pt 2): p. H147-55.

22. Falloon, B.J., et al., *Comparison of small artery sensitivity and morphology in pressurized and wire-mounted preparations.* Am J Physiol, 1995. **268**(2 Pt 2): p. H670-8.

23. Fatigati, V. and R.A. Murphy, *Actin and tropomyosin variants in smooth muscles. Dependence on tissue type.* J Biol Chem, 1984. **259**(23): p. 14383-8.

24. Ford, L.E., C.Y. Seow, and V.R. Pratusevich, *Plasticity in smooth muscle, a hypothesis.* Can J Physiol Pharmacol, 1994. **72**(11): p. 1320-4.

25. Gerthoffer, W.T. and S.J. Gunst, *Invited review: focal adhesion and small heat shock proteins in the regulation of actin remodeling and contractility in smooth muscle.* J Appl Physiol, 2001. **91**(2): p. 963-72.

26. Gibbons, G.H. and V.J. Dzau, *The emerging concept of vascular remodeling.* N Engl J Med, 1994. **330**(20): p. 1431-8.

27. Gillis, J.M., M.L. Cao, and A. Godfraind-De Becker, *Density of myosin filaments in the rat anococcygeus muscle, at rest and in contraction. II.* J Muscle Res Cell Motil, 1988. **9**(1): p. 18-29.

28. Godfraind-De Becker, A. and J.M. Gillis, *Analysis of the birefringence of the smooth muscle anococcygeus of the rat, at rest and in contraction. I.* J Muscle Res Cell Motil, 1988. **9**(1): p. 9-17.

29. Gordon, A.M., A.F. Huxley, and F.J. Julian, *The variation in isometric tension with sarcomere length in vertebrate muscle fibres.* J Physiol, 1966. **184**(1): p. 170-92.

30. Gordon, A.R. and M.J. Siegman, *Mechanical properties of smooth muscle. I. Length-tension and force-velocity relations.* Am J Physiol, 1971. **221**(5): p. 1243-9.

31. Gunst, S.J., *Effect of length history on contractile behavior of canine tracheal smooth muscle.* Am J Physiol, 1986. **250**(1 Pt 1): p. C146-54.

32. Gunst, S.J., *Effects of muscle length and load on intracellular Ca2+ in tracheal smooth muscle.* Am J Physiol, 1989. **256**(4 Pt 1): p. C807-12.

33. Gunst, S.J., et al., *Mechanisms for the mechanical plasticity of tracheal smooth muscle.* Am J Physiol, 1995. **268**(5 Pt 1): p. C1267-76.

34. Hai, C.M., *Length-dependent myosin phosphorylation and contraction of arterial smooth muscle.* Pflugers Arch, 1991. **418**(6): p. 564-71.

35. Hai, C.M. and R.A. Murphy, *Ca2+, crossbridge phosphorylation, and contraction.* Annu Rev Physiol, 1989. **51**: p. 285-98.

36. Harris, D.E. and D.M. Warshaw, *Length vs. active force relationship in single isolated smooth muscle cells.* Am J Physiol, 1991. **260**(5 Pt 1): p. C1104-12.

37. Herlihy, J.T. and R.A. Murphy, *Length-tension relationship of smooth muscle of the hog carotid artery.* Circ Res, 1973. **33**(3): p. 275-83.

38. Herlihy, J.T. and R.A. Murphy, *Force-velocity and series elastic characteristics of smooth muscle from the hog carotid artery.* Circ Res, 1974. **34**(4): p. 461-6.

39. Herrera, A.M., K.H. Kuo, and C.Y. Seow, *Influence of calcium on myosin thick filament formation in intact airway smooth muscle.* Am J Physiol Cell Physiol, 2002. **282**(2): p. C310-6.

40. Herrera, A.M., E.C. Martinez, and C.Y. Seow, *Electron microscopic study of actin polymerization in airway smooth muscle.* Am J Physiol Lung Cell Mol Physiol, 2004. **286**(6): p. L1161-8.

41. Higgs, H.N. and T.D. Pollard, *Regulation of actin filament network formation through ARP2/3 complex: activation by a diverse array of proteins.* Annu Rev Biochem, 2001. **70**: p. 649-76.

42. Hudgins, P.M. and G.B. Weiss, *Differential effects of calcium removal upon vascular smooth muscle contraction induced by norepinephrine, histamine and potassium.* J Pharmacol Exp Ther, 1968. **159**(1): p. 91-7.

43. Hurwitz, L., et al., *Evidence for two distinct types of potassium-activated calcium channels in an intestinal smooth muscle.* J Pharmacol Exp Ther, 1980. **214**(3): p. 574-80.

44. Huxley, A.F. and R. Niedergerke, *Structural changes in muscle during contraction; interference microscopy of living muscle fibres.* Nature, 1954. **173**(4412): p. 971-3.

45. Kamm, K.E. and J.T. Stull, *The function of myosin and myosin light chain kinase phosphorylation in smooth muscle.* Annu Rev Pharmacol Toxicol, 1985. **25**: p. 593-620.

46. Kamm, K.E. and J.T. Stull, *Dedicated myosin light chain kinases with diverse cellular functions.* J Biol Chem, 2001. **276**(7): p. 4527-30.

47. Kim, H.R., et al., *Cytoskeletal remodeling in differentiated vascular smooth muscle is actin isoform dependent and stimulus dependent.* Am J Physiol Cell Physiol, 2008. **295**(3): p. C768-78.

48. Kim, I., et al., *Ca2+-calmodulin-dependent protein kinase II-dependent activation of contractility in ferret aorta.* J Physiol, 2000. **526 Pt 2**: p. 367-74.

49. Kuo, K.H., et al., *Structure-function correlation in airway smooth muscle adapted to different lengths.* Am J Physiol Cell Physiol, 2003. **285**(2): p. C384-90.

50. Kuo, K.H., et al., *Myosin thick filament lability induced by mechanical strain in airway smooth muscle.* J Appl Physiol, 2001. **90**(5): p. 1811-6.

51. Lakie, M. and L.G. Robson, *Thixotropy in frog single muscle fibres.* Exp Physiol, 1990. **75**(1): p. 123-5.

52. Lin, Y.C. and L. Redmond, *CaMKIIbeta binding to stable F-actin in vivo regulates F-actin filament stability.* Proc Natl Acad Sci U S A, 2008. **105**(41): p. 15791-6.

53. Maekawa, M., et al., *Signaling from Rho to the actin cytoskeleton through protein kinases ROCK and LIM-kinase.* Science, 1999. **285**(5429): p. 895-8.

54. Mahajan, R.K., et al., *Actin filaments mediate Dictyostelium myosin assembly in vitro.* Proc Natl Acad Sci U S A, 1989. **86**(16): p. 6161-5.

55. Mangel, A.W., et al., *Depolarization-induced contractile activity of smooth muscle in calcium-free solution.* Am J Physiol, 1982. **242**(1): p. C36-40.

56. Masuo, M., et al., *A novel mechanism for the Ca(2+)-sensitizing effect of protein kinase C on vascular smooth muscle: inhibition of myosin light chain phosphatase.* J Gen Physiol, 1994. **104**(2): p. 265-86.

57. Mehta, D. and S.J. Gunst, *Actin polymerization stimulated by contractile activation regulates force development in canine tracheal smooth muscle.* J Physiol, 1999. **519 Pt 3**: p. 829-40.

58. Mehta, D., et al., *Role of Rho in Ca(2+)-insensitive contraction and paxillin tyrosine phosphorylation in smooth muscle.* Am J Physiol Cell Physiol, 2000. **279**(2): p. C308-18.

59. Mehta, D., M.F. Wu, and S.J. Gunst, *Role of contractile protein activation in the length-dependent modulation of tracheal smooth muscle force.* Am J Physiol, 1996. **270**(1 Pt 1): p. C243-52.

60. Millar-Craig, M.W., C.N. Bishop, and E.B. Raftery, *Circadian variation of blood-pressure.* Lancet, 1978. **1**(8068): p. 795-7.

61. Moreland, R.S., S. Moreland, and R.A. Murphy, *Dependence of stress on length, Ca2+, and myosin phosphorylation in skinned smooth muscle.* Am J Physiol, 1988. **255**(4 Pt 1): p. C473-8.

62. Morgan, K.G. and S.S. Gangopadhyay, *Invited review: cross-bridge regulation by thin filament-associated proteins.* J Appl Physiol, 2001. **91**(2): p. 953-62.

63. Mulvany, M.J. and D.M. Warshaw, *The active tension-length curve of vascular smooth muscle related to its cellular components.* J Gen Physiol, 1979. **74**(1): p. 85-104.

64. Naghshin, J., et al., *Adaptation to chronic length change in explanted airway smooth muscle.* J Appl Physiol, 2003. **95**(1): p. 448-53; discussion 435.

65. Nichols, W.W. and M.F. O'Rourke, *McDonald's Blood Flow in Arteries: Theoretical, experimental and clinical principles.* 4th ed. ed. 1998, London, UK: Arnold.

66. North, A.J., et al., *Actin isoform compartments in chicken gizzard smooth muscle cells.* J Cell Sci, 1994. **107 (Pt 3)**: p. 445-55.

67. Obara, K. and H. Yabu, *Effect of cytochalasin B on intestinal smooth muscle cells.* Eur J Pharmacol, 1994. **255**(1-3): p. 139-47.

68. O'Brien, E., J. Sheridan, and K. O'Malley, *Dippers and non-dippers.* Lancet, 1988. **2**(8607): p. 397.

69. Ohashi, K., et al., *Rho-associated kinase ROCK activates LIM-kinase 1 by phosphorylation at threonine 508 within the activation loop.* J Biol Chem, 2000. **275**(5): p. 3577-82.

70. Opazo Saez, A., et al., *Tension development during contractile stimulation of smooth muscle requires recruitment of paxillin and vinculin to the membrane.* Am J Physiol Cell Physiol, 2004. **286**(2): p. C433-47.

71. Pantaloni, D. and M.F. Carlier, *How profilin promotes actin filament assembly in the presence of thymosin beta 4.* Cell, 1993. **75**(5): p. 1007-14.

72. Patton, C., S. Thompson, and D. Epel, *Some precautions in using chelators to buffer metals in biological solutions.* Cell Calcium, 2004. **35**(5): p. 427-31.

73. Pavalko, F.M., et al., *Phosphorylation of dense-plaque proteins talin and paxillin during tracheal smooth muscle contraction.* Am J Physiol, 1995. **268**(3 Pt 1): p. C563-71.

74. Pratusevich, V.R., C.Y. Seow, and L.E. Ford, *Plasticity in canine airway smooth muscle.* J Gen Physiol, 1995. **105**(1): p. 73-94.

75. Prewitt, R.L., D.C. Rice, and A.D. Dobrian, *Adaptation of resistance arteries to increases in pressure.* Microcirculation, 2002. **9**(4): p. 295-304.

76. Price, J.M., D.L. Davis, and E.B. Knauss, *Length-dependent sensitivity in vascular smooth muscle.* Am J Physiol, 1981. **241**(4): p. H557-63.

77. Price, J.M., D.L. Davis, and E.B. Knauss, *Length-dependent sensitivity at lengths greater than Lmax in vascular smooth muscle.* Am J Physiol, 1983. **245**(3): p. H379-84.

78. Rasmussen, H., Y. Takuwa, and S. Park, *Protein kinase C in the regulation of smooth muscle contraction.* Faseb J, 1987. **1**(3): p. 177-85.

79. Ratz, P.H., et al., *Regulation of smooth muscle calcium sensitivity: KCl as a calcium-sensitizing stimulus.* Am J Physiol Cell Physiol, 2005. **288**(4): p. C769-83.

80. Ratz, P.H., A.S. Miner, and S.E. Barbour, *Calcium-independent phospholipase A(2) participates in KCl-induced calcium sensitization of vascular smooth muscle.* Cell Calcium, 2009.

81. Ratz, P.H. and R.A. Murphy, *Contributions of intracellular and extracellular Ca2+ pools to activation of myosin phosphorylation and stress in swine carotid media.* Circ Res, 1987. **60**(3): p. 410-21.

82. Rembold, C.M., *Resistance to stretch, [Ca2+]i, and activation of swine arterial smooth muscle.* J Muscle Res Cell Motil, 1992. **13**(1): p. 27-34.

83. Rembold, C.M. and R.A. Murphy, *Muscle length, shortening, myoplasmic [Ca2+], and activation of arterial smooth muscle.* Circ Res, 1990. **66**(5): p. 1354-61.

84. Rembold, C.M., et al., *Paxillin phosphorylation, actin polymerization, noise temperature, and the sustained phase of swine carotid artery contraction.* Am J Physiol Cell Physiol, 2007. **293**(3): p. C993-1002.

85. Rice, R.V., et al., *The organization of contractile filaments in a mammalian smooth muscle.* J Cell Biol, 1970. **47**(1): p. 183-96.

86. Rokolya, A. and H.A. Singer, *Inhibition of CaM kinase II activation and force maintenance by KN-93 in arterial smooth muscle.* Am J Physiol Cell Physiol, 2000. **278**(3): p. C537-45.

87. Safar, M.E., *Hypertension, systolic blood pressure, and large arteries.* Med Clin North Am, 2009. **93**(3): p. 605-19, Table of Contents.

88. Safar, M.E., B.I. Levy, and H. Struijker-Boudier, *Current perspectives on arterial stiffness and pulse pressure in hypertension and cardiovascular diseases.* Circulation, 2003. **107**(22): p. 2864-9.

89. Safar, M.E., et al., *Recent advances on large arteries in hypertension.* Hypertension, 1998. **32**(1): p. 156-61.

90. Schmidt, J.M., et al., *Interaction of talin with actin: sensitive modulation of filament crosslinking activity.* Arch Biochem Biophys, 1999. **366**(1): p. 139-50.

91. Seow, C.Y., *Response of arterial smooth muscle to length perturbation.* J Appl Physiol, 2000. **89**(5): p. 2065-72.

92. Seow, C.Y., *Myosin filament assembly in an ever-changing myofilament lattice of smooth muscle.* Am J Physiol Cell Physiol, 2005. **289**(6): p. C1363-8.

93. Seow, C.Y., V.R. Pratusevich, and L.E. Ford, *Series-to-parallel transition in the filament lattice of airway smooth muscle.* J Appl Physiol, 2000. **89**(3): p. 869-76.

94. Shaw, L., et al., *Inhibitors of actin filament polymerisation attenuate force but not global intracellular calcium in isolated pressurised resistance arteries.* J Vasc Res, 2003. **40**(1): p. 1-10; discussion 10.

95. Sherwood, A., et al., *Nighttime blood pressure dipping: the role of the sympathetic nervous system.* Am J Hypertens, 2002. **15**(2 Pt 1): p. 111-8.

96. Sica, D.A., *What are the influences of salt, potassium, the sympathetic nervous system, and the renin-angiotensin system on the circadian variation in blood pressure?* Blood Press Monit, 1999. **4 Suppl 2**: p. S9-S16.

97. Smolensky, A.V. and L.E. Ford, *The extensive length-force relationship of porcine airway smooth muscle.* J Appl Physiol, 2007. **102**(5): p. 1906-11.

98. Smolensky, A.V., et al., *Length-dependent filament formation assessed from birefringence increases during activation of porcine tracheal muscle.* J Physiol, 2005. **563**(Pt 2): p. 517-27.

99. Somlyo, A.V. and A.P. Somlyo, *Electromechanical and pharmacomechanical coupling in vascular smooth muscle.* J Pharmacol Exp Ther, 1968. **159**(1): p. 129-45.

100. Speich, J.E., et al., *ROK-induced cross-link formation stiffens passive muscle: reversible strain-induced stress softening in rabbit detrusor.* Am J Physiol Cell Physiol, 2005. **289**(1): p. C12-21.

101. Speich, J.E., et al., *Adjustable passive length-tension curve in rabbit detrusor smooth muscle.* J Appl Physiol, 2007. **102**(5): p. 1746-55.

102. Staessen, J.A., et al., *Predicting cardiovascular risk using conventional vs ambulatory blood pressure in older patients with systolic hypertension. Systolic Hypertension in Europe Trial Investigators.* Jama, 1999. **282**(6): p. 539-46.

103. Steinsland, O.S., R.F. Furchgott, and S.M. Kirpekar, *Biphasic vasoconstriction of the rabbit ear artery.* Circ Res, 1973. **32**(1): p. 49-58.

104. Syyong, H., et al., *Adaptive response of pulmonary arterial smooth muscle to length change.* J Appl Physiol, 2008. **104**(4): p. 1014-20.

105. Tang, D., D. Mehta, and S.J. Gunst, *Mechanosensitive tyrosine phosphorylation of paxillin and focal adhesion kinase in tracheal smooth muscle.* Am J Physiol, 1999. **276**(1 Pt 1): p. C250-8.

106. Tang, D.D. and S.J. Gunst, *Depletion of focal adhesion kinase by antisense depresses contractile activation of smooth muscle.* Am J Physiol Cell Physiol, 2001. **280**(4): p. C874-83.

107. Tang, D.D. and S.J. Gunst, *The small GTPase Cdc42 regulates actin polymerization and tension development during contractile stimulation of smooth muscle.* J Biol Chem, 2004. **279**(50): p. 51722-8.

108. Tang, D.D., C.E. Turner, and S.J. Gunst, *Expression of non-phosphorylatable paxillin mutants in canine tracheal smooth muscle inhibits tension development.* J Physiol, 2003. **553**(Pt 1): p. 21-35.

109. Tang, D.D., et al., *The focal adhesion protein paxillin regulates contraction in canine tracheal smooth muscle.* J Physiol, 2002. **542**(Pt 2): p. 501-13.

110. Tang, D.D., W. Zhang, and S.J. Gunst, *The adapter protein CrkII regulates neuronal Wiskott-Aldrich syndrome protein, actin polymerization, and tension development during contractile stimulation of smooth muscle.* J Biol Chem, 2005. **280**(24): p. 23380-9.

111. Tanko, L.B., et al., *A new method for combined isometric and isobaric pharmacodynamic studies on porcine coronary arteries.* Clin Exp Pharmacol Physiol, 1998. **25**(11): p. 919-27.

112. Tseng, S., et al., *F-actin disruption attenuates agonist-induced [Ca2+], myosin phosphorylation, and force in smooth muscle.* Am J Physiol, 1997. **272**(6 Pt 1): p. C1960-7.

113. Uvelius, B., *Isometric and isotonic length-tension relations and variaitonsin cell length in longitudinal smooth muscel from rabbit urinary bladder.* Acta Physiol Scand, 1976. **97**(1): p. 1-12.

114. Van Heijst, B.G., et al., *The effect of length on the sensitivity to phenylephrine and calcium in intact and skinned vascular smooth muscle.* J Muscle Res Cell Motil, 1999. **20**(1): p. 11-8.

115. Vandekerckhove, J. and K. Weber, *At least six different actins are expressed in a higher mammal: an analysis based on the amino acid sequence of the amino-terminal tryptic peptide.* J Mol Biol, 1978. **126**(4): p. 783-802.

116. Verdecchia, P., et al., *Circadian blood pressure changes and left ventricular hypertrophy in essential hypertension.* Circulation, 1990. **81**(2): p. 528-36.

117. Wang, L., P.D. Pare, and C.Y. Seow, *Selected contribution: effect of chronic passive length change on airway smooth muscle length-tension relationship.* J Appl Physiol, 2001. **90**(2): p. 734-40.

118. Wang, Z., F.M. Pavalko, and S.J. Gunst, *Tyrosine phosphorylation of the dense plaque protein paxillin is regulated during smooth muscle contraction.* Am J Physiol, 1996. **271**(5 Pt 1): p. C1594-602.

119. Watanabe, N., et al., *p140mDia, a mammalian homolog of Drosophila diaphanous, is a target protein for Rho small GTPase and is a ligand for profilin.* Embo J, 1997. **16**(11): p. 3044-56.

120. Waugh, W.H., *Role of calcium in contractile excitation of vascular smooth muscle by epinephrine and potassium.* Circ Res, 1962. **11**: p. 927-40.

121. Wingard, C.J., A.K. Browne, and R.A. Murphy, *Dependence of force on length at constant cross-bridge phosphorylation in the swine carotid media.* J Physiol, 1995. **488 (Pt 3)**: p. 729-39.

122. Winton, F.R., *The influence of length on the responses of unstriated muscle to electrical and chemical stimulation, and stretching.* J Physiol, 1926. **61**(3): p. 368-82.

123. Wright, G. and E. Hurn, *Cytochalasin inhibition of slow tension increase in rat aortic rings.* Am J Physiol, 1994. **267**(4 Pt 2): p. H1437-46.

124. Xu, J.Q., J.M. Gillis, and R. Craig, *Polymerization of myosin on activation of rat anococcygeus smooth muscle.* J Muscle Res Cell Motil, 1997. **18**(3): p. 381-93.

125. Yoo, J., et al., *Mechanosensitive modulation of myosin phosphorylation and phosphatidylinositol turnover in smooth muscle.* Am J Physiol, 1994. **267**(6 Pt 1): p. C1657-65.

126. Youn, T., S.A. Kim, and C.M. Hai, *Length-dependent modulation of smooth muscle activation: effects of agonist, cytochalasin, and temperature.* Am J Physiol, 1998. **274**(6 Pt 1): p. C1601-7.

127. Zhang, W. and S.J. Gunst, *Dynamic association between alpha-actinin and beta-integrin regulates contraction of canine tracheal smooth muscle.* J Physiol, 2006. **572**(Pt 3): p. 659-76.

128. Zhang, W., et al., *Activation of the Arp2/3 complex by N-WASp is required for actin polymerization and contraction in smooth muscle.* Am J Physiol Cell Physiol, 2005. **288**(5): p. C1145-60.

VITA

Melissa L. Bednarek was born on February 14, 1976 in Williamsville, New York. She graduated from Newfane Senior High School in 1994. She then completed a Bachelor of Science degree, with majors in Biology and Psychology, at St. Bonaventure University in 1998. Melissa then moved to Philadelphia, Pennsylvania to complete a Masters in Physical Therapy degree from the Medical College of Pennsylvania (MCP) Hahnemann University (now known as Drexel University) in 2000. After successfully passing the physical therapy licensure exam, she became a full-time acute care physical therapist at Lancaster General Hospital in Lancaster, Pennsylvania. After 4 years of clinical practice, Melissa returned to graduate school as a full-time student at the Medical College of Virginia (MCV) Campus of Virginia Commonwealth University in Richmond, Virginia. She completed her Doctor of Philosophy degree through the Department of Physiology and Biophysics in 2009. She remained in academia by accepting a position as an Assistant Professor in the Department of Physical Therapy at Chatham University in Pittsburgh, Pennsylvania.